DOCTOR OF PHILOSOPHY

Continuum models for fungal growth

Al-Taie, Ali Hussein Shuaa

Award date:
2011

DOCTOR OF PHILOSOPHY

Continuum models for fungal growth

Ali Hussein Shuaa Al-Taie

2011

University of Dundee

Continuum Models for Fungal Growth

By

Ali Hussein Shuaa Al-Taie

Doctor of Philosophy

Division of Mathematics

University of Dundee

Dundee

October 2011

Contents

List of Figures

List of Tables

Acknowledgements

Firstly, I would like to thank my supervisor, Dr Fordyce Davidson, without whom this thesis would not have been possible. His insight into the subject and attention to detail have been inspirational, and his guidance and support invaluable. My thanks also go out to every one else in department who have helped me in so many ways over the years.

I wish also to thank the other members of staff of the Department of Mathematics. I am also grateful to Mr Nick Dawes for providing me with mathematical software and solving any technical problems I encountered. I am greatly indebted to my father, mother, brothers, sisters, children and the rest of my family for encouragement, prayers and support they have provided me during my studies. My sincere thanks are due to my wife, Khalida, who has managed patiently to look after our children, Hussein, Zeinab, Mujtaba, Fatima and Muqtada so that I could concentrate on my studies. May ALLAH bless them all.

My great pleasure and appreciations go to my friends Mohannad Al-Tameemi, Faik Mayah, Ebraheem Alzahrani, Ali Al-Hachami, Marc Sturrock, Asad Hafudh and for their moral support and encouragement throughout my studies.

Finally, I would like to thank ministry of higher education and scientific research, the Iraqi Cultural Attache and College of Management and Economics at Wassit University for their financial support and otherwise.

Declaration

I declare that the following thesis is my own composition and that it has not been submitted before in application for a higher degree.

Ali Hussein Shuaa Al-Taie

Certification

This is to certify that Ali Hussein Shuaa Al-Taie has complied with all the requirements for the submission of this Doctor of Philosophy thesis to the University of Dundee.

Dr Fordyce Davidson

Abstract

Fungi generally exist as unicellular organisms (yeasts) or in a vegetative state in which a mycelium, i.e. an interconnected network of tubes (hyphae) is formed. The mycelium can operate over a very large range of scales (each hypha is only a few microns in diameter, yet mycelia can be kilometres across).

Fungi are of fundamental importance to many natural processes: certain species have major roles in decomposition and nutrient cycling in the soil; some form vital links with plant roots allowing nutrient transfer. Other species are essential to industrial processes: citric acid production for use in soft drinks; brewing and baking; treatment of industrial effluent and ground toxins.

Unfortunately, certain species can cause devastating damage to crops, serious disease in humans or can damage building materials.

In this thesis we constructed new models for the development of fungal mycelia. At this scale, partial differential equations representing the interaction of biomass with the underling substrate is the appropriate choice. Models are essentially based on those derived by Davidson and co workers (see e.g. Boswell et al. (2007).

These models are of a complex mathematical structure, comprising both parabolic and hyperbolic parts. Thus, their analytic and numerical properties are non-trivial.

The objectives of this thesis are to:

(i) obtain a solid understanding of the physiology of growth and function and the varying mathematical techniques used in model construction.

(ii) revisit existing models to reinterpret the various model components in a simplified form.

(iii) construct models to compare the growth dynamics of different phenotype for new species to see if these "scale " appropriately.

Chapter 1

Introduction

Mathematics has been applied to a wide range of biological areas over the last century (Hardy, 1940). It is of no surprise, then, that mathematics has played a key role in the understanding of the growth and behaviour of fungal mycelial. This will be the topic of this thesis.

Depending on (Edelstein, 1982). Our aim is to develop a model for the growth of fungi which we can use to create a source term in a single root model to account for nutrient uptake by the fungi. Therefore, we will focus on the hyphal loss or death. The original model that we assume that fungal growth can be described by is: the hyphal tip density n and the hyphal length density ρ. Sometimes, one tip of fungi splits up into two. It is less clear whether anastomosis occurs in some fungi. There are reports that it does Giovanetti et al. (2011).

The thesis is ordered as follows. In Chapter 2, some biological background and some mathematical background concerning the fungal models is given. Specifically we look at:

- Biological Background.

- Modelling background.
- Mathematical techniques.
- Reaction diffusion equations.
- Convection - diffusion equations.

In Chapter 3, we extend the model of (Edelstein, 1982), namely

$$\frac{\partial \rho}{\partial t} = J_n - d(\rho),$$
$$\frac{\partial n}{\partial t} = -\frac{\partial (J_n)}{\partial x} + \sigma(\rho, n),$$

with flux $J_n = nv$, where we investigated from effect hyphal death on development of fugal network, when $d(\rho) = \gamma_1 \rho^k$. In particular, we consider the following generic phenotypes:

- FHD: Lateral branching plus tip - hypha anastomosis.
- FXD: Lateral branching with density limitation.
- YWD: Dichotomous branches, tip-tip anastomoses.
- YHD: Dichotomous branches, tip-hyphae anastomoses.

Other patterns of branching for examples: FHTD: Lateral branching, tip-hypha anastomosis, tip death, YWTD: dichotomous branching tip - tip anastomoses tip death, etc.

In each case we applied similar techniques: non- dimensionalisation, stability of uniform solutions, travelling wave solution and numerical solution of the initial value problem to the different types of branching. To avoid unnecessary repetition we put this in tables.

Also in Chapter 1, we study the other case for hyphal death, $d(\rho) = \frac{d\rho^k}{\rho_o^k + d\rho^k}$, where k positive number, we use the Michaelis constant which is equivalent to the half maximum hyphal death rate. To shorten the process we put a lot of cases in tables under the following headings: Biological type, symbols, branching rule σ, choice of scales, dimensionless equation for propagation, steady states and traveling wave solutions.

In chapter 4, we added diffusion for previous models and the system takes this form:

$$\begin{aligned} \frac{\partial \rho}{\partial t} &= |J| - d(\rho), \\ \frac{\partial n}{\partial t} &= -\nabla J + \sigma(\rho, n), \end{aligned}$$

In this model we assume that flux J is take the form:

$$J = \underbrace{-D_n \frac{\partial n}{\partial x}}_{\text{diffusion}} + \underbrace{nv}_{\text{convection}}.$$

The following cases are described as below:

- We discuss two cases, $d(\rho) = 0$ and $d(\rho) \neq 0$.
- When $d(\rho) = 0$, we study the cases for values of D_n and v as:
  1. $D_n \neq 0$, $v \neq 0$: tip diffusion and convection,
  2. $D_n \neq 0$, $v = 0$: tip diffusion,
  3. $D_n = 0$, $v \neq 0$: tip convection.
- We study the same above cases when $d(\rho) \neq 0$.
- We illustrate the relation between wavespeed c and diffusion D_n. We noted that when diffusion D_n is increasing then wavespeed c is still increasing.

In Chapter 5, we develop our system by adding substrate s, the system is given below:

$$\begin{aligned}\frac{\partial \rho}{\partial t} &= |J| - d(\rho),\\ \frac{\partial n}{\partial t} &= -\nabla J + \sigma(\rho, n),\\ \frac{\partial s}{\partial t} &= \Delta s + f(\rho, n),\end{aligned}$$

where

$$J = -D_n \frac{\partial n}{\partial x} + vns.$$

We show, the effects of substrate on the development of fungal networks. This Chapter illustrates the effects of parameters on the development of fungal networks.

In Chapter 6, we study radially symmetric fronts and compare them to 1-D travelling waves. We present extensions of our work from Chapters 3-5 to two spatial dimensions. We expect spatial domain to be in 2 - dimension. In this chapter, we consider the following 2-D spatially extended

- Fungal growth equations

$$\begin{aligned}\frac{\partial \rho}{\partial t} &= [(nv_1)^2 + (nv_2)^2]^{\frac{1}{2}} - d(\rho),\\ \frac{\partial n}{\partial t} &= -\frac{\partial (nv)}{\partial r} - \frac{(nv)}{r} + \sigma(\rho, n)\end{aligned}$$

- Fungal growth system with substrate

$$\begin{aligned}\frac{\partial \rho}{\partial t} &= [(nv_1 s)^2 + (nv_2 s)^2]^{\frac{1}{2}} - d(\rho),\\ \frac{\partial n}{\partial t} &= -\frac{\partial (nvs)}{\partial r} - \frac{(nvs)}{r} + \sigma(\rho, n, s)\\ \frac{\partial s}{\partial t} &= -f_s(\rho, n, s)\end{aligned}$$

Finally, in Chapter 7 we conclude by summarising a number of important points, and then suggest some possible topics for future work.

Chapter 2

Biological and Modelling Background

2.1 Introduction

Mathematical biology is the application of mathematics to biological systems (Murray, 2002). Mathematical biology contributes understanding at all levels of systems, from the order of molecules to ecosystem. In this thesis we focused on one small, but important part: the growth of fungi.

2.2 Biological Background

A glossary of biological terms is given in an Appendix at the end of this thesis.

2.2.1 Fungi

Fungi are not classed as animals or plants, they have a Kingdom of their own to which they belong. They range from being just a single cell, like the yeasts, to others that cover hundreds of acres of land (Hadley, 2002). Most fungi are said to be filamentous. This is because the main body of the fungus is made up of thin, thread-like filaments that are called hyphae, which form the mycelium.

To date, 100,000 species of fungi have been discovered (Assinder and Rutter, 2001). It is thought that there are over one million species still to be found (Hadley, 2002). The fungi that most people are familiar with are those that form fruit bodies or mushrooms. Fungi can live in many habitats including the arctic, tropical rainforest, fresh and salt water. However, most fungi live in soil (Moore, 2001).

Many useful products have been isolated from fungi which have been of great benefit to humans including antibiotics; agents to lower cholesterol and Immune system suppressants. Certain activities of fungi are also used to produce food and drink.

The fungi used in the manufacture of: beer; chocolate; cheese; bread; fizzy drinks and enzymes for washing powders. (Hadley, 2002; Moore, 2001; Assinder and Rutter, 2001)

2.2.2 Mycelium

At one time or another, we have all come across food that has become contaminated in some forgotten corner of our refrigerator and observed the filamentous growth of fungi as a “mold”. This mat is in fact the filamentous growth of fungi and is called the mycelium and represents the ‘body” of the fungus. A fragment of mycelium is referred to as a hypha.

2.2.3 A hypha

A hypha (plural hyphae) is a long, branching filamentous cell of a fungus (and also of unrelated Actinobacteria). In most fungi, hyphae are the main mode of vegetative growth, and are collectively called a mycelium; yeasts are unicellular fungi that do not grow as hyphae (Madigan and Martinko, 2005).

2.2.4 Fungal Colonies

Many species of fungi produce small secondary structures such as sclerotia, coremia or conidia within their colonies. These produced in uniform, sporadic fashion or as a result of external cues. In some circumstances, a seemingly homogeneous growth environment will nevertheless result in synchronous formation of such structures so that an apparent spatial pattern results. The pattern is usually periodic along the radius of colony. Examples of these phenomenon are known to occur in *Sclerotium rolfsii* Okon et al. (1972), *Penicillium claviform* Watkinson (1975) as well as *Nectria cinnabarina* (Bourret et al., 1969) although the differences in the details of patterning is wide. Conjectures as to the causes of these spatial patterns include endogenous biochemical oscillations (Winfree, 1980), the combined nutrient statutes of the colony and medium (Humpherson-Jones and Cooke, 1977), accumulation and utilization of reserve material Watkinson (1975), and the combination of enhanced translocation and inhibition of tip growth (Okon et al., 1972).

since secondary structures are often produced by modifications of hyphae, variable hypha density may be a necessary precursor of some of these structures. Indeed in *Sclerotium rolfsii* radial density striations are often encountered, especially in conditions favouring synchronous formation of sclerotia (Hadar and

Edelstein, unpublished observations). It is of interest to determine whether density striations occur in any model fungi which combine the basic branching control mechanisms outlined in this in this thesis.
Two examples which apparently demonstrates density bands is fungal types:

(i) FX: Lateral branches with density limitation.

(ii) YH: Dichotomous branches tip - hyphae anastomoses.

2.3 Modelling Background

Models describe our beliefs about how the world functions. In mathematical modelling, we translate those beliefs into the language of mathematics. This has many advantages

(i) Mathematics is a very precise language. This helps us to formulate ideas and identify underlying assumptions.

(ii) Mathematics is a concise language, with well-defined rules for manipulations.

(iii) All the results that mathematicians have proved over hundreds of years are at our disposal.

(iv) Computers can be used to perform numerical calculations.

There is a large element of compromise in mathematical modelling. The majority of interacting systems in the real world are far too complicated to model in their entirety. Hence the first level of compromise is to identify the most important

parts of the system. These will be included in the model, the rest will be excluded. The second level of compromise concerns the amount of mathematical manipulation which is worthwhile. Although mathematics has the potential to prove general results, these results depend critically on the form of equations used. Small changes in the structure of equations may require enormous changes in the mathematical methods. Using computers to handle the model equations may never lead to elegant results, but it is much more robust against alterations.

2.3.1 What objectives can modelling achieve?

Mathematical modelling can be used for a number of different reasons. How well any particular objective is achieved depends on both the state of knowledge about a system and how well the modelling is done. Examples of the range of objectives are:

(i) Developing scientific understanding, through quantitative expression of current knowledge of a system (as well as displaying what we know, this may also show up what we do not know);

(ii) test the effect of changes in a system;

(iii) aid decision making, including
   (1) tactical decisions by managers;
   (2) strategic decisions by planners.

Stages of modelling is helpful to divide up the process of modelling into four broad categories of activity, namely formulation, analysis, interpretation and test, see Fig. 2.1.

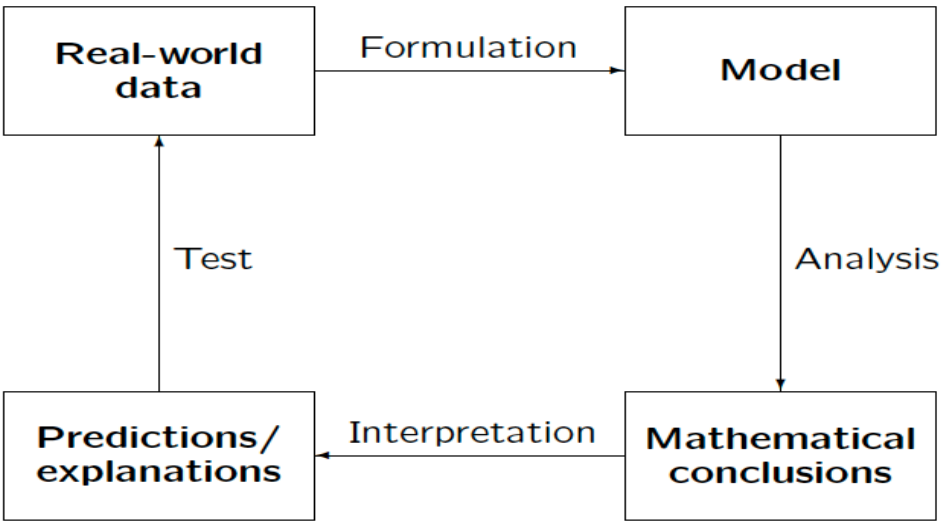

Figure 2.1: Stages of modelling, see (Vetterling, 1987).

2.4 Biological Modelling

The understanding of the growth and function of the fungal developed by used mathematical modelling (Edelstein, 1982; Prosser, 1995; Davidson, 2007a,b; Schnepf and Roose, 2006; Schnepf et al., 2008a,b) This includes complex interactions within their environment, such as real time descriptions of the colonization of soil like structures, and translocation phenomena (Boswell et al., 2002, 2003a,b, 2007; Jolicoeur et al., 2003; Tlalka et al., 2003; Darrah et al., 2006; Schnepf and Roose, 2006; Boswell, 2008; Jager et al., 2008; Schnepf et al., 2008a,b).

Necessary, modelling frameworks need to link environmental condition to community structure, biotic interactions and function (Falconer et al., 2007, 2008). We focus on a specific area in which we hope to make progress (Schnepf and Roose, 2006; Schnepf et al., 2008a,b; Davidson, 2007a). The main focus at the macro-scale is the interactions of fungi with the environment.

To examine growth and function of the fungi, there are three main modelling approaches: (i) continuous, (ii)discrete and (iii) hybrid discrete continuum automaton modelling, for example, (Boswell et al., 2003a, 2007; Edelstein, 1982; Davidson, 1998; Boswell et al., 2002, 2003a; Schnepf and Roose, 2006; Schnepf et al., 2008a,b) are common approach to modelling by using properties of fungal mycelia growing, as continuous variables so that the model comprises a system of (non-linear) partial differential equations (PDEs).

Mathematical models for the growth of filamentous fungi was suggested by Edelstein and Segel (1982) and she describes in general biological processes such as the creation of new branches, the divide of a tip with another tip or its neighbouring hypha (anastomosis).

In next section, we will focus on a simple model, and include additional processes as necessary when test our models.

2.5 Mathematical Techniques

2.5.1 First order equation

Our work depends on first order hyperbolic equations, therefore, in this section, we will examine first - order partial differential equation. We will find some curves, called characteristics, provide important information on the nature of the solution. Thus, we focus on techniques based on separation of variables and series transform methods to solution techniques based to the characteristics curves.

2.5.2 Constant - coefficient advection equation

The equation

$$vn_x + n_t = 0, \qquad v = \text{constant} \tag{2.1}$$

$n = n(x,t)$ is called an advection equation. Above equation (2.1) arises in mathematical models that involve the movement of a wave in one direction with no change in the shape of the wave. To solve this equation, we are finding curves in the (x,t) - plane along which (2.1) reduces to an ordinary differential equation. Let C be a curve defined by $x = x(t)$. Then, on C we have $n(x,t) = n(x(t),t)$. Differentiation of n along C yields

$$\frac{dn}{dt} = \frac{\partial n}{\partial x}\frac{dx}{dt} + \frac{\partial n}{\partial t}, \tag{2.2}$$

comparing the right of (2.2) with the left side of (2.1), we see that if we set

$$\frac{dx}{dt} = v \qquad on \quad C \tag{2.3}$$

then

$$\frac{dn}{dt} = 0 \qquad on \quad C \tag{2.4}$$

A curve along which (2.3) holds, is called a characteristic curve, or simply a characteristic of Equation (2.1).
Equation (2.4) implies that the solution n is constant along a characteristic. Solving the characteristic equation (2.3) yields

$$x = vt + x_o, \qquad x_o = constant. \tag{2.5}$$

Thus, the characteristics of the constant - coefficient equation (2.1) are seen to be straight lines in the (x, t) plane. Note that at time $t = 0$ the characteristics defined by equation (2.5) intersects the x axis at position x_o. Also, for every unit increase of t, a point on the characteristics moves v unit in the positive x direction if v is positive and v units in the negative x direction if v is negative.

2.5.3 Initial - Value Problem

Consider the initial - value problem (IVP)

$$vn_x + n_t = 0, \qquad -\infty < x < +\infty, \quad t > 0, \tag{2.6a}$$

$$n(x, 0) = f(x). \tag{2.6b}$$

An IVP of the form (2.6 a, b) is also referred to as a Cauchy Problem. From equation (2.5) we note that the point (x, t) and $(x - vt, 0)$ lie on the same characteristics, see Fig. 2.2. Since n is constant along a characteristics,

$$n(x, t) = n(x - vt, 0) = f(x - vt).$$

This establishes the following result.

Theorem 1.1. If $f(x)$ is continuously differentiable, then

$$n(x, t) = f(x - vt),$$

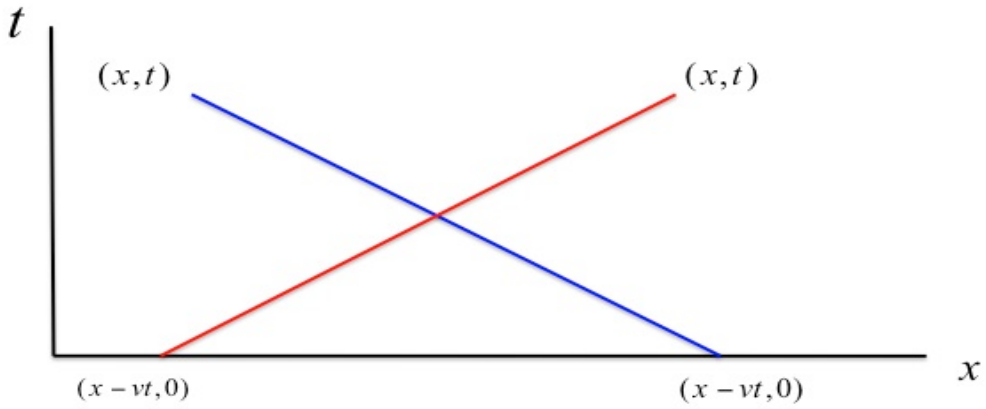

Figure 2.2: A characteristic of Equation (2.6) red line for the case $v > 0$, blue line for the case $v < 0$.

solves the initial - value problem defined by equation (2.6 a, b).

Let us assume that f is continuously differentiable then

$$n_x = f'(x - vt) \quad \text{and} \quad n_t = f'(x - vt) \cdot (-v),$$

are continuous. Thus, $n(x, t)$ has the required differentiability to be called a solution of Equation (2.1). In many applications f is allowed to be only piecewise continuously differentiable or even piecewise continuous. In this case $n(x, t) = f(x - vt)$ is still referred to as a solution of the initial - value problem (2.6 a, b), but it is called a weak, or generalized, solution.

2.5.4 Initial - Boundary - Value Problem (IBVP)

An initial - value problem for the constant - coefficient, first order wave equation has the from

$$vn_x + n_t = 0, \qquad x > 0, \quad t > 0, \tag{2.7a}$$

$$n(x,0) = f(x) \qquad x > 0, \tag{2.7b}$$

$$n(0,t) = \mathrm{g}(t) \qquad t > 0. \tag{2.7c}$$

The initial condition is given by (2.7b) and the boundary condition by (2.7c).
We first consider the case that v is positive. Then the characteristic through the origin divides the first quadrant into two region, see Fig. 2.3.

$$R_1 : x > vt \quad and \quad R_2 : x < vt.$$

In R_1 the solution n is determined by the initial condition to be $n(x,t) = f(x-vt)$. Given a point $(\bar{x}, \bar{t})$ in R_2 we can trace back along the characteristic $x = v(t-\bar{t})+\bar{x}$ point $(0, \bar{t} - \bar{x}/v)$. This show that in R_2

$$n(x,t) = n(0, t - x/v) = \mathrm{g}(t - x/v)$$

and we note that the solution to (2.7a) - (2.7c) is given by

$$n(x,t) = \begin{cases} f(x - vt), & x > vt, \quad v > 0, \\ \mathrm{g}(\frac{vt-x}{v}) & x < vt, \quad v > 0 \end{cases} \tag{2.8}$$

The condition for $n(x,t)$ defined by equation (2.8) to be continuous across the line $x = vt$ is that $f(0) = \mathrm{g}(0)$.
Now, if $v < 0$, the initial - boundary - value problem (2.7) is not well posed.

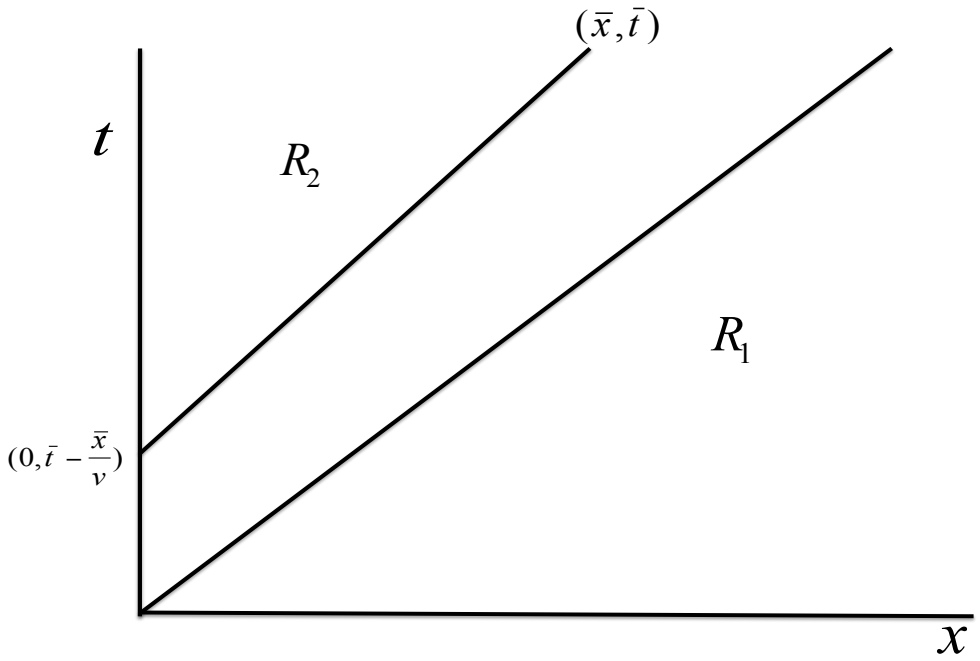

Figure 2.3: R_1, region of influence of initial condition $f(x)$; R_2, region of influence of boundary condition g(x).

To see this, see that for $x_o > 0$, the point $(x_o, 0)$ and $(0, x_o/|v|)$ lie on the same characteristic. The initial condition (2.7b) states $n(x_o, 0) = f(x_o)$, while the boundary condition (2.7c) gives $n(0, x_o/|v|) = \mathrm{g}(x_o/|v|)$. The fact that n is constant along a characteristic requires that

$$f(x_o) = \mathrm{g}(x_o/|v|) \tag{2.9}$$

for arbitrary $x_o > 0$. Thus, the boundary condition g and the initial condition f must satisfy the compatibility condition (2.9), and we note that for general f and g the initial boundary value problem (2.7a -c) will not have a solution (Fig .2.4). In many application that involve a first - order differential equation of the form equation (2.1), we find that x plays the role of a space variable and t a time variable.

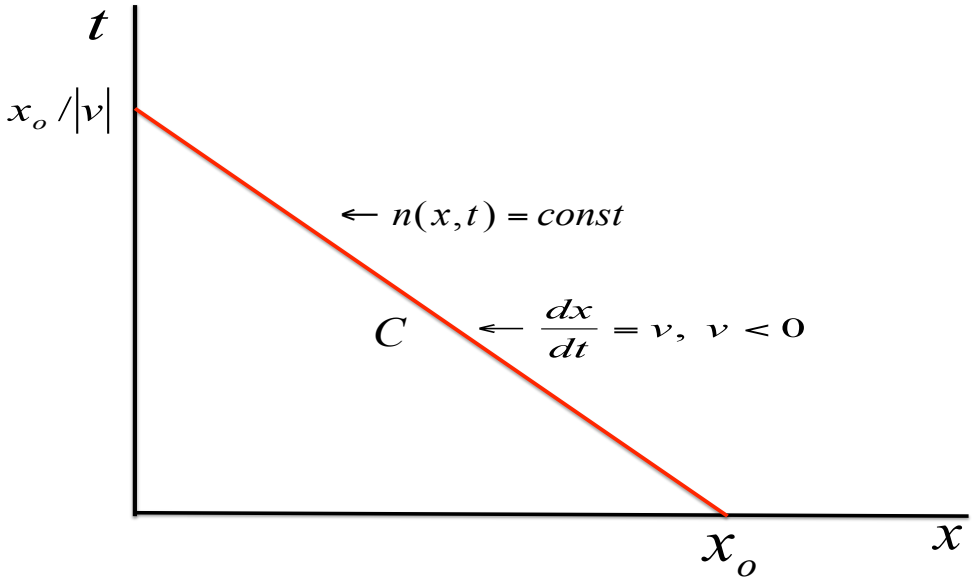

Figure 2.4: The solution cannot be specified at two points on a same characteristics.

2.5.5 Linear and Quasi - Linear Equations

The general first order, quasi - linear equation for $n(x,t)$ has the form

$$a(x,t,n)n_x + b(x,t,n)n_t = c(x,t,n) \tag{2.10}$$

An initial - value problem consists of (2.10) together with an initial condition

$$n(x,0) = f(x) \tag{2.11}$$

If c is identically zero, (2.10) is said to be homogeneous. If a and b are independent of n, (2.10) is called almost linear. If a and b are independent of n and c has the form $c(x,t,n) = d(x,t)n + S(x,t)$ then (2.10) is linear DuChateau and Zachmann (1989).

For the constant - coefficients, the homogenous equation $vn_x + n_t = 0$, the characteristic curves are the straight lines defined by $dx/dt = v$.

Now, the initial - value problem defined by (2.10) and (2.11).

As a first step, let us introduce a curve C defined by

$$C : \begin{cases} x = x(r), & x(0) = s, \\ t = t(r) & t(0) = 0. \end{cases}$$

We used r to fix a position along C and s to specify where the curve C intersects the x - axis. Let the restriction of $n(x,t)$ to the curve C, be written as $n = n(x(r), t(r))$. Using the chain rule to differentiate with respect to r, we find

$$\frac{dn}{dr} = \frac{\partial n}{\partial x}\frac{dx}{dr} + \frac{\partial n}{\partial t}\frac{dt}{dr}$$

If we set $\frac{dx}{dr} = a$ and $\frac{dt}{dr} = b$, then, along C, the partial differential equation (2.10) reduces to the ordinary differential equations $\frac{dn}{dr} = c$. The equations

$$\frac{dx}{dr} = a, \qquad \frac{dt}{dr} = b; \qquad \frac{dn}{dr} = c$$

are called the characteristic equations of Equation (2.10).

2.6 Reaction-Diffusion Equation

2.6.1 Derivation of a simple model for fungal growth

We derive the equation describing fungal tip density as conservation law. Let V be an arbitrary finite volume, which is bounded by the surface S. Consider n be the hyphal tip density in that volume, v be the vector of extension rates, (nv) be the flux through the surface and u_n the unit outward normal vector to S. The total amount of tips contained in V is

$$\int_V n(x,t)dV.$$

The flux of tips into V is

$$-\int_S (nv)\cdot u_n dS.$$

Since $\mathbf{u_n}$ point outward, therefore, we note that the minus sign. The number of tips created or destroyed in V per unit time is described by

$$\int_V f dV.$$

The change in tip density in V with time must be equal to the flux of tips into V plus the number of tips created or destroyed, i.e.,

$$\frac{d}{dt}\int_V n dV = -\int_S (nv)\cdot u_n dS + \int_V f dV.$$

Here V does not change with time. Therefore, we swap the integration and differentiation operators, and using the divergence theorem. We obtain

$$\int_V \frac{\partial n}{\partial t} dV = -\int_V \nabla \cdot (nv) dV + \int_V f dV.$$

From the above expression as V is arbitrary, we conclude that

$$\frac{\partial n}{\partial t} = -\nabla \cdot (nv) + f. \tag{2.12}$$

As a simplest case, we consider the new tip creation to be linearly proportional to the existing tip density, i.e. $f = \alpha n$, where α is the tip branching rate. This would, in biological terms, correspond to apical branching, where one tip splits into two. The other type of branching would be lateral branching where a new hypal grows from the side of an existing hypha. However, mycorrhizal fungi are known to branch mainly apically (Edelstein, 1982).

The hyphal length density is dependent on hyphal growth and death. Hyphal growth occurs due to elongation of a small region just behind the hyphal tip. Therefore, the hyphae can be viewed as the "trail" left behind the tip and the increase of hyphal density can be written as $n|v|$. The simplest way to describe the death rate is to consider it linearly proportional to the hyphal length density ρ, i.e., the rate of death is $d\rho$ where d is the hyphal death rate (Drew et al., 2003; Jakobsen et al., 1992). Hence, the equation describing the hyphal length density

$$\frac{\partial \rho}{\partial t} = n|v| - \gamma_1 \rho. \tag{2.13}$$

2.6.2 Analytical solutions

We can consider hyphal and tip length densities to depend only on horizontal distance from the root-fungus interface. Hence we have to solve the one dimensional problem in Cartesian coordinates. Let us consider a semi-infinite domain. The non-dimensional equations are

$$\frac{\partial \rho}{\partial t} = n - \gamma\rho, \tag{2.14}$$

$$\frac{\partial n}{\partial t} = -\frac{\partial n}{\partial x} + \sigma(n, \rho), \tag{2.15}$$

If we suppose $\sigma(n, \rho) = n$ then the equation (2.15) is a hyperbolic equation and can be solved using the method of characteristics. Let x and t be function of a parameter τ, i.e., $x = x(\tau), t = t(\tau)$. Then the characteristic equations are

$$\frac{\partial t}{\partial \tau} = 1, \tag{2.16}$$

$$\frac{\partial x}{\partial \tau} = 1, \tag{2.17}$$

and the partial differential equation (2.15) becomes the ODE

$$\frac{dn}{d\tau} = n. \tag{2.18}$$

From equation (2.16) and (2.17) we find that the characteristics are straight parallel lines (Fig. 2.5). The red line in Fig. 2.5 separates the regions determined by the initial and boundary conditions.

Furthermore, some of our work depends on reaction diffusion equations, then we will focus on it in this section. The reaction-diffusion equation is a mathematical model that has been used to describe how the concentration of one or more substances disperses through space under the influence of two processes: local

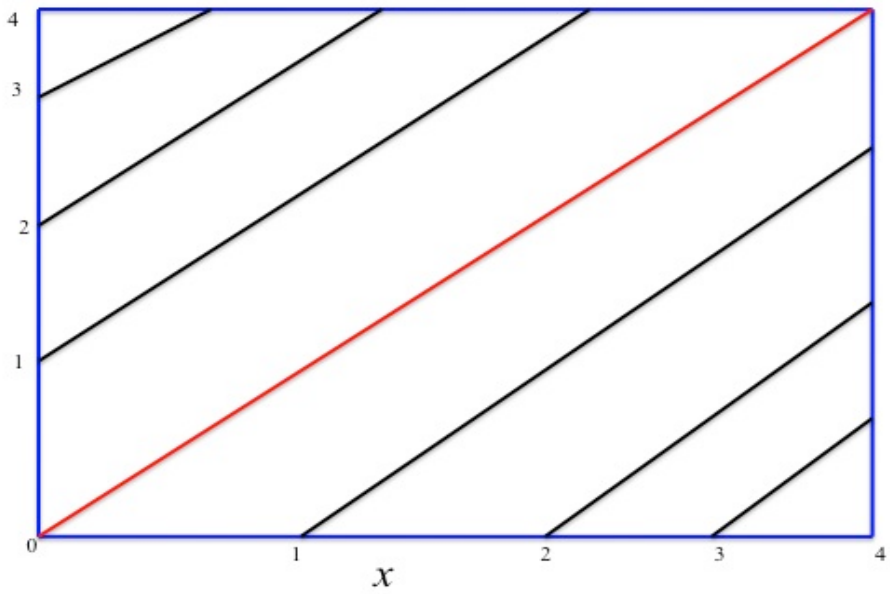

Figure 2.5: Characteristics of equation (2.15)

reactions in which the substances interact with each other, and diffusion which causes the substances to spread out in space.

Guided by (Edelstein-Kehet, 2005; Murray, 2002), in order to derive the reaction-diffusion equation, we first consider *Fickian* diffusion which says that the flux, J, of material, which can be cells, amount of chemical, number of animals and so on, is proportional to the gradient of the concentration of the material. That is, in one dimension

$$J \propto -\frac{\partial c}{\partial x} \quad \Longrightarrow \quad J = -D\frac{\partial c}{\partial x} \tag{2.19}$$

where $c(x,t)$ is the concentration of the species and D is its diffusivity. The minus sign simply indicates that diffusion transports matter from a high to a low concentration with the magnitude dependent on the difference.

We now write a general conservation equation, which says that the rate of change of the amount of material in a region is equal to the rate of flow across the boundary plus any that is created within the boundary.

If the region is $x_o < x < x_1$ and no material is created, then we have

$$\frac{\partial}{\partial t}\int_{x_o}^{x_1} c(x,t)dx = J(x_o,t) - J(x_1,t).$$

If we take $x_1 = x_o + \Delta x$, take the limit as $\Delta x \to 0$ and use (2.19) we get the classical diffusion equation in one dimension, namely,

$$\frac{\partial c}{\partial t} = -\frac{\partial J}{\partial x} = \frac{\partial D(\frac{\partial c}{\partial x})}{\partial x}, \tag{2.20}$$

which, if D is constant, becomes

$$\frac{\partial c}{\partial t} = D\frac{\partial^2 c}{\partial x^2}, \tag{2.21}$$

often referred to as the heat equation. We now consider diffusion in three space dimensions. Let S be an arbitrary surface enclosing a volume V. The general conservation equation says that the rate of change of the amount of material in V is equal to the rate of flow of material across S into$V$ plus the material created in V. Thus

$$\frac{\partial}{\partial t}\int_V c(x,t)dv = -\int_S J \cdot ds + \int_V f dv, \tag{2.22}$$

where J is the flux of material and f, which represents the source of material, may be a function of c, x and t. Applying the divergence theorem to the surface integral and assuming $c(x,t)$ is continuous, (2.22) becomes

$$\int_V [\frac{\partial c}{\partial t} + \nabla \cdot J - f(c,x,t)]dv = 0. \tag{2.23}$$

Since the volume V is arbitrary the integrand must be zero and so the conservation

equation for c is given by

$$\frac{\partial c}{\partial t} = -\nabla \cdot J + f(c, x, t). \tag{2.24}$$

This equation holds for a general flux transport J. If, for example, we choose the transport process to be classical diffusion, then

$$J = -D\nabla c, \tag{2.25}$$

and (2.24) becomes

$$\frac{\partial c}{\partial t} = \nabla(D\nabla c) + f(c, x, t), \tag{2.26}$$

where D may be a function of x and c. Situations where D is space-dependent are arising in more and more modelling situations of biomedical importance, from diffusion of genetically engineered organisms in heterogeneous environments to the effect of white and grey matter in the growth and spread of brain tumours, for additional details see (Swanson et al., 2000, 2002a,b). The source term f in an ecological context, for example, could represent the birth and death process and c the population density.

If we further generalise (2.26) to the situation in which there are, for example, several interacting species or chemicals we then have a vector $c_i(x, t), i = 1, ..., m$ of densities or concentrations each diffusing with its own diffusion coefficient D_i and interacting according to the vector source term f. Then (2.26) becomes

$$\frac{\partial \underline{\mathbf{c}}}{\partial t} = \nabla \cdot (D\nabla \underline{c}) + \mathbf{f(c)}, \tag{2.27}$$

where now D is a matrix of the diffusivities which, if there is no cross diffusion among the species, is simply a diagonal matrix. In (2.27), $\nabla \underline{\mathbf{c}}$ is a second rank

tensor so $\nabla \cdot D\nabla \underline{\mathbf{c}}$ is a vector, see (Mehrer, 2007; Murray, 2002).

Cross-diffusion can arise in genuinely practical models, for examples see (Kuto and Yamada, 2004; Okubo and Levin, 2001; Ruan, 1996). Moreover, cross-diffusion systems can pose interesting mathematical problems particularly regarding their well-posedness. Equation 2.27 is referred to as a reaction-diffusion system.

2.6.3 Fisher's equation

We consider the following ODE model for population growth

$$u^{'}(t) = a(u(t))u(t), \quad u(t) = u_o \quad \text{at} \quad t = 0 \tag{2.28}$$

where $u(t)$ denotes the population size at time t, and $a(u)$ plays the role of the population dependent growth rate. The model asserts that the population changes at a rate that is proportional to the present population size. Moreover, if we suppose

$$a(u) = \alpha(1 - \frac{u(t)}{u_\infty}),$$

for constant positive parameters, α, u_∞, then the population grows when the population is smaller than the 'limiting value" u_∞ and the population size decreases if u exceeds this value. Thus the model predicts behaviour that is qualitatively consistent with the way we observe populations to behave. This autonomous differential equation has critical points at $u = 0$ and $u = u_\infty$ and it is easy to see that the critical point at zero is unstable while the other is a stable critical point. Then the population $u(t)$ will tend to the limiting value u_∞ as t tends to infinity, regardless of the initial population size. This equation is a special case

of the more general autonomous equation, $u^{'}(t) = F(u(t))$.

Now the partial differential equation

$$\frac{\partial u(x,t)}{\partial t} - \frac{\partial^2 u(x,t)}{\partial x^2} = F(u(t)) \quad x \in R^n, \quad t > 0, \tag{2.29}$$

can be viewed as an attempt to incorporate the mechanism of diffusion into the population model. We are going to discuss equations of this form in the case $n = 1$ where the equation can be written more generally as

$$\frac{\partial u(x,t)}{\partial t} - \frac{\partial^2 b(u(x,t))}{\partial x^2} = F(u(t)), \qquad b^{'}(u) > 0, \tag{2.30}$$

Equations of this form arise in a variety of biological applications and in modelling certain chemical reactions and are referred to as reaction diffusion equations.

To clear the reaction diffusion equation with positive constant parameters, D, α and u_∞:

$$\frac{\partial u(x,t)}{\partial t} - D\frac{\partial^2 u(x,t)}{\partial x^2} = \alpha u(x,t)(1 - \frac{u(x,t)}{u_\infty}). \tag{2.31}$$

This is know as **Fisher's equation** and it is usually viewed as a population growth model. The various parameters in the equation have the following dimensions

$$\begin{aligned} D &\quad \text{denotes diffusivity} \quad (L^2T^{-1}), \\ \alpha &\quad \text{denotes growth rate} \quad (T^{-1}), \\ u_\infty &\quad \text{denotes carrying capacity} \\ &\qquad \text{(number of individuals)}. \end{aligned}$$

To reduction to dimensionless form, it is often useful to rewrite the partial differential equation in terms of dimensionless variables. We define

$$\begin{aligned} \tau &= \alpha t \quad \text{time scaled to the growth rate} \\ z &= x\sqrt{\frac{\alpha}{D}} \quad \text{distance scaled to diffusion length} \\ v &= \frac{u(x,t)}{u_\infty} \quad \text{population scaled to carrying capacity} \end{aligned}$$

and then the equation becomes

$$\frac{\partial v(z,\tau)}{\partial \tau} - \frac{\partial^2 v(z,\tau)}{\partial z^2} = v(1-v). \tag{2.32}$$

Now, in order to investigate the existence of travelling wave solutions, we suppose $v(z,\tau) = V(z-c\tau)$ with $V(s)$ tending to constant values as s tends to plus or minus infinity. Then

$$-cV^{'}(s) - V^{''}(s) = V(s)(1-V(s)), \quad -\infty < s = z - c\tau < \infty. \tag{2.33}$$

This second order equation reduces to the following autonomous dynamical system

$$\begin{aligned} V^{'}(s) &= W(s), \\ W^{'}(s) &= -cW(s) - V(s)(1-V(s)), \end{aligned} \tag{2.34}$$

This system has critical points at $(0,0)$ and $(1,0)$. Since

$$J_{(V,W)} = \begin{bmatrix} 0 & 1 \\ 2V-1 & -c \end{bmatrix}$$

we can classify the critical points according to the eigenvalues of this matrix.

$$\text{at} \quad (0,0) \quad \lambda_{\pm} = \frac{1}{2}(-c \pm \sqrt{c^2 - 4})$$

a stable node if $c > 2$ and stable focus if $0 < c < 2$,

$$\text{at} \quad (1,0) \quad \lambda_{\pm} = \frac{1}{2}(-c \pm \sqrt{c^2 + 4}),$$

a saddle point for all values of c. In the case $0 < c < 2$, the origin is a stable focus and the orbits of the system are curves in the (V, W) - plane.

$$\left\{ \begin{array}{ll} V = V(s), & V_{(-\infty)} = V_o \\ W = W(s), & W_{(-\infty)} = W_o \end{array} \right\} \quad -\infty < s < \infty$$

with $(V(s), W(s)) \to (0,0)$ as $s \to \infty$. Since the origin is a focus, the orbits are such that V and W assume both positive and negative values as the curve spirals toward the origin. Negative values for V are not physically meaningful in the population interpretation of $V = u$. Therefore, we conclude that there are no relevant travelling wave solutions for wave speeds between zero and 2, see Figs. 2.6. In the case $c > 2$ the origin is a stable node and the orbits in the fourth quadrant that are attracted to the origin approach the node with V positive and W negative. Then these are physically relevant orbits. If there exists an orbit with $V_o = 1, W_o = 0$ that is attracted to the origin, then this orbit, which is in fact a heteroclinic orbit joining the two critical points, corresponds to a travelling wave solution to the Fisher's equation. The component $V = V(s)$ of the heteroclinic orbit is a smooth function such that $V'(s) = W(s) < 0$ for all s. In addition, $V(s)$ tends to 1 as s tends to minus infinity and $V(s)$ tends to 0 as s tends to plus infinity so that 0 and 1 are the state values ahead of and behind the wave, respectively. The monotone decreasing function V is the wave form that is

propagated at speed $c > 2.$, see Figs. 2.7.

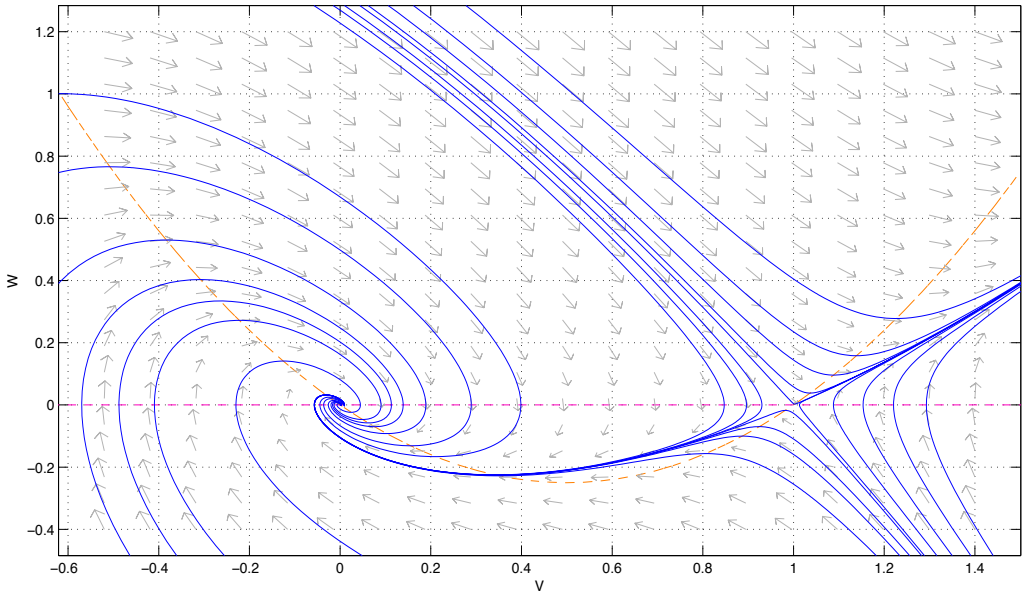

Figure 2.6: The (V, W)-plane: Solution to the system (2.34), note that a trajectories connects the saddle point $(1, 0)$ to the stable spiral $(0, 0)$ for $c = 0.5$. The dashed lines represents null-clines. The arrows denote the direction of the vector field.Solutions are produced using MATLAB pplane7.

2.6.4 Proof of Existence of the Travelling Wave solution

To verify that this heteroclinic orbit actually exists, consider the following Fig2.8 in the (V, W) - plane. Let the triangular region,OAB, where the stable node is located at point O, the saddle point is at A, and OB is the line $W + bV = 0$ for some $b > 0$ to be carefully chosen later. The parabola $W = \frac{1}{c}V(1 - V)$ is the curve along which $W^{'} = 0$ and $V^{'} = W < 0$. In addition,

$$W^{'} < 0 \text{ and } V^{'} = 0 \text{ along the line OA,}$$

$$W^{'} > 0 \text{ and } V^{'} = 0 \text{ along the line AB.}$$

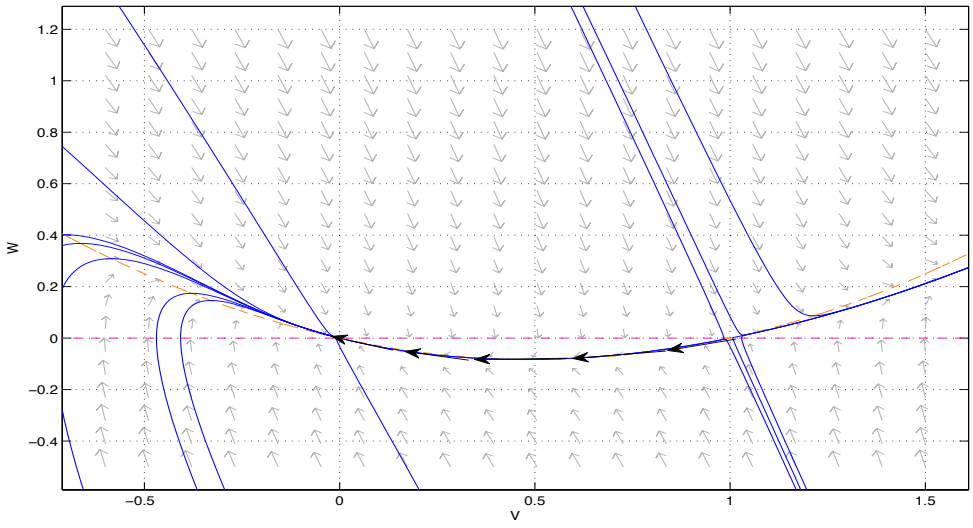

Figure 2.7: The (V, W)-plane: Solution to the system (2.34), note that a trajectories connects the point $(1, 0)$ to the point $(0, 0)$ for $c = 3$. The dashed lines represents null-clines. The black arrows are the profile of the corresponding travelling wave. Solutions are produced using MATLAB pplane7.

Then trajectories that are inside OAB do not leave this region (in the forward direction) through OA or AB. Now consider the region in the neighbourhood of point A.

If, by letting s tend to $-\infty$, we trace backward along an orbit which cuts the arc PQ near the point P, we see that such an arc must pass out of OAB above the point A. On the other hand, tracing backward along an orbit which cuts the arc PQ near the point Q, we see that such an arc must pass out of OAB below the point A. It follows that there exists an orbit which passes through the point A as s tends to $-\infty$, see Fig. 2.9 taken from DuChateau and Zachmann (1989)

We let the line OB, whose equation is $W + bV = 0$ for some positive b. If a trajectory crosses OB from right to left at $s = s_o$ then the expression $W(s) + bV(s) = 0$ decreases from a positive value when $s < s_o$ on the right of OB to a negative value when $s > s_o$ on the left side of OB. Then in order to have a

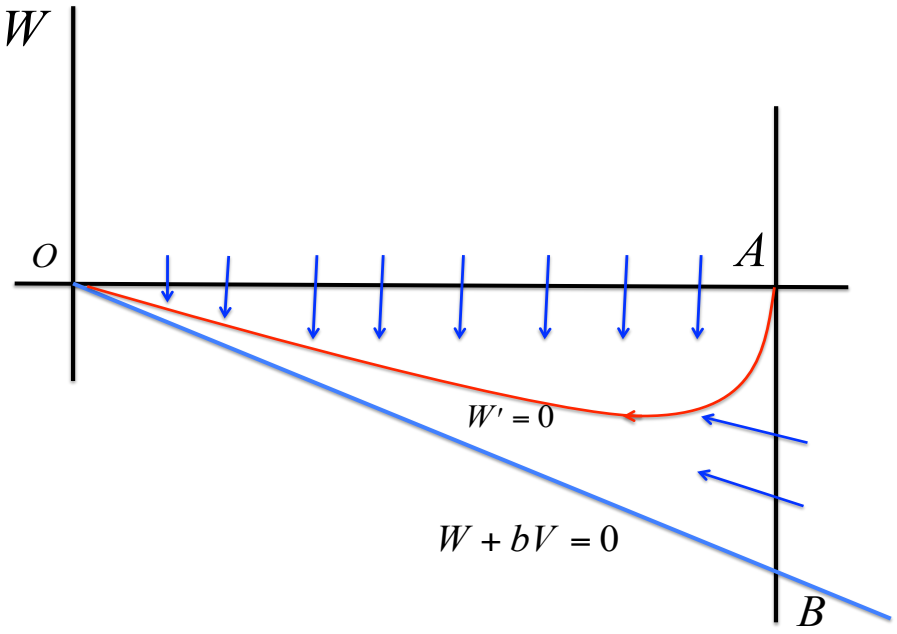

Figure 2.8: V positive and W negative near stable node, see DuChateau and Zachmann (1989)

trajectory exit the triangle OAB through OB at $(V(s_o), W(s_o))$, we must have

$$W^{'}(s_o) + bV^{'}(s_o) < 0 \quad \text{and} \quad W(s_o) + bV(s_o) = 0.$$

On the other hand, the equations of the dynamical system (2.34) imply,

$$\begin{aligned} W^{'}(s) + bV^{'}(s) &= -cW(s) - V(s)(1 - V(s)) + bW(s) \\ &= (b - c)W(s) - V(s)(1 - V(s)). \end{aligned}$$

In particular, along OB

$$\begin{aligned} W^{'}(s_o) + bV^{'}(s_o) &= (b - c)(-bV(s_o)) - V(s_o)(1 - V(s_o)) \\ &= V(s_o)[-b(b - c) - 1 + V(s_o)], \end{aligned}$$

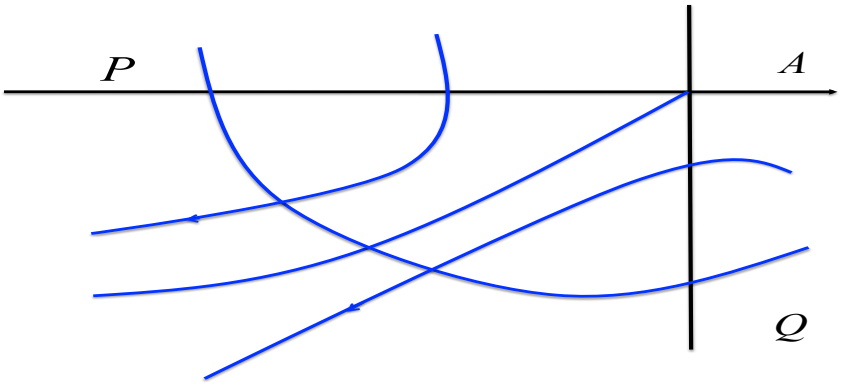

Figure 2.9: V positive and W negative near stable node, see DuChateau and Zachmann (1989)

and for $b = c/2 > 0$

$$W^{'}(s_o) + bV^{'}(s_o) \quad = V(s_o)[\tfrac{c^2}{4} - 1 + V(s_o)] > 0 \quad if \quad c^2 > 4.$$

Then for $c^2 > 4$, no trajectory can exit OAB through OB. Then forward orbits do not exit through any of the sides of the triangle and we say the triangle OAB is a trapping region for the dynamical system. It follows that the trajectory that tends to A as s tends to minus infinity must also tend to O as s tends to plus infinity. This is a consequence of the fact that any triangle $OA^{'}B^{'}$ that is similar to OAB is also a trapping region (i.e., it does not permit orbits to exit through any of the sides) and as $A^{'}$, $B^{'}$ tend toward O, the orbits in the triangle are forced toward O. This proves the existence of the orbit joining the saddle at A to the stable node at O. Then the component $V(s)$ satisfies (2.33) and the conditions $V(s) \to 1$ as $s \to -\infty$, $V(s) \to 0$ as $s \to \infty$. and $v(x,t) = V(x - ct)$ is a TWS for the equation (2.32) as long as $c^2 > 4$. i.e., there is a minimum speed but no maximum.

2.7 Convection - Diffusion Equation

The convection-diffusion equation is a parabolic partial differential equation, which describes physical phenomena where particles or energy (or other physical quantities) are transferred inside a physical system due to two processes: diffusion and convection. In its simplest form (when the diffusion coefficient and the convection velocity are constant and there are no sources or sinks) the equation takes the form: (Bejan, 2004; Bird, 1960; Probstein, 1994).

$$\frac{\partial n}{\partial t} = D_n \nabla^2 n - \overrightarrow{v} \cdot \nabla n.$$

The two terms on the right hand side represent different physical processes: the first corresponds to normal diffusion while the second describes convection or advection, which is why the equation is also known as the advection - diffusion equation. Moreover, n is the variable of interest, the constant D_n is the diffusivity for species or heat transfer, and $\overrightarrow{v}$ is the velocity of the convecting process.
Next chapters, we will illustrate many cases for the convection-diffusion equation. In Chapter 3 and Chapter 4 we will discuss and explain convection - diffusion equation minutely for our modelling. Now let us consider an extended model:

$$\begin{aligned} \frac{\partial \rho}{\partial t} &= |J| - d(\rho), \\ \frac{\partial n}{\partial t} &= -\nabla J + \sigma(\rho, n), \end{aligned} \tag{2.35}$$

where $\rho(x,t)$, $n(x,t)$, $d(\rho)$ and $\sigma(\rho,n)$ will be explicitly defined next Chapter. In this model, we assume that flux J takes the form:

$$J = \underbrace{-D_n \frac{\partial n}{\partial x}}_{\text{diffusion}} + \underbrace{nv}_{\text{convection}}. \tag{2.36}$$

substituting (2.36) in (2.35) we get

$$\begin{aligned}\frac{\partial \rho}{\partial t} &= |-D_n\frac{\partial n}{\partial x}+nv|-d(\rho),\\ \frac{\partial n}{\partial t} &= -\frac{\partial}{\partial x}(-D_n\frac{\partial n}{\partial x}+nv)+\sigma(\rho,n),\end{aligned} \tag{2.37}$$

i.e.

$$\begin{aligned}\frac{\partial \rho}{\partial t} &= |-D_n\frac{\partial n}{\partial x}+nv|-d(\rho),\\ \frac{\partial n}{\partial t} &= D_n\frac{\partial^2 n}{\partial x^2}-\frac{\partial (nv)}{\partial x}+\sigma(\rho,n).\end{aligned} \tag{2.38}$$

We will discuss special cases. From (2.38), if we take $D_n = d = 0$ and $\sigma(\rho, n) = 0$, then we have the equations

$$\frac{\partial \rho}{\partial t} = nv, \tag{2.39a}$$

$$\frac{\partial n}{\partial t} = -\frac{\partial (nv)}{\partial x}, \tag{2.39b}$$

Then the solution for equation (2.39a) is

$$\rho(x,t) = \int vn(x,t)\,dt + f_1(x),$$

and the solution of (2.39b) is $n(x,t) = f_2(x-vt)$, therefore

$$\rho(x,t) \;\; = \;\; \int vf_2(x-vt)dt, + f_3(x),$$

Fig. 2.10(a), shows the profiles $\rho(x,t)$, $n(x,t)$, and the relation between v and wave speed is equal, see Fig. 2.10(b). In the next stage we assume that $d = 0$,

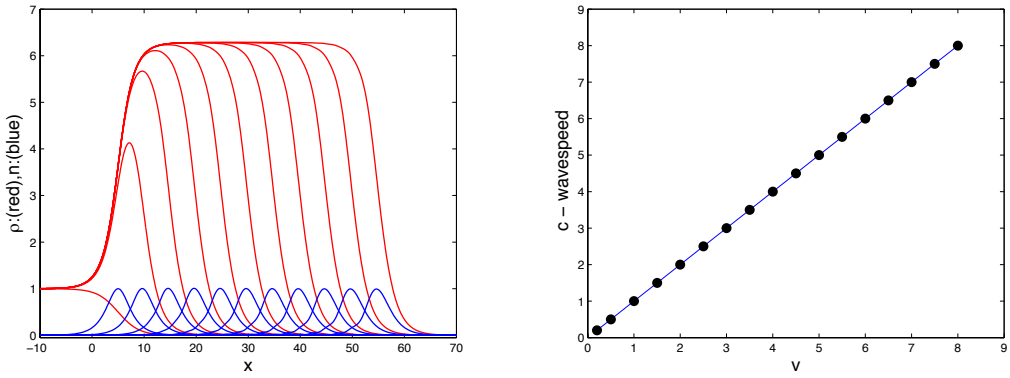

(a) (b)

Figure 2.10: The profiles for $n(x,t)$ (blue) and $\rho(x,t)$ (red) move from left to right with speed v. Here we have $v = 1$. The relationship between v and wave speed. Using pdepe code in MATLAB

$\sigma(\rho, n) = 0$, and $D_n \neq 0$, then system (2.35) becomes

$$\begin{aligned} \frac{\partial \rho}{\partial t} &= |-D_n \frac{\partial n}{\partial x} + nv|, \\ \frac{\partial n}{\partial t} &= D_n \frac{\partial^2 n}{\partial x^2} - \frac{\partial (nv)}{\partial x}. \end{aligned} \tag{2.40}$$

The method of separation of variables is a powerful tool with which to solve the following linear partial differential equation Jones and Sleeman (1983).

$$\frac{\partial n}{\partial t} = D_n \frac{\partial^2 n}{\partial x^2} - \frac{\partial (nv)}{\partial x}, \tag{2.41}$$

where $D_n = 1$. To begin with, we seek solution of Eq (2.41) in the form

$$n(x,t) = X(x)T(t).$$

Substitution of this in equation.(2.41) leads to the identity,

$$\frac{\partial n}{\partial t} = X\frac{dT}{dt}, \quad \frac{\partial n}{\partial x} = T\frac{dX}{dx} \quad \Rightarrow \quad \frac{\partial^2 n}{\partial x^2} = T\frac{d^2X}{dx^2},$$

therefore

$$\begin{aligned} X\frac{dT}{dt} &= T(\frac{d^2X}{dx^2} - \frac{dX}{dx}), \\ \frac{1}{T}\frac{dT}{dt} &= \frac{1}{X}(\frac{d^2X}{dx^2} - \frac{dX}{dx}), \end{aligned}$$

Now $\frac{1}{T}\frac{dT}{dt}$ is a function of t only, while $\frac{1}{X}(\frac{d^2X}{dx^2} - \frac{dX}{dx})$ is a function of x only. Consequently, the equation

$$\frac{1}{T}\frac{dT}{dt} = \frac{1}{X}(\frac{d^2X}{dx^2} - \frac{dX}{dx}),$$

must be equal to a constant, say λ. Thus X and T must satisfy the ordinary differential equations

$$\begin{aligned} \frac{dT}{dt} - \lambda T &= 0, \\ \frac{d^2X}{dx^2} - \frac{dX}{dx} - \lambda X &= 0. \end{aligned}$$

These have the general solutions

$$\begin{aligned} T(t) &= e^{\lambda t}, \\ X(x) &= (\frac{1 \pm\sqrt{1+4\lambda}}{2})x. \end{aligned}$$

Hence (2.41) has a general solution of the form

$$n(x,t) = A_{\pm}e^{(\frac{1\pm\sqrt{1+4\lambda}}{2})x+\lambda t}.$$

Fig. (2.11a, b and c), show the profiles $\rho(x,t)$, $n(x,t)$ when $v = D_n$, $v > D_n$ and $v < D_n$.

Fig. 2.11(d) show the wavespeed is increasing when the velocity v is increasing. The relation between v and wavespeed are equal $v = c$, where D_n fixed.

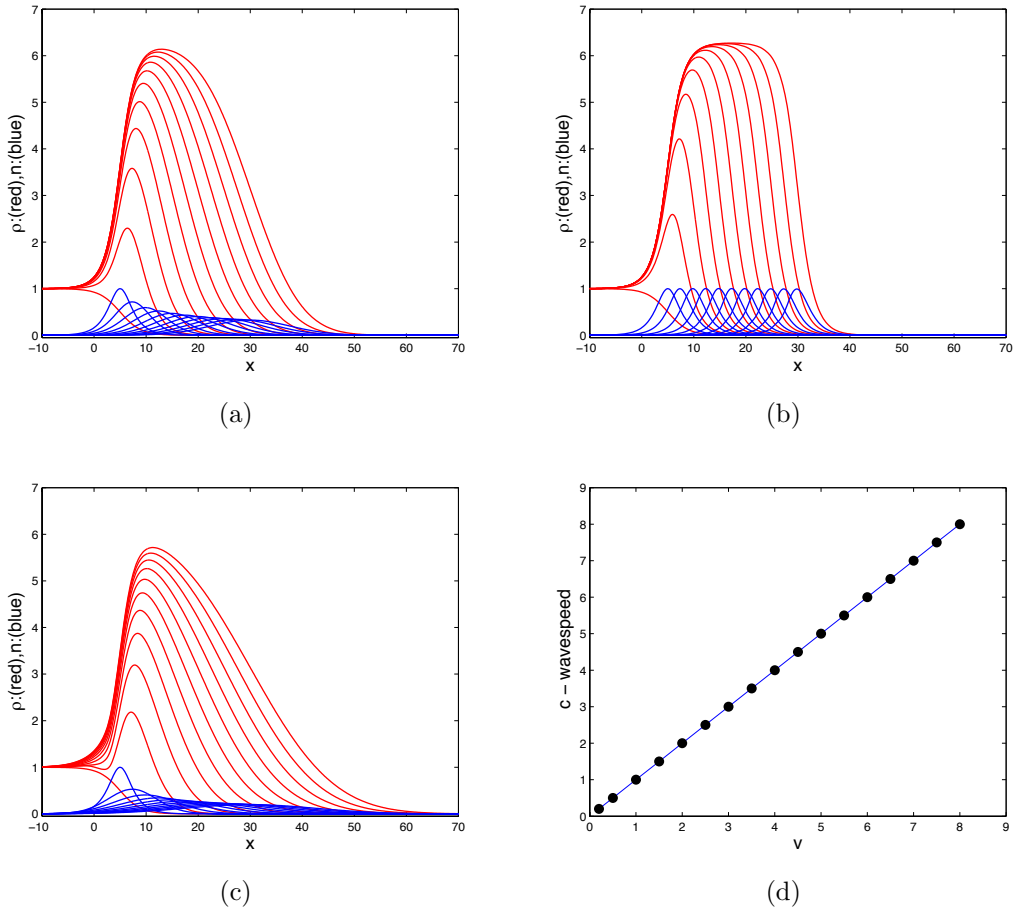

Figure 2.11: The profiles for $n(x,t)$ (blue) and $\rho(x,t)$ (red) move from left to right with speed v. Here we have (a) $v = D_n = 0.5$ (b) $v > D_n$, 0.5, 0.001 respectively, (c) $v < D_n, 0.5$, 1.5 respectively (d) The relationship between wavespeed c and v, $D_n = 0.01$. The speed c was computed using MATLAB by tracking the point $x(t)$ given by $\rho(x,t) = 1/2$.

In this these, we consider equations of the general form

$$\begin{aligned} \frac{\partial \rho}{\partial t} &= |J| - d(\rho, n), \\ \frac{\partial n}{\partial t} &= -\nabla \cdot J + \sigma(\rho, n), \end{aligned} \tag{2.42}$$

where ρ and n are continuos variables, d and $\sigma(\rho, n)$ are suitable smooth functions and J_n represents the flux and species n.

Typically, J_n contain both "diffusive" and "convective" terms, e.g.

$$J_n = D_n \frac{\partial n}{\partial x} + nv, \quad \text{in 1- D} \tag{2.43}$$

To study 2.42, we use a combination of the techniques discussed above, we study steady states, the associated kinetic problem, travelling wave solutions and we non- dimensionalisation techniques.

Chapter 3

Modelling The Propagation of Fungal Colonies

3.1 Basic Formulation

A mathematical description of growth and branching in fungi can be derived in terms of continuous variables such as densities of filaments and tips. The general concept of continuum modelling yields the following equations of fungal growth in which a balance is kept for the accumulation of hyphal filaments and their tips.

Hyphae are immobile. They are created only through the motion of tips-essentially the trail left behind tips as they moves. The rate of local length accumulation depends on the number of tips present as well as on their rate of motion. This suggests the following equation:

$$\frac{\partial \rho}{\partial t} = nv - d. \tag{3.1}$$

Here, the variables are as follows: $\rho = \rho(x,t)$ - hyphal density in unit of filament length per unit area; $n = n(x,t)$ - tip density (number per unit area); v - tips extension rate; $d = d(\rho)$ - hyphal death rate. Tips do undergo motion so that the flux of tips enters into the equation for tip densities. Assuming that tip growth is a directed motion, in one dimension this equation would take the form Edelstein and Segel (1982);

$$\frac{\partial n}{\partial t} = -\frac{\partial}{\partial x}(nv) + \sigma(\rho, n), \tag{3.2}$$

where $\sigma = \sigma(\rho, n)$ - net creation of tips. From the basic tip - growth mechanism: a number of tips n growing at the rate v (in length per unit time) gives rise to a hyphal accumulation rate of nv (in hyphal length per unit time). (Edelstein, 1982) discussed and analysed the above model when $d(\rho, n) = 0$ for a variety of biologically relevant functions $\sigma(\rho, n)$. More generally, we can describe hyphal growth by the system below:

$$\begin{aligned} \frac{\partial \rho}{\partial t} &= J_n - d(\rho), \\ \frac{\partial n}{\partial t} &= -\frac{\partial (J_n)}{\partial x} + \sigma(\rho, n). \end{aligned} \tag{3.3}$$

This second balance equation for tip densities accommodates the fact that tip move (with flux $J_n = nv$) and are moreover created by branching or eliminated by anastomosis (Segel, 1981).

The ratio of hyphal length per tips is called the hyphal growth unit (Caldwell and Trinci, 1973); (Bull and Trinc, 1977). This unit represents the average length of hypha committed to supporting a single tip.

3.2 Mathematical Study of Branching Phenotypes

The two terms $\sigma(\rho, n)$ and $d(\rho, n)$ in system (3.3) have as yet to be specified. If hyphal death does occur, a simple way to incorporate it would be to setting

$$d(n, \rho) = \gamma_1 \rho^k,$$

where k is some positive number and γ_1 is the rate constant for hyphal autolysis It is interesting to point out that autolysis of hyphae is known to occur in certain fungi (eg. *Sclerotium rolfisii*) (Edelstein, 1982).

Table 3.1: Types of net creation of tips

$\sigma(\rho, n)$	Tip production / loss	Symbol	Parameters description
$\alpha_1 n$	Dichotomous branching	Y	α_1 is the number of tips produced per tip per unit time
$\alpha_2 \rho$	Lateral branching	F	α_2 is the number of branches produced per unit length hypha per unit time
$-\alpha_3 n$	Tip loss	T	α_3 is the loss rate of tips (constant for tip death)
$-\beta_1 n^2$	Tip - tip anastomosis	W	β_1 is the rate of tip reconnections per unit time
$-\beta_2 n\rho$	Tip - hypha anastomosis	H	β_2 is the rate of tip reconnections per unit length hypha per unit time
$-\beta_3 \rho^2$	Tip - death due to overcrowding	X	β_3 is the rate at which overcrowding density limitation) eliminates branching

The choice of term is discussed in (Edelstein, 1982) and are self explanatory, appart from the last X term. Here tip death due to overcrowding is modelled by the term $-\beta_3 \rho^2$.

3.3 Tip Creation

Table 3.1 illustrates the possible forms for $\sigma(\rho, n)$, differentiates tip production or loss and parameters description ($\alpha_{1,2,3}$ and $\beta_{1,2,3}$).

3.3.1 Cases of net creation of tips

Defining σ_{br} = branching rate (creation of tips per unit time per unit area or per unit length), σ_{mort} = loss rate (elimination of tips per unit time per unit area or per unit length).
The term $\sigma(\rho, n)$ is actually a difference of two terms:

$$\sigma(\rho, n) = \sigma_{br} - \sigma_{mort},$$

Combining a single branching type with a single tip-degrading influence can yield six distinct "species" of fungi. Of these, four apply somewhat more broadly to fungi in which true anastomosis is absent. These are,

$$\sigma = \alpha_2\rho - \beta_2 n\rho, \tag{3.4a}$$

$$\sigma = \alpha_2\rho - \beta_3\rho^2, \tag{3.4b}$$

$$\sigma = \alpha_1 n - \beta_1 n^2, \tag{3.4c}$$

$$\sigma = \alpha_1 n - \beta_2 n\rho. \tag{3.4d}$$

For ease of notation in discussing these types, shorthand symbols will be used as follows: F for lateral branching; Y for dichotomous branching; H for tip-hyphae anastomosis; W for tip-tip anastomosis; T for tip death; X represents tip elimination by hyphal toxins (tip - death due to overcrowding); D for hyphal death. In theory, a combination of different branching types could be expressed

Table 3.2: Main phenotypes considered

Symbol	Biological Type
FHD	Lateral branches tip-hyphae anastomoses with hyphal death
FXD	Lateral branches with density limitation with hyphal death
YWD	Dichotomous branches, tip-tip anastomoses with hyphal death
YHD	Dichotomous branches, tip-hyphae anastomoses with hyphal death

during phases of growth of a particular species of fungi.

Table 3.2 illustrates different types of branching.

3.4 Hyphal Death

With $d(\rho, n) = 0$, (Edelstein, 1982) studied each of these phenotypes. In the next sections, we will study and discuss the different cases for $d(\rho)$ and $\sigma(\rho, n)$. Therefore, firstly, let us take $d(\rho) = \gamma_1 \rho^k$, where k be defined before, then our system becomes

$$\begin{aligned} \frac{\partial \rho}{\partial t} &= nv - \gamma_1 \rho^k, \\ \frac{\partial n}{\partial t} &= -\frac{\partial (nv)}{\partial x} + \sigma(\rho, n) \end{aligned} \tag{3.5}$$

where, $\sigma(\rho, n) = \alpha_1 n - \alpha_3 n + \alpha_2 \rho - \beta_1 n^2 - \beta_2 n\rho - \beta_3 \rho^2$.

3.4.1 Non-dimensionalisation

Incorporating all tip-hyphae interactions into system (3.5) results in the system below

$$\begin{aligned}\frac{\partial \rho}{\partial t} &= nv - \gamma_1 \rho^k, \\ \frac{\partial n}{\partial t} &= -\frac{\partial (nv)}{\partial x} + \alpha_1 n - \alpha_3 n + \alpha_2 \rho - \beta_1 n^2 - \beta_2 n\rho - \beta_3 \rho^2.\end{aligned} \tag{3.6}$$

To facilitate the analysis of this system and to assist in its numerical integration, we non - dimensionalise the equations. To do so, we choose a reference time τ, a reference length scale $\bar{x}$ and reference scales for hyphal density, $\bar{\rho}$, and tip density, $\bar{n}$. Setting

$$\rho^* = \frac{\rho}{\bar{\rho}}, \quad n^* = \frac{n}{\bar{n}}, \quad t^* = \frac{t}{\tau}, \quad and, \quad x^* = \frac{x}{\bar{x}}, \tag{3.7}$$

and substituting into (3.6) yields

$$\begin{aligned}\frac{\partial \rho^*}{\partial t^*} &= (\frac{\tau v \bar{n}}{\bar{\rho}}) n^* - (\frac{\gamma_1 \tau \bar{\rho}^k}{\bar{\rho}}) \rho^{*k}, \\ \frac{\partial n^*}{\partial t^*} &= -(\frac{\tau v \bar{n}}{\bar{x}\bar{n}}) \frac{\partial n^*}{\partial x^*} + (\frac{\alpha_1 \tau \bar{n}}{\bar{n}}) n^* - (\frac{\alpha_3 \tau \bar{n}}{\bar{n}}) n^* + (\frac{\alpha_2 \tau \bar{\rho}}{\bar{n}}) \rho^* \\ &\quad - (\frac{\beta_1 \tau \bar{n}^2}{\bar{n}}) n^{*2} - (\frac{\beta_2 \tau \bar{\rho} \bar{n}}{\bar{n}}) n^* \rho^* - (\frac{\beta_3 \tau \bar{\rho^2}}{\bar{n}}) \rho^{*2}.\end{aligned} \tag{3.8}$$

Now, setting $\bar{x} = \tau v$ and $\bar{\rho}/\bar{n} = \bar{x}$, (3.8) becomes

$$\begin{aligned}\frac{\partial \rho^*}{\partial t^*} &= (\frac{\tau v}{\tau v}) n^* - \hat{d} \rho^{*k}, \\ \frac{\partial n^*}{\partial t^*} &= -(\frac{\bar{x}}{\bar{x}}) \frac{\partial n^*}{\partial x^*} + (\alpha_1 \tau) n^* - (\alpha_3 \tau) n^* + (\alpha_2 v \tau^2) \rho^* \\ &\quad - (\beta_1 \tau \bar{n}) n^{*2} - (\beta_2 \tau^2 v \bar{n}) n^* \rho^* - (\beta_3 \tau^2 v \bar{\rho}) \rho^{*2},\end{aligned} \tag{3.9}$$

where $\tau = 1/\gamma_1$, $\hat{d} = (\gamma_1 \tau \bar{\rho}^k/\bar{\rho})$ and on cancelling get,

$$\begin{aligned}
\frac{\partial \rho^*}{\partial t^*} &= n^* - \hat{d}\rho^{*k}, \\
\frac{\partial n^*}{\partial t^*} &= -\frac{\partial n^*}{\partial x^*} + (\frac{\alpha_1}{\gamma_1})n^* - (\frac{\alpha_3}{\gamma_1})n^* + (\frac{\alpha_2 v}{{\gamma_1}^2})\rho^* \\
&\quad - (\frac{\beta_1 \bar{n}}{\gamma_1})n^{*2} - (\frac{\beta_2 v \bar{n}}{{\gamma_1}^2})n^*\rho^* - (\frac{\beta_3 v \bar{\rho}}{{\gamma_1}^2})\rho^{*2}.
\end{aligned} \tag{3.10}$$

The remaining choice of $\bar{n}$ or $\bar{\rho}$ depends on the exact branching kinetics chosen as will now be demonstrated for the phenotypes described in Table 3.2.

3.5 FHD: Lateral Branching Plus Tip - Hypha Anastomosis

In this case the model system is

$$\begin{aligned}
\frac{\partial \rho^*}{\partial t^*} &= n^* - \hat{d}\rho^{*k}, \\
\frac{\partial n^*}{\partial t^*} &= -\frac{\partial n^*}{\partial x^*} + (\frac{\alpha_2 v}{{\gamma_1}^2})\rho^* - (\frac{\beta_2 v \bar{n}}{{\gamma_1}^2})n^*\rho^*,
\end{aligned} \tag{3.11}$$

after dropping stars, hats and chosen $\bar{n} = \alpha_2/\beta_2$, the system (3.11) becomes

$$\begin{aligned}
\frac{\partial \rho}{\partial t} &= n - d\rho^k, \\
\frac{\partial n}{\partial t} &= -\frac{\partial n}{\partial x} + \alpha\rho(1-n),
\end{aligned} \tag{3.12}$$

where $\alpha = (\alpha_2 v/\gamma_1^2)$. The parameter α gives a measure of the number of tips produced per unit hyphae per unit time. Here d represents the rate of spontaneous hyphal death.

3.5.1 Stability of uniform solutions

To build a picture of solution structure, we first look for uniform steady states of system (3.12), and therefore seek solutions of the algebraic equations $n - d\rho^k = 0$, $\alpha\rho(1-n) = 0$. Clearly, there are two steady states: $(0,0)$ and $(\sqrt[k]{\frac{1}{d}}, 1)$. Following standard procedures, it follows that $(0,0)$ is a saddle point and $(\sqrt[k]{\frac{1}{d}}, 1)$ is a stable node of the kinetic problem associated with (3.12). Fig.3.1 illustrates the (ρ, n) - plane, showing trajectories from the saddle point $(0,0)$ to the stable point $(\sqrt[k]{\frac{1}{d}}, 1)$, for this associated ode system.

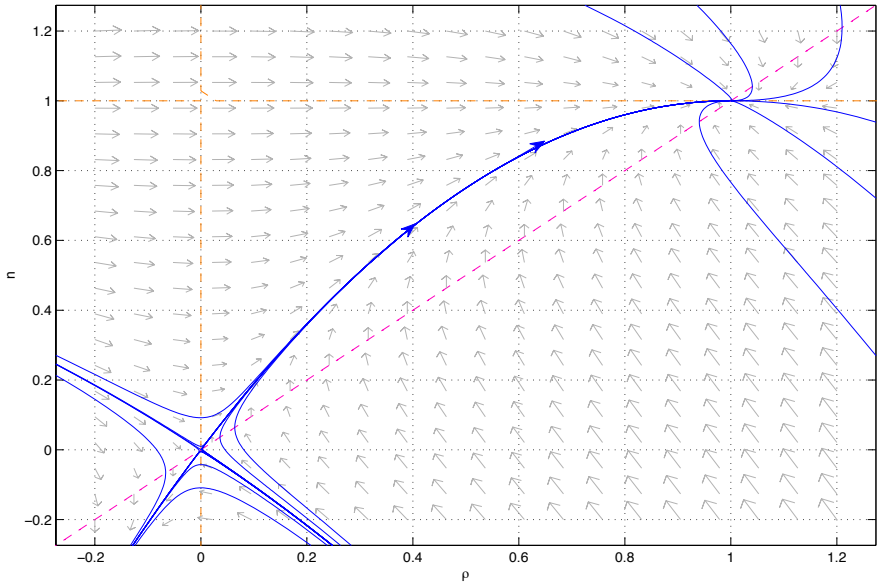

Figure 3.1: The (ρ, n)- plane for the ordinary differential equation $\rho' = n - d\rho^k$ and $n' = \alpha\rho(1-n)$, here $\alpha = 1$, $d = 1$ and $k = 1$. The solid blue line corresponds to the model a trajectory connects the saddle point $(0,0)$ to the stable node $(\sqrt[k]{\frac{1}{d}}, 1)$. The dashed lines corresponds the model to the null-cline. Solutions are produced using MATLAB pplane7.

Hence we seek travelling wave solutions to (3.12). A mathematical way of saying this that we seek solutions of the form

$$\begin{aligned} \rho(x,t) &= P(z), \\ n(x,t) &= N(z), \end{aligned} \tag{3.13}$$

where $z = x - ct$. Here $P(z)$, $N(z)$ represent density profiles, and c can be interpreted as the rate of propagation of the colony edge. For these to be biologically meaningful, we require P and N to be bounded, non negative functions of z. Then $\rho(x,t)$ and $n(x,t)$ are a travelling wave, and it moves at a constant speed c in the positive $x-$direction if c positive. Clearly if $(x - ct)$ is constant, so are $\rho(x,t)$ and $n(x,t)$. It also means the coordinate system moves with speed c. The wave speed c generally has to be determined. The dependent variable z is sometimes called the wave variable. When we look for travelling wave solutions of an equation or system of equations in x and t in the form (3.13), we have

$$\begin{aligned} \frac{\partial \rho}{\partial t} &= \frac{dP}{dz}.\frac{\partial z}{\partial t} = \frac{dP}{dz}(-c) = -c\frac{dP}{dz}, \\ \frac{\partial n}{\partial t} &= \frac{dN}{dz}.\frac{\partial z}{\partial t} = \frac{dN}{dz}(-c) = -c\frac{dN}{dz}, \\ \frac{\partial n}{\partial x} &= \frac{dN}{dz}.\frac{\partial z}{\partial x} = \frac{dN}{dz}(1) = \frac{dN}{dz}. \end{aligned} \tag{3.14}$$

Thus we can reduce the system (3.12) to a set of two ordinary differential equation:

$$\begin{aligned} \frac{dP}{dz} &= \frac{-1}{c}[N - dP^k], \\ \frac{dN}{dz} &= \frac{1}{(1-c)}[\alpha P(1-N)], \quad c \neq 1, -\infty < z < \infty, \end{aligned} \tag{3.15}$$

with $(P,N)(-\infty) = (\sqrt[k]{\frac{1}{d}}, 1)$ and $(P,N)(\infty) = (0,0)$. These can be analysed using phase plane techniques as described in a lucid exposition by (Odell, 1980). The steady states of system (3.15) are again $(0,0)$ and $(\sqrt[k]{\frac{1}{d}}, 1)$. However, the

stability of the steady states now depends on the value of c; it can be shown that $(0,0)$ is saddle point and $(\sqrt[k]{\frac{1}{d}},1)$ unstable node when $c>1$; $(0,0)$ is unstable spiral and $(\sqrt[k]{\frac{1}{d}},1)$ saddle point when $0<c<1$; $(0,0)$ is saddle point and $(\sqrt[k]{\frac{1}{d}},1)$ stable node when $c<0$ see Fig. (3.2a, b and c).

Fig. (3.2a) illustrate the type of phase plane solution to system 3.15 obtained under the assumption that $c>1$, it illustrates trajectories connecting in the (P,N) - plane, from the unstable node $(\sqrt[k]{\frac{1}{d}},1)$ to the saddle point $(0,0)$. This trajectory depends on value of c and α. c represent direction of this trajectory and value of α if it is small close to the line $P=N$(null cline) and it is moving away when the value of α increase. The results seems clear, the system have more than one equilibrium point $dP/dz=0$, $dN/dz=0$ is satisfy. $(0,0)$ and $(\sqrt[k]{\frac{1}{d}},1)$ are two intersection points for N and P null-clines.

Two equilibria of system (3.15) is thus ensured. Provided conditions: there is a trajectory of system (3.15) connecting these in the (P,N) plane and this trajectory remains in the positive (P,N) quadrant, are also met. The potential for a heteroclinic trajectory representing a bounded travelling wave solution is established.

The equilibrium in positive (P,N) quadrant is such that $N\neq 0$ and $P\neq 0$ implying that the wave level at $z\to-\infty$ is $P\neq 0$ and $N\neq 0$. There are many interesting implications of hyphal death. Tip density in the interior of the colony is maintained at a nonzero level. Biologically, this means that, while old hyphae are weeded out, new growth is continually taking place so that the density level is regulated in the older sections colony. Travelling waves are in fact waves of tips and branching of the leading tips and branching which grow ahead of colony.

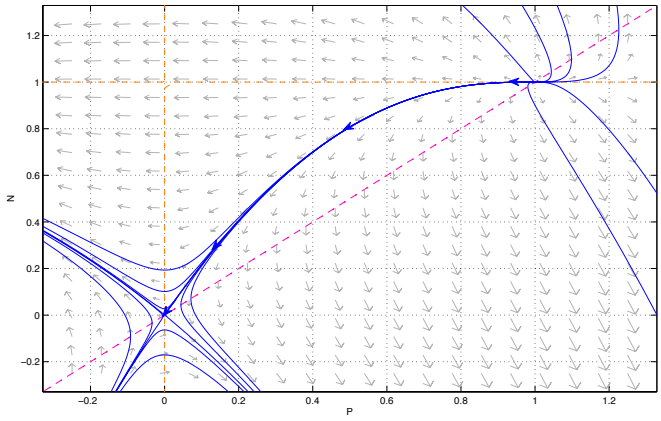

(a)

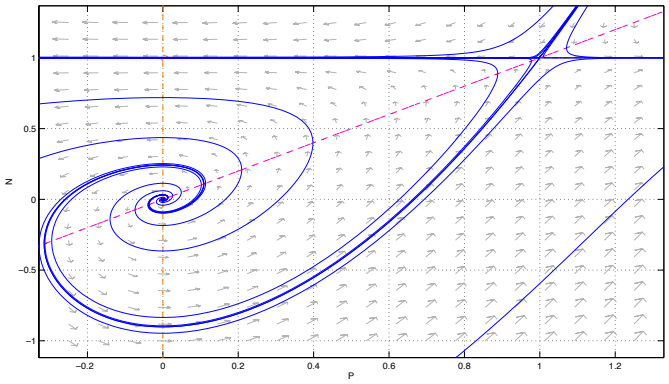

(b)

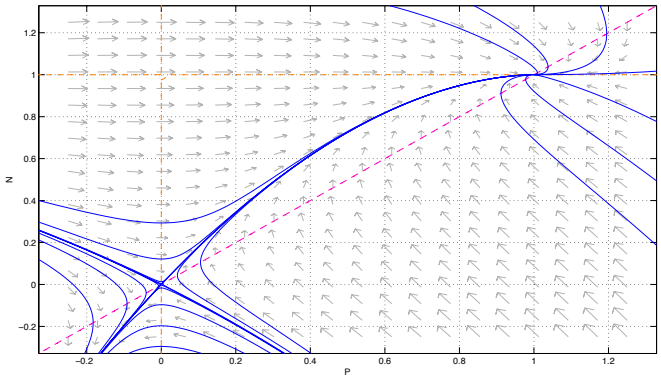

(c)

Figure 3.2: (a) The (P, N)-plane : note that a trajectories connects the unstable node $(\sqrt[k]{\frac{1}{d}}, 1)$ to the saddle point $(0, 0)$ for $c > 1$, $d = 1$ and $k = 1$. The trajectories moves away of the line $P = N$ when α is increased, where value of $\alpha = 2.5$ and $c = 2 > 0$. This exhibits a heteroclinic trajectory which remains in the positive (N, P) quadrant. (b) $c = 0.5$. (c) $c = -2$. Solutions are produced using MATLAB pplane7.

3.5.2 Numerical solution of the initial value problem

Using pdepe code in MATLAB, solution to the system (3.12) for $d = 8$, $k = 3$ and α values of 2 and 5, respectively, are illustrated in Fig. (3.3 a, b). From these figures, it is clear that the parameter α modulates the growth rate. We notes, the second propagates at a considerably faster rate than the first with respect to same normalized units $\bar{n}$. Fig. 3.4 illustrates that the slope for this straight line equals values of wave speed c, where t represent the horizontal coordinates and the position of x represented by vertical coordinates, where the straight line represented the line which connected between mid point for profile of tips or branching ($\rho(x,t) = 1/2$).

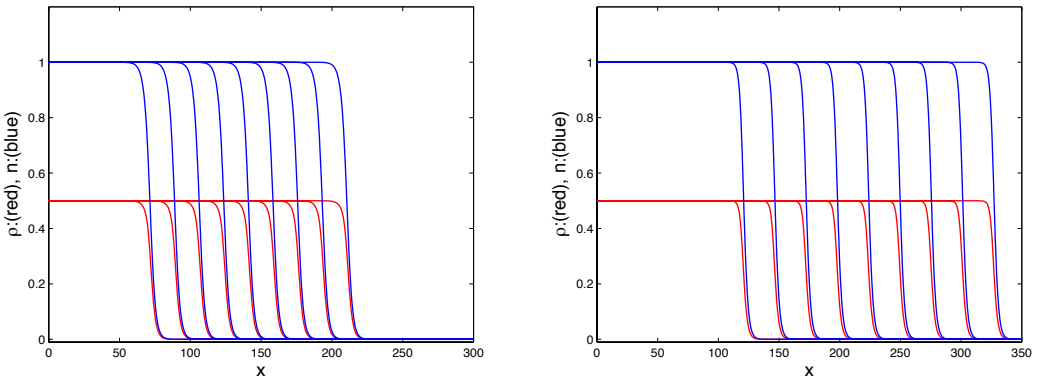

(a) (b)

Figure 3.3: Solution to the system (3.12) with the parameters $d = 8, k = 3$ and α taking value of (a) 2, (b) 5. (The wave speed $c = 3.441$ for $\alpha = 2$, $c = 5.105$ for, $\alpha = 5$). Units of density and distance are normalized units $\bar{n}$, ρ is red and n is blue. The time spacings: $10m$ where $m = 1, 2, ..., 9$.

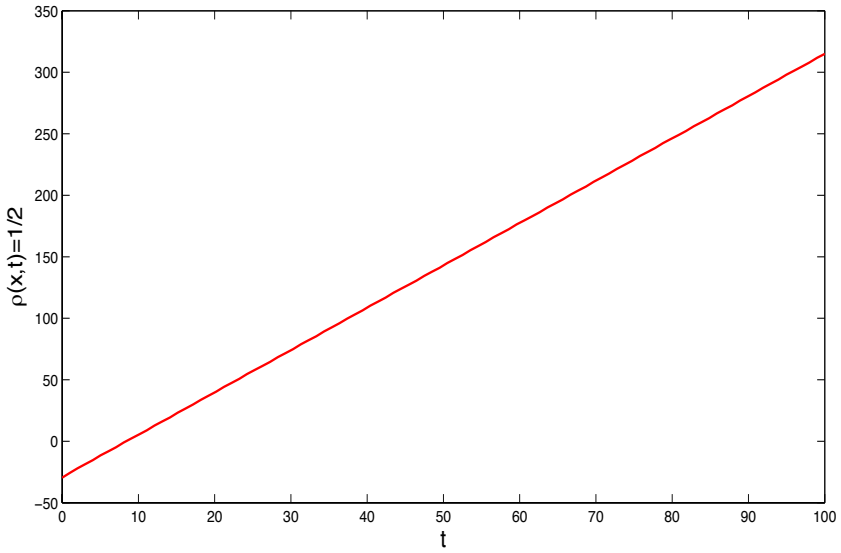

Figure 3.4: The straight line represented the relation between t and the position of x is $\rho(x,t) = 1/2$ at values of $\alpha = 2$, $d = 8$ and $k = 3$, (slope $= 3.441$).

Now, we plot relationship between c and α, see Fig. 3.5, that is clear the wave speed c is increasing when α an increase function of α. Since $\alpha = (\alpha_2 v/{\gamma_1}^2)$, therefore the growth rate is increasing with α_2 while keeping v and γ_1 are fixed, also the growth rate is increasing with v while keeping α_2 and γ_1 are fixed, while, the growth rate is decreasing with γ_1 increases while keeping α_2 and v are fixed. We note that changing the rate of anastomosis, β_2, cannot alter the colony growth rate, since the growth parameter α has no dependence on β_2. However, increasing β_2 would decrease the density levels accumulated in the interior. Fig. 3.5 illustrates the relation between waves speed c and α values.

Fig 3.6. illustrates the relation between waves speed c and d and it illustrates the relation between waves speed c and k.

Since the wave speed has dependence on α, d and k, the profile of branching rise with k increases while keeping α and d are fixed see Fig (3.7a, b). While, the profile of branching dropped with d increases while keeping α and k are fixed see Fig (3.8a, b).

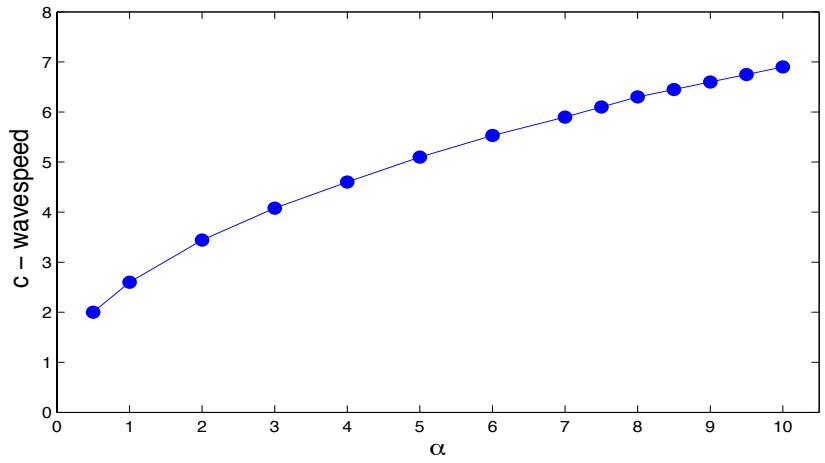

Figure 3.5: The relation between waves speed c and α values.

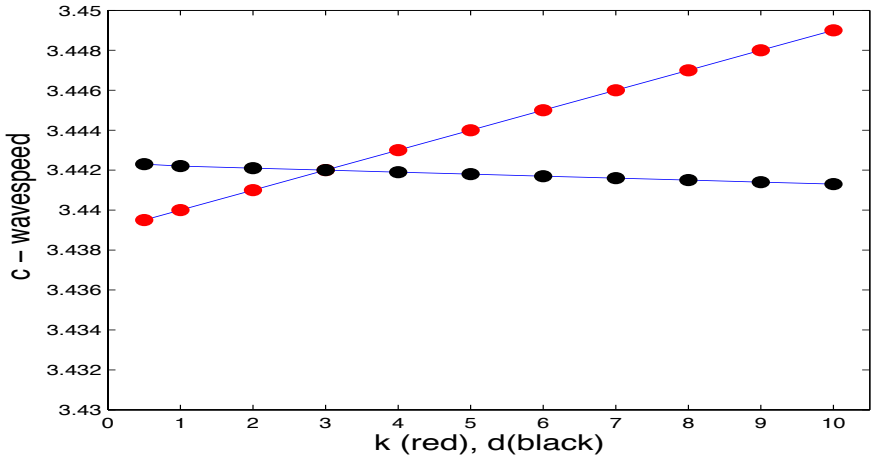

Figure 3.6: We note slightly alter the wave speed with k and d. The relation between waves speed c and k values while keeping $\alpha = 2$ and $d = 8$ fixed, here k is red dots, and the relation between waves speed c and d values while keeping $\alpha = 2$ and $k = 3$ fixed, here d is black dots.

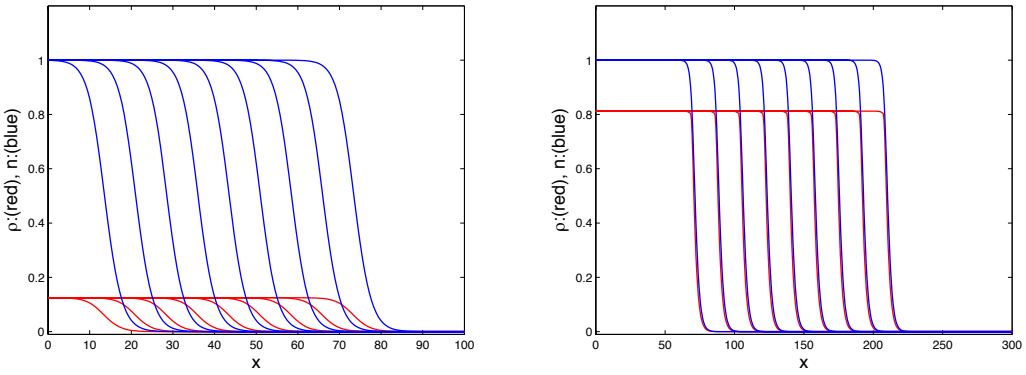

(a) (b)

Figure 3.7: Solution to the system (3.12) with the parameters $\alpha = 2, d = 8$ and k taking value of (a) 1 (b) 10. Units of density and distance are normalized as before. For rise with k increases while keeping α and d are fixed. ρ is (red) and n is (blue). The time spacings: $10m$ where $m = 1, 2, ..., 9$.

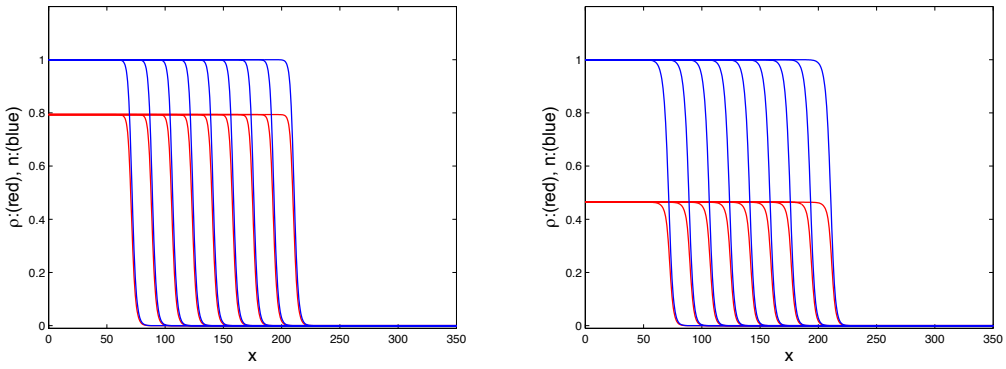

(a) (b)

Figure 3.8: Solution to the system (3.12) with the parameters $\alpha = 8, k = 3$ and d taking value of (a) 2 (b) 10. Units of density and distance are normalized as above. Branching profile (red) decays with d increases while keeping α and k are fixed. The time spacings: $10m$ where $m = 1, 2, ..., 9$.

In the next sections, we will study lateral branching with density limitation (FXD), dichotomous branching, the tip - tip anastomoses (YWD), and dichotomous branches, and tip-hyphae anastomoses (YHD).

3.6 FXD: Lateral Branching with Density Limitation

Many species of fungi produce small secondary structures such as sclerotia, coremia or conidia within their colonies. These produced in random, sporadic fashion or as a result of external cues. In some circumstances, a seemingly homogeneous growth environment will nevertheless result in synchronous formation of such structures so that an apparent spatial pattern results. The pattern is usually periodic along the radius of colony. Examples of these phenomenon are known to occur in *Sclerotium rolfsii* (Okon et al., 1972), *Penicillium claviform* (Watkinson, 1975) as well as *Nectria cinnabarina* (Bourret et al., 1969) although the differences in the details of patterning is wide. Conjectures as to the causes of these spatial patterns include endogenous biochemical oscillations (Winfree, 1980), the combined nutrient statutes of the colony and medium Humpherson-Jones and Cooke (1977), accumulation and utilization of reserve material (Watkinson, 1975), and the combination of enhanced translocation and inhibition of tip growth (Okon et al., 1972).

Since secondary structures are often produced by modifications of hyphae, variable hypha density may be a necessary precursor of some of these structures. Indeed in *Sclerotium rolfsii* radial density striations are often encountered, especially in conditions favouring synchronous formation of sclerotia (Hadar and

Edelstein, unpublished observations). It is of interest to determine whether density striations occur in any model fungi which combine the basic branching control mechanisms outlined in this in this thesis.

One example which apparently demonstrates density bands is fungal type FXD as we will now show. The model system in this case is

$$\begin{aligned} \frac{\partial \rho}{\partial t} &= nv - \gamma_1 \rho^k, \\ \frac{\partial n}{\partial t} &= -\frac{\partial nv}{\partial x} + \alpha_2 \rho - \beta_3 \rho^2. \end{aligned} \tag{3.16}$$

By the similar techniques to those of previous type; FHD. Here $\bar{\rho} = (\alpha_2/\beta_3)$ we get the form

$$\begin{aligned} \frac{\partial \rho}{\partial t} &= n - d\rho^k, \\ \frac{\partial n}{\partial t} &= -\frac{\partial n}{\partial x} + \alpha\rho(1-\rho), \end{aligned} \tag{3.17}$$

where $\alpha = (\alpha_2 v/\gamma_1^2)$ and d is as define before. The parameter α represent the rate of hyphal branching per unit length hypha per unit time. $\alpha(1-\rho)\rho$ thus represents the number of branches produced per unit time per unit length of hyphae.

3.6.1 Stability of uniform solutions

We now look for uniform steady states of system (3.17), and therefore seek solutions of the algebraic equations $n - d\rho^k = 0$, $\alpha\rho(1-\rho) = 0$. Clearly, there are two steady states: $(0,0)$ and $(1,d)$. Following standard procedures, it follows that $(0,0)$ is a saddle point and $(1,d)$ is a stable spiral if $(d < 2\sqrt{\alpha}/k)$ and stable node if $(d \geq 2\sqrt{\alpha}/k)$ of the kinetic problem associated with (3.17). Fig. 3.9 illustrates the (ρ, n) - plane, showing trajectories from the saddle point $(0,0)$ to the stable

spiral $(1, d)$, for this associated ode system.

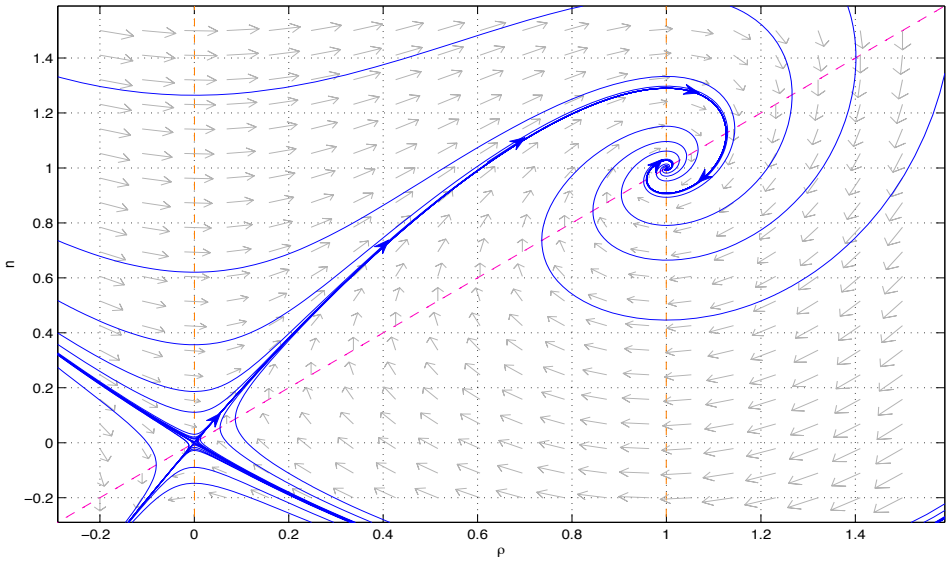

Figure 3.9: (ρ, n)- plane for ordinary differential equation $\rho' = n - d\rho^k$ and $n' = \alpha\rho(1-\rho)$, here $\alpha = 2.5, d = 1$ and $k = 1$. The solid blue line corresponds to the model a trajectory connects the saddle point $(0, 0)$ to the stable spiral $(1, 1)$. The dashed lines corresponds the model to the null-cline. Solutions are produced using MATLAB pplane7.

3.6.2 Travelling wave solution

As above, thus we can reduce the system (3.17) to a set of two ordinary differential equation:

$$\begin{aligned} \frac{dP}{dz} &= \frac{-1}{c}[N - dP^k], \\ \frac{dN}{dz} &= \frac{1}{(1-c)}[\alpha P(1-P)], \quad c \neq 1, -\infty < z < \infty. \end{aligned} \tag{3.18}$$

System (3.18) has two uniform steady states points $(0, 0)$ and $(1, d)$. Their stability depends on the value of c, $(0, 0)$ is saddle point and $(1, d)$ unstable spiral when $c > 1$. $(0, 0)$ is unstable spiral and $(1, 1)$ saddle point when $0 < c < 1$. $(0, 0)$ is saddle point and $(1, d)$ stable spiral when $c < 0$ see Fig. (3.10a, b and c).

We seek bounded, non-negative solution of system (3.18). Necessary condition for the existence of such solutions as above. Fig. (3.10 a) illustrates trajectories connecting these in the (P, N) - plane, from the unstable spiral $(1, d)$ to the saddle point $(0, 0)$. This trajectory depends on value of c and α. c represent direction of this trajectory and value of α if it is small close to the line $P = N$(null cline) and it is moving away when the value of α increase. The results seems clear, the system have more than one equilibrium point $dP/dz = 0$, $dN/dz = 0$ is satisfy. $(0, 0)$ and $(1, d)$ are two intersection points for N and P null-clines.

Two equilibria of system (3.18) is thus ensured. Provided conditions: there is a trajectory of system (3.18) connecting these in the (P, N) plane and this trajectory remains in the positive (P, N) quadrant, are also met. The potential for a heteroclinic trajectory representing a bounded travelling wave solution is established. There are many interesting implications. Tip density in the interior of the colony is maintained at a nonzero level. The equilibrium in positive (P, N) quadrant is such that $N \neq 0$ and $P \neq 0$ implying that the wave level at $z \to -\infty$ are $N \neq 0$ and $P \neq 0$.

The different c values gives different travelling wave profiles; uniform biomass and moving rings (fairy ring). Fig. (3.10(a)) illustrates the spiral heteroclinic trajectory which winds its way from $(1, d)$ unstable spiral to $(0, 0)$ saddle point when $c > 1$ in this version results in spatial variations of densities with respect to the wave variable z.

Fig. (3.10(b)) illustrates the spiral heteroclinic trajectory which winds its way from $(0, 0)$ unstable spiral to $(1, d)$ saddle point when $0 < c < 1$. While Fig. (3.10(c)) illustrates the spiral heteroclinic trajectory which winds its way from $(0, 0)$ saddle point to $(0, 0)$ stable spiral when $c < 0$.

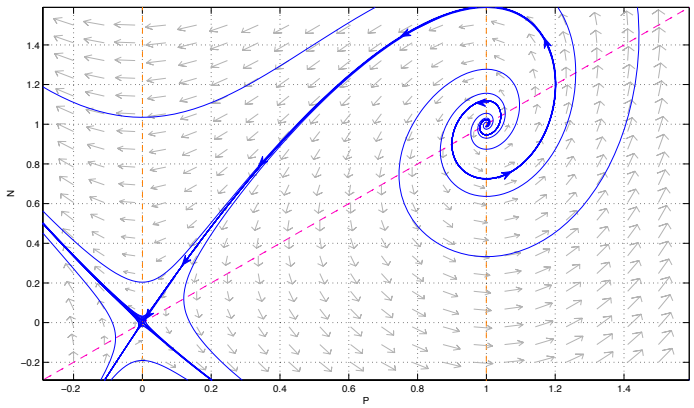

(a)

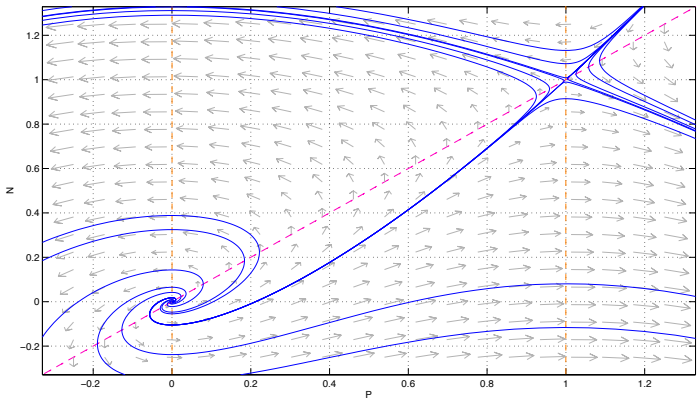

(b)

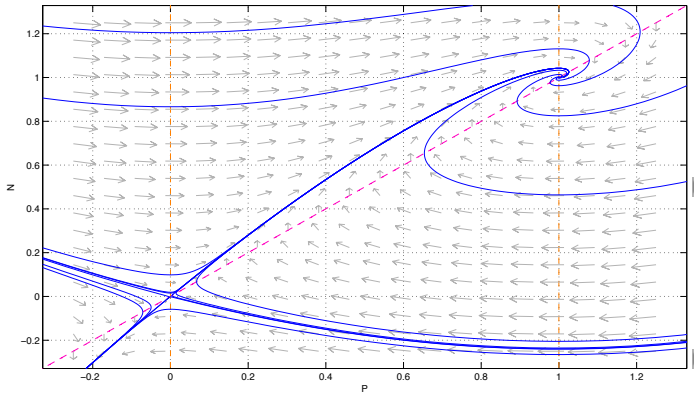

(c)

Figure 3.10: (a) (P, N)- plane : note that trajectory connects a from the unstable node $(1, 1)$ to the saddle point $(0, 0)$ for $c > 1$ and (a) $\alpha = 2.5, d = 1$ and $k = 1$. That is clear the trajectories are moving away of the line $P = N$ when values of α are increasing. A heteroclinic trajectory which remains in positive (P, N) quadrant. (b) $c = 0.5$. (c) $c = -2$. Solutions are produced using MATLAB pplane7.

3.6.3 Numerical solution of the initial value problem

Using pdepe code in MATLAB. Solution to the system (3.17) for $d = 1$, $k = 3$ and α values of 2 and 5, respectively, are illustrated in Fig. (3.11 a, b). This parameter α thus modulates the growth rate. Of these, the second propagates at a considerably faster rate than the first with respect to same normalized units.

As above, we can calculated wavespeed $c \approx slope$. Fig. 3.11(c), details the relationship between c and α, and it illustrates that c increases when α increases. Since $\alpha = (\alpha_2 v/{\gamma_1}^2)$, therefore the growth rate is increasing with α_2 while keeping v and γ_1 are fixed, the growth rate is increasing with v while keeping α_2 and γ_1 are fixed, while the growth rate is decreasing with γ_1 increases while keeping α_2 and v are fixed. This would make the colony grow more quickly out of the the hostile zone. Changing the rate of anastomosis, β_3, cannot alter the colony growth rate, since the growth parameter α has no dependence on β_3. Biological mean, new growth is continually taking place, while old hyphae are eradicated. We notes slightly alter the wave speed with k and d see Fig. 3.12 and Fig. 3.13 if a large value for imaginary part of the eigenvalues then the oscillation for profile of ρ and n are increasing and a small value for imaginary part of the eigenvalues then the slightly oscillation for profile of ρ and n or close to stable node.

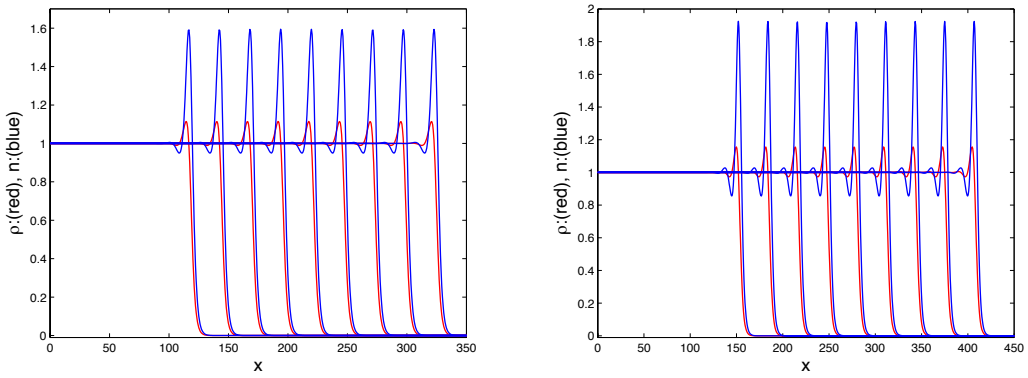

(a) (b)

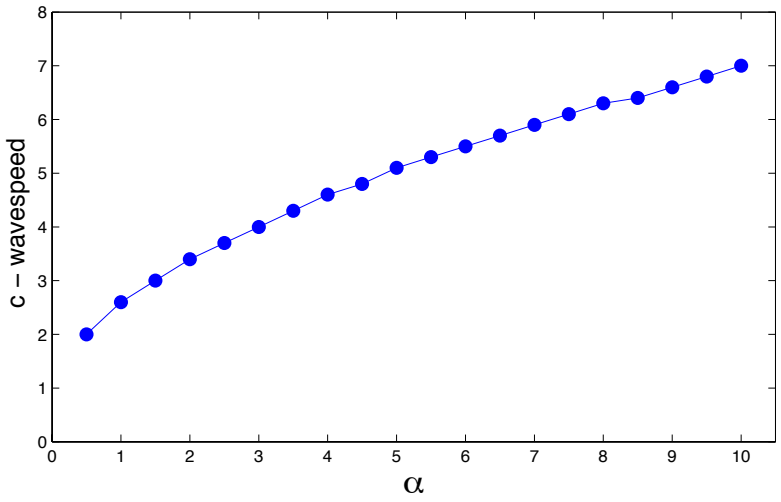

(c)

Figure 3.11: Solution to the system (3.17) with the parameters $d = 1, k = 3$ and α taking value of (a) 2, (b) 5. (The wave speed $c = 3.441$ for, $\alpha = 2$ and $c = 5.105$ and for $\alpha = 5$). Units of density and distance are normalized units $\bar{\rho}$. (c) The relation between waves speed c and α values, higher α values the propagation speed is large. The time spacings: $10m$ where $m = 1, 2, ..., 9$.

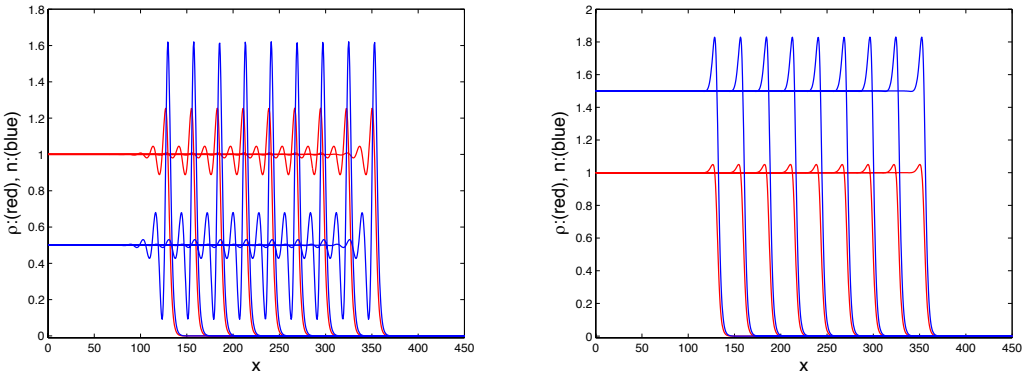

(a) (b)

Figure 3.12: Solution to the system (3.17) with the parameters $\alpha = 6, k = 3$ and d taking value of (a) 0.5, (b) 2. (The wave speed $c = 5.5254$ for $d = 0.5$, $c = 5.539$ for, $d = 2$). Units of density and distance are normalized units $\bar{\rho}$. The time spacings: $10m$ where $m = 1, 2, ..., 9$.

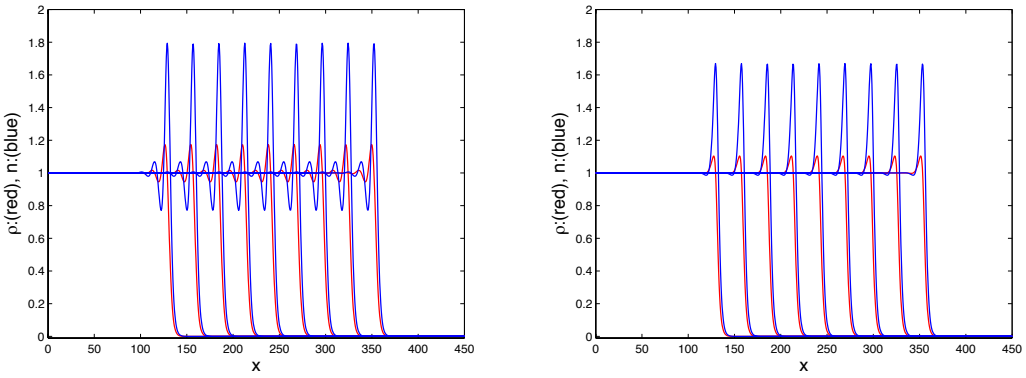

(a) (b)

Figure 3.13: Solution to the system (3.17) with the parameters $\alpha = 6, d = 1$ and k taking value of (a) 2, (b) 4. (The wave speed $c = 5.5296$ for $k = 2$, $c = 5.5371$ and $k = 4$). Units of density and distance are normalized units $\bar{\rho}$. The time spacings: $10m$ where $m = 1, 2, ..., 9$.

3.7 YWD: Dichotomous Branches, Tip-Tip Anastomoses

The model system in this case is

$$\begin{aligned} \frac{\partial \rho}{\partial t} &= nv - \gamma_1 \rho^k, \\ \frac{\partial n}{\partial t} &= -\frac{\partial nv}{\partial x} + \alpha_1 n - \beta_1 n^2. \end{aligned} \tag{3.19}$$

As above the equations would then take the form:

$$\begin{aligned} \frac{\partial \rho}{\partial t} &= n - d\rho^k \\ \frac{\partial n}{\partial t} &= -\frac{\partial n}{\partial x} + \alpha n(1-n), \end{aligned} \tag{3.20}$$

where $\alpha = (\alpha_1/\gamma_1)$ and d denoted before. This single parameter α represents the rate of tip production per unit length hypae per unit time. $\alpha(1-n)n$ this represent number of tips produced per unit time per unit length of tips.

As above, using the same code in MATLAB. Solution to the system (3.20) for $d = 8, k = 3$ and α values of 0.5 and 3 are illustrated in Fig. 3.14(a). This parameter α, thus modulates the growth rate. Of these, the second propagates at a considerably faster rate than the first with respect to same normalized units $\bar{n}$. Fig. 3.14(a). shows hyphal distributions produced by such colonies for $d = 8$, $k = 3$ and α values of 0.5 and 3. Fig. 3.14(c), details the relationship between c and α, and it illustrates that c is increasing when α increase.

In response to environmental stresses of various kinds, a possible fungal strategy could be to increase the rate of branching, α_1 while keeping γ_1 fixed. This would make the colony grow more quickly out of the hostile zone. Changing the rate of anastomosis, β_1, cannot alter the colony growth rate, we know the growth parameter α has no dependence on β_1 . However, increasing β_1 would decrease

the density levels accumulated in the interior, thus minimizing the extent of colonisation of unsuitable areas.

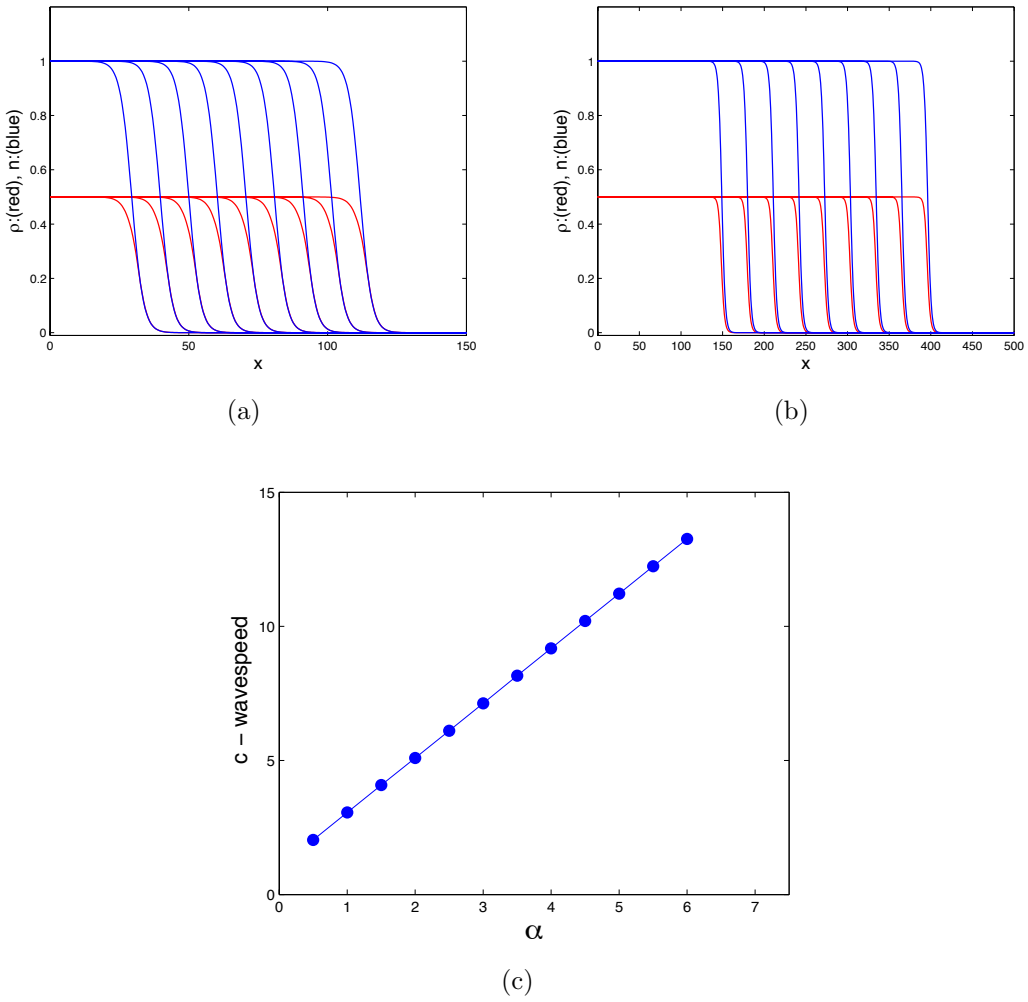

Figure 3.14: Solution to the system (3.20) with the parameters $d = 8, k = 3$ and α taking values of (a) 0.5. (b) 3. Units of density and distance are normalized units $\bar{n}$. (The wave speed $c = 2.0369$ for $\alpha = 0.5$ and $c = 7.1394$ for $\alpha = 3$). The time spacings: $10m$ where $m = 1, 2, ..., 9$. (c) The relation between waves speed c and α values, higher α values the propagation speed is large.

3.8 YHD: Dichotomous Branches, Tip-Hyphae Anastomoses

The model system in this case is

$$\begin{aligned} \frac{\partial \rho}{\partial t} &= nv - \gamma_1 \rho^k, \\ \frac{\partial n}{\partial t} &= -\frac{\partial nv}{\partial x} + \alpha_1 n - \beta_2 n\rho. \end{aligned} \tag{3.21}$$

Here the non-dimensionalised equations would then take the form:

$$\begin{aligned} \frac{\partial \rho}{\partial t} &= n - d\rho^k \\ \frac{\partial n}{\partial t} &= -\frac{\partial n}{\partial x} + \alpha n(1-\rho), \end{aligned} \tag{3.22}$$

where $\alpha = (\alpha_1/\gamma_1)$ and d denoted before. This single parameter α represent the rate of tip production per unit length hyphae per unit time. By the similar techniques to those a previous sections there are two uniform steady states: $(0, 0)$ and $(1, d)$.

Following standard proceeders it can be easily show that $(0, 0)$ is a saddle point and $(1, d)$ is a stable spiral.

The same processes in the previous sections are applied. Solution to the system (3.22) for $d = 1$, $k = 1$ and α values of 0.5 and 3 are illustrated in Fig. (3.15a, b). This parameter α thus modulates the growth rate. Of these, the second propagates at a considerably faster rate than the first with respect to same normalized units.Fig. (3.15a, b) shows hyphal distributions produced by such colonies $d = 1$, $k = 1$ and α values of 0.5 and 3. It is evident that density striation result when α is increased. Tip densities which are essentially similar have peaks leading those of hyphae by approximately two dimensionless unit.

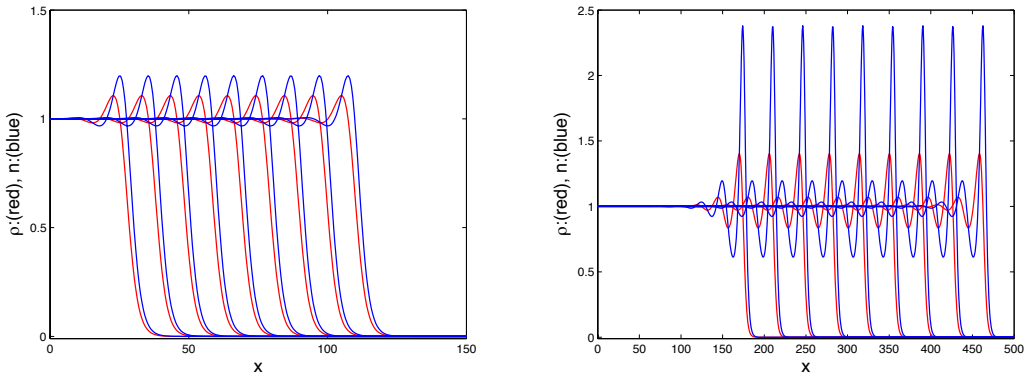

(a) (b)

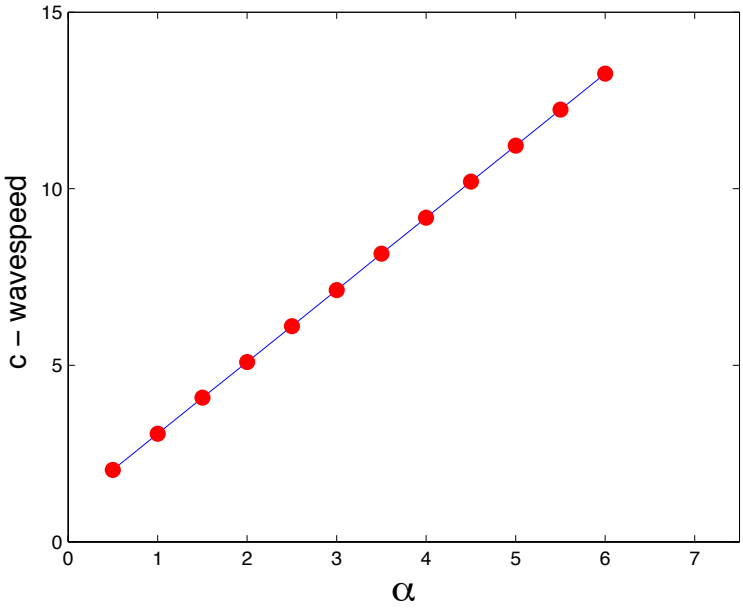

(c)

Figure 3.15: Solution to the system (3.22) with the parameters $d = k = 1$ and α taking values of (a) 0.5 and (b) 3. (The wave speed $c = 2.0367$ for $\alpha = 0.5$ and $c = 7.1399$ for $\alpha = 3$) c and α values, higher α values the propagation speed is large. The time spacings: $10m$ where $m = 1, 2, ..., 9$. (c) The relation between waves speed Units of density and distance are normalized units $\bar{\rho}$.

Fig.3.15(c), details the relationship between c and α, and it illustrates that c is increasing when α increase.

Since $\alpha = (\alpha_1/\gamma_1)$, therefore the grow is increasing when α_1 is increasing while keeping γ_1 is fixed, but the grow is decreasing when γ_1 is increasing while keeping α_1 is fixed, since the growth parameter α has no dependence on β_1, therefore β_1, can not alter the colony growth rate.

3.9 Other Patterns of Branching

3.9.1 YTD: Dichotomous branches with tip loss

The model system in this case is

$$\begin{aligned} \frac{\partial \rho}{\partial t} &= nv - \gamma_1 \rho^k, \\ \frac{\partial n}{\partial t} &= -\frac{\partial nv}{\partial x} + \alpha_1 n - \alpha_3 n. \end{aligned} \tag{3.23}$$

The equations would then take the form:

$$\begin{aligned} \frac{\partial \rho}{\partial t} &= n - d\rho^k \\ \frac{\partial n}{\partial t} &= -\frac{\partial n}{\partial x} + n(\alpha - \beta), \end{aligned} \tag{3.24}$$

where $\alpha = (\alpha_1/\gamma_1)$, $\beta = (\alpha_3/\gamma_1)$ and d denoted before. This single parameter $(\alpha - \beta)$ represent the rate of tip growth per unit length hyphae per unit time. There is one steady state: $(0, 0)$. Solution to system 3.24 for $\alpha = 2$, $\beta = 1$ and $\alpha = 1$, $\beta = 2$ respectively are illustrated in Fig. (3.16a, b).There is no traveling wave in this case, we noted that the profile like peak is increasing and it move right side when $\alpha > \beta$, but move in negative direction and increasing for $\alpha < \beta$.

Thus no propagation of colony. We used *Waterfall* plot in pdepe code see Fig. 3.16 to give us more clearly.

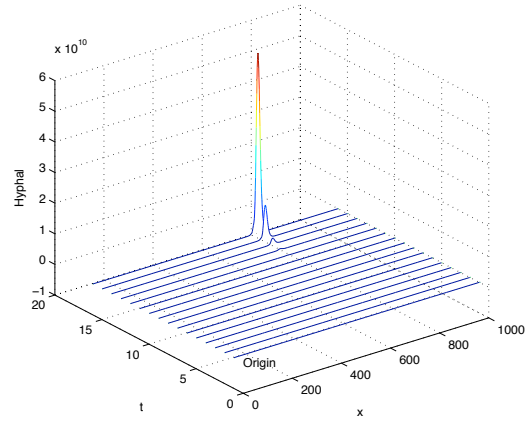

(a)

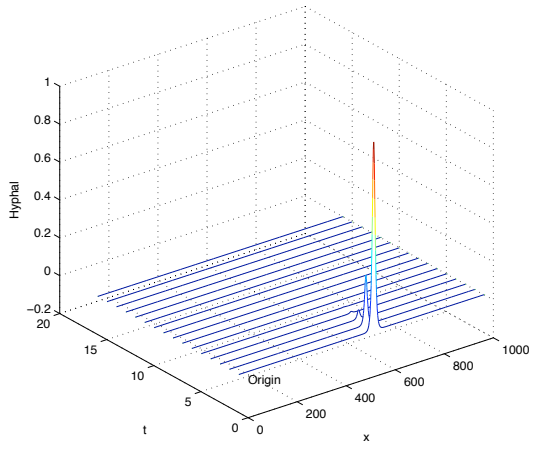

(b)

Figure 3.16: Solution to the system (3.24) with the parameters $d = k = 1$, α and β taking values of (a) $2, 1$ and (b) $1, 2$ respectively. Solutions are produced using MATLAB pdede.

From the numerical solutions for the previous types, FHD and FXD types are equal in wave speed c for a given value of α. As well as YWD, YHD types are equal in wave speed c for a given values of α. The wave speed c in the types YWD, YHD is faster than the types of FHD, FXD see Fig. 3.17. Here, the FHD and FXD are equal or approximately equal for a given values of parameters α. YWD and YHD are approximately equal for a given values of parameters α.
To avoid repeating the same previous technique, we made the table for each biological type was illustrate properties for every one of them, see Table 3.3. Also it shows briefly the existence or absence of travelling wave, according to the conditions mentioned previously.

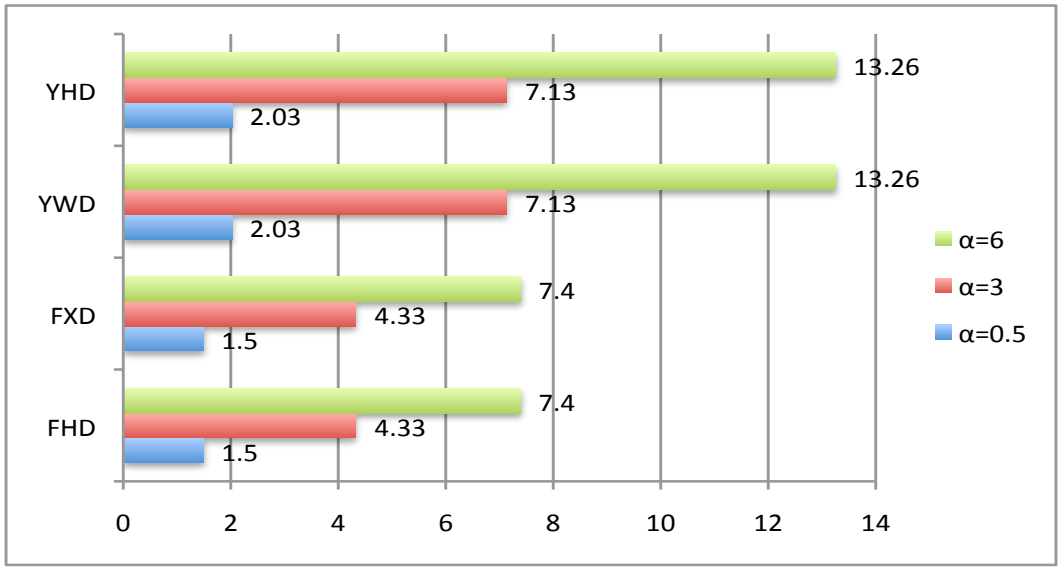

Figure 3.17: The chart shows the wave speed c for different values of α for four phenotypes. It is clear the wave speed for FHD, FXD- types are equal and YWD, YHD types are equal for the same value of α. The waves speed in YWD, YHD types are larger than from FHD and FXD types for the same values of α. Here values of $d = k = 1$.

Table 3.3: Branching type with $d(\rho) = d\rho^k$

Biological Type	Symbol	Branching Rule σ	Choice of scales	Dimensionless equation for propagation	Steady state	Traveling wave
Lateral branches tip-hypha anastomoses	FHD	$\sigma = \rho(\alpha_2 - \beta_2 n)$	$\bar{n} = \alpha_2/\beta_2$ $\tau = 1/\gamma_1$ $\bar{\rho} = \alpha_2 v/\gamma_1\beta_2$	$dP/dz = \frac{-1}{c}[N - dP^k]$ and $dN/dz = \frac{1}{(1-c)}[\alpha P(1-N)]$	(0,0) $(\sqrt[k]{\frac{1}{d}}, 1)$	all satisfied for $c > 1$
Lateral branches with density limitation	FXD	$\sigma = \rho(\alpha_2 - \beta_3\rho)$	$\bar{\rho} = \alpha_2/\beta_3$ $\tau = 1/\gamma_1$ $\bar{n} = \alpha_2\gamma_1/v\beta_3$	$dP/dz = \frac{-1}{c}[N - dP^k]$ $dN/dz = \frac{1}{(1-c)}[\alpha P(1-P)]$	(0,0) $(1, d)$	all satisfied for $c > 1$
Dichotomous branches, tip-tip anastomoses	YWD	$\sigma = n(\alpha_1 - \beta_1 n)$	$\bar{n} = \alpha_1/\beta_1$ $\tau = 1/\gamma_1$ $\bar{\rho} = v\alpha_1/\gamma_1\beta_1$	$dP/dz = \frac{-1}{c}[N - dP^k]$ $dN/dz = \frac{1}{(1-c)}[\alpha N(1-N)]$	(0,0) $(\sqrt[k]{\frac{1}{d}}, 1)$	all satisfied for $c > 1$
Dichotomous branches tip - hyphae anastomoses	YHD	$\sigma = n(\alpha_1 - \beta_2\rho)$	$\bar{\rho} = \alpha_1/\beta_2$ $\tau = 1/\gamma_1$ $\bar{n} = \alpha_1\gamma_1/v\beta_2$	$dP/dz = \frac{-1}{c}[N - dP^k]$ $dN/dz = \frac{1}{(1-c)}[\alpha N(1-P)]$	(0,0) $(1, d)$	all satisfied for $c > 1$
Lateral branches tip-tip anastomoses	FWD	$\sigma = \alpha_2\rho - \beta_1 n^2$	$\bar{\rho} = \alpha_2 v^2/\beta_1\gamma_1^2$ $\tau = 1/\gamma_1$ $\bar{n} = \alpha_2 v/\beta_1\gamma_1$	$dP/dz = \frac{-1}{c}[N - dP^k]$ $dN/dz = \frac{1}{(1-c)}[\alpha(P - N^2)]$	(0,0) $(d^{(\frac{-2}{2k-1})}, d^{(\frac{-1}{2k-1})})$	all satisfied for $c > 1$
Dichotomous branches with density limitation	YXD	$\sigma = \alpha_1 n - \beta_3\rho^2$	$\bar{\rho} = \alpha_1\gamma_1/\beta_3 v$ $\tau = 1/\gamma_1$ $\bar{n} = \alpha_1\gamma_1^2/\beta_3 v^2$	$dP/dz = \frac{-1}{c}[N - dP^k]$ $dN/dz = \frac{1}{(1-c)}[\alpha(N - P^2)]$	(0,0) $(d^{(\frac{-1}{k-2})}, d^{(\frac{-2}{k-2})})$	all satisfied for $c > 1$
Dichotomous branches, tip death	YTD	$\sigma = \alpha_1 n - \alpha_3 n$	$\tau = 1/\gamma_1$	$dP/dz = \frac{-1}{c}[N - dP^k]$ $dN/dz = \frac{1}{(1-c)}[N(\alpha - \beta)]$	$(0, 0)$	fails: no travelling wave
Lateral branches tip death	FTD	$\sigma = \alpha_2\rho - \alpha_1 n$	$\tau = 1/\gamma_1$	$dP/dz = \frac{-1}{c}[N - dP^k]$ $dN/dz = \frac{1}{(1-c)}[\alpha P - \beta N]$	$(0, 0)$	fails: no travelling wave if $k = d = 1$

3.10 More Complex Phenotypes

In this section we combine three types of branching inuence can yield many distinct phenotypes.

Table 3.4: More Complex phenotypes of biological branches

$\sigma(\rho, n)$	Symbol	Biological Type
$\alpha_2\rho - \beta_1 n^2 - \alpha_3 n$	FHTD	Lateral branches, tip - hypha anastomoses, tip death with hyphal death
$\alpha_2\rho - \beta_3\rho^2 - \beta_1 n^2$	FWTD	Lateral branches, tip - tip anastomoses, tip death with hyphal death
$\alpha_2\rho - \beta_3\rho^2 - \beta_2 n\rho$	FWXD	Lateral branches, tip - tip anastomoses, density limitation with hyphal
$\alpha_2\rho - \alpha_3 n - \beta_2 n\rho$	FHXD	Lateral branches, tip - hypha anastomoses, density limitation with hyphal death
$\alpha_1 n - \beta_1 n^2 - \alpha_3 n$	YWTD	Dichotomous branching, tip - tip anastomoses, tip death with hyphal death
$\alpha_1 n - \beta_1 n^2 - \beta_3\rho^2$	YWXD	Dichotomous branching, tip - tip anastomoses, density limitation with hyphal death
$\alpha_1 n - \beta_2 n\rho - \beta_3\rho^2$	YHXD	Dichotomous branching, tip - hypha anastomoses, density limitation with hyphal death
$\alpha_1 n - \alpha_3 n - \beta_2 n\rho$	YHTD	Dichotomous branching, tip - hypha anastomoses, tip death with hyphal death

with $\rho(x,t)$, $n(x,t)$, α_1, α_2, α_3, β_1, β_2 and β_2 defined above. In theory, a combination of different branching types could be expressed during phases of growth of a particular species of fungi. When $d \neq 0$, we shows more cases for net creation of tips, for examples, see Table 3.4. In this section we combining a three types of branching influence can yield many distinct phenotypes.

3.10.1 FHTD: Lateral Branching, Tip-Hypha Anastomosis, Tip Death with Hyphal Death

Now we will study FHTD type of fungi and the other the type of fungi are take a similar technique. The model system in this case is

$$\begin{aligned} \frac{\partial \rho}{\partial t} &= nv - \gamma_1 \rho^k, \\ \frac{\partial n}{\partial t} &= -\frac{\partial nv}{\partial x} + \alpha_2 \rho - \alpha_1 n - \beta_2 n\rho, \end{aligned} \tag{3.25}$$

with non-dimensionalisation.

$$\begin{aligned} \frac{\partial \rho}{\partial t} &= n - d\rho^k, \\ \frac{\partial n}{\partial t} &= -\frac{\partial n}{\partial x} + \alpha\rho(1-n) - \beta n, \end{aligned} \tag{3.26}$$

where $\alpha = (\alpha_2 v/\gamma_1^2)$, $\beta = (\alpha_2/\gamma_1)$. We will consider d = k = 1. By the similar techniques to those a previous sections, as first step, we look for uniform steady states of system (3.26) is seek solution of $n - \rho = 0$, $\alpha\rho(1-n) - \beta n = 0$. There are two steady states :$(0,0)$ and $(\frac{\alpha-\beta}{\alpha}, \frac{\alpha-\beta}{\alpha})$. Following standard proceeding it can be easily show that $(0,0)$ is a saddle point and $(\frac{\alpha-\beta}{\alpha}, \frac{\alpha-\beta}{\alpha})$ is stable node for all $\alpha, \beta > 0$ and $\alpha > \beta$.

Introducing $z = x - ct$ a set of two ordinary differential equation is obtained:

$$\begin{aligned} \frac{dP}{dz} &= \frac{-1}{c}[N - P], \\ \frac{dN}{dz} &= \frac{1}{(1-c)}[\alpha P(1-N) - \beta N], \quad c \neq 1, -\infty < z < \infty \end{aligned} \tag{3.27}$$

System (3.27) has two steady states points, $(0,0)$ and $(\frac{\alpha-\beta}{\alpha}, \frac{\alpha-\beta}{\alpha})$. Their stability depends on the value of c, $(0,0)$ is saddle point and, $(\frac{\alpha-\beta}{\alpha}, \frac{\alpha-\beta}{\alpha})$ stable node when $c > 1$. $(0,0)$ is unstable node and, $(\frac{\alpha-\beta}{\alpha}, \frac{\alpha-\beta}{\alpha})$ saddle point when $0 < c < 1$, $(0,0)$ is saddle point and, $(\frac{\alpha-\beta}{\alpha}, \frac{\alpha-\beta}{\alpha})$ stable node when $c < 0$.

Two Solution to the system (3.26) for α values of 0.1, 1, and for β value of 0.001 are illustrated in Fig. (3.18a, b). Two Solution to the system (3.26) for β values of 0.001, 0.5, and for α value of 1 are illustrated in Fig. (3.18b, c). Of these, the second propagates at a considerably faster rate than the first with respect to same normalized units. Altering α essentially selects for faster wave as the most stable solution to system (3.26) and same for β but the profile for ρ and n decreases, see Fig. 3.18(c).

All of the biological types (FWTD), (FXWD) , (FHXD) and (FHTD) achieve the required conditions above. The other biological types are illustrated in Table (3.5). Using the same processes as the last sections, we can investigate the following: non-dimensionalisation quantities, stability of uniform solutions, travelling wave solution and numerical solution of the initial value problem. These types are (YWTD), (YXWD), (YHXD), and (YHTD), and all of the biological types achieve the required conditions above.

From Table 3.3 and Table (3.5), we not the steady states in Table 3.3 depended on the parameters d and k, while the steady states in Table 3.5 depended on the parameters α and β, Table 3.5 if β is very small then the steady states will depend on α. In Table 3.3 YTD and FTD no travelling waves, while In Table each biological types have travelling waves.

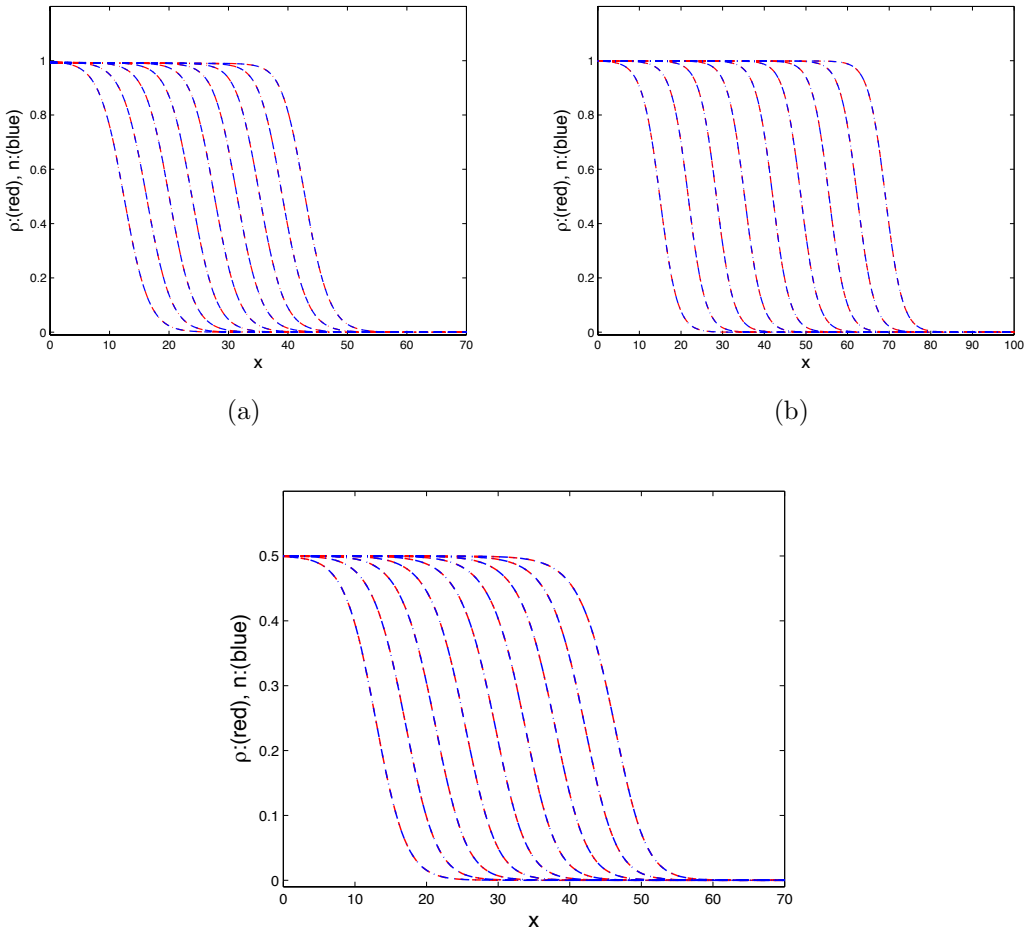

Figure 3.18: Solution to the system (3.26) with the parameter α and β taking values of (a) 0.1, 0.001 and (b) 1, 0.001. That is clear the points of stability are $(0,0)$ and $(0.999, 0.999)$ at α= 1, $\beta = 0.001$, and $(0,0)$, $(0.99, 0.99)$ at α= 1 and β = 0.001. The wave speed $c = 0.255$ for $\alpha = 1$, $\beta = 0.001$ and $c = 1.74$ for $\alpha = 1$, $\beta = 0.001$. (c) $\alpha = 1$, and $\beta = 0.5$, that is clear the points of stability are $(0,0)$ and $(0.5, 0.5)$ and here, $c = 0.457$. The time spacings: $10m$ where $m = 1, 2, ..., 9$.

Table 3.5: More complex phenotypes: Branching type with $d(\rho) = d\rho^k$

Biological Type	Symbol	Branching Rule σ	Choice of scales	Dimensionless equation for propagation	Steady state	Condition satisfied
Lateral branches tip-tip anastomosis tip death	FWTD	$\sigma = \alpha_2\rho - \beta_1 n^2 - \alpha_1 n$	$\bar{\rho} = v/\beta_1$ $\tau = 1/\gamma_1$ $\bar{n} = \gamma_1/\beta_1$	$dP/dz = \frac{-1}{c}[N - P]$ and $dN/dz = \frac{1}{(1-c)}[\alpha P - N(\beta + N)]$	$(0,0)$ $(\alpha - \beta, \alpha - \beta)$	all satisfied for $c > 1$ and $\alpha > \beta$
Lateral branches tip-tip anastomosis with density limitation	FXWD	$\sigma = \alpha_2\rho - \beta_3\rho^2 - \beta_1 n^2$	$\bar{\rho} = \gamma_1^2/\beta_3 v$ $\tau = 1/\gamma_1$ $\bar{n} = \gamma_1^3/\beta_3 v^2$	$dN/dz = \frac{1}{(1-c)}[P(\alpha - P) - \beta N^2]$	$(0,0)$ $(\frac{\alpha}{1+\beta}, \frac{\alpha}{1+\beta})$	all satisfied for $c > 1$
Lateral branches tip-hypha anastomosis with density limitation	FHXD	$\sigma = \alpha_2\rho - \beta_3\rho^2 - \beta_2 n\rho$	$\bar{\rho} = \gamma_1/\beta_2$ $\tau = 1/\gamma_1$ $\bar{n} = \gamma_1^2/v\beta_2$	$dN/dz = \frac{1}{(1-c)}[P(\alpha - \beta P - N)]$	$(0,0)$ $(\frac{\alpha}{1+\beta}, \frac{\alpha}{1+\beta})$	all satisfied for $c > 1$
Lateral branches tip-hypha anastomosis tip death	FHTD	$\sigma = \alpha_2\rho - \alpha_1 n - \beta_2 n\rho$	$\bar{\rho} = \alpha_2 v/\gamma_1\beta_2$ $\tau = 1/\gamma_1$ $\bar{n} = \alpha_2/\beta_2$	$dN/dz = \frac{1}{(1-c)}[\alpha P(1 - N) - \beta N]$	$(0,0)$ $(\frac{\alpha-\beta}{\alpha}, \frac{\alpha-\beta}{\alpha})$	all satisfied for $c > 1$
Dichotomos branching tip-tip anastomosis tip death	YWTD	$\sigma = \alpha_1 n - \beta_1 n^2 - \alpha_3 n$	$\bar{\rho} = v/\beta_1$ $\tau = 1/\gamma_1$ $\bar{n} = \gamma_1/\beta_1$	$dN/dz = \frac{1}{(1-c)}[N(\alpha - N)]$	$(0,0)$ (α, α)	all satisfied for $c > 1$
Dichotomos branching tip-tip anastomosis with density limitation	YXWD	$\sigma = \alpha_1 n - \beta_1 n^2 - \beta_3\rho^2$	$\bar{\rho} = v/\beta_1$ $\tau = 1/\gamma_1$ $\bar{n} = \gamma_1/\beta_1$	$dN/dz = \frac{1}{(1-c)}[N(\alpha - N) - \beta P^2]$	$(0,0)$ $(\frac{\alpha}{1+\beta}, \frac{\alpha}{1+\beta})$	all satisfied for $c > 1$
Dichotomos branching tip-hypha anastomosis with density limitation	YHXD	$\sigma = \alpha_1 n - \beta_2 n\rho - \beta_3\rho^2$	$\bar{\rho} = \gamma_1^2/\beta_3 v$ $\tau = 1/\gamma_1$ $\bar{n} = \gamma_1^3/v^2\beta_3$	$dN/dz = \frac{1}{(1-c)}[\alpha N - P(\beta N + P)]$	$(0,0)$ $(\frac{\alpha}{1+\beta}, \frac{\alpha}{1+\beta})$	all satisfied for $c > 1$
Dichotomos branching tip-hypha anastomosis with density limitation	YHTD	$\sigma = \alpha_1 n - \alpha_3 n - \beta_2 n\rho$	$\bar{\rho} = \gamma_1/\beta_2$ $\tau = 1/\gamma_1$ $\bar{n} = \gamma_1^2/v\beta_2$	$dN/dz = \frac{1}{(1-c)}[\alpha N(\alpha - P)]$	$(0,0)$ (α, α)	all satisfied for $c > 1$

3.11 Alternative Hyphal Death Terms

$$d(\rho, n) = \frac{d\rho^k}{\rho_o^k + \rho^k}$$

This term $d(\rho) = \frac{d\rho^k}{\rho_o^k + \rho^k}$ has two features that we wish to explain.
The first is the "delay" in hyphal death: for low values of ρ, the death rate is does to zero. This models, a resilience of the network to mild to no directs crowding. The second feature is the saturation at the death rate. This could represent the situation where hyphal aggregates are formed at high densities.

3.11.1 A Closer Look: Michaelis-Menten constant

Now, we will study the effects of hyphal death (loss) on the development of fungal networks, when $d(\rho) = \frac{d\rho^k}{\rho_o^k + \rho^k}$, where k is the positive number. Fig 3.19 illustrates the function $d(\rho) = \frac{d\rho^k}{\rho_o^k + \rho^k}$.

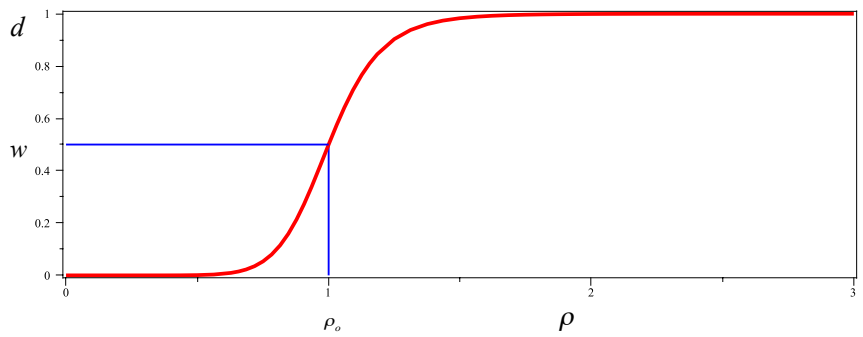

Figure 3.19: The horizontal axis represented ρ direction, that is clear value of ρ_o here equal 1 and ρ_o called Michaelis-Menten constant. The vertical axis represented d, w represented the value of $\frac{1}{2}d$, here equal 0.5 and $k = 10$.

3.11.2 FHD: Lateral Branching Plus Tip - Hypha Anastomosis

$$\begin{aligned} \frac{\partial \rho}{\partial t} &= nv - \frac{d\rho^k}{({\rho_o}^k + \rho^k)}, \\ \frac{\partial n}{\partial t} &= -\frac{\partial (nv)}{\partial x} + \alpha_2 \rho - \beta_2 n\rho, \end{aligned} \tag{3.28}$$

$\rho(x,t), n(x,t), v, \alpha_2$ and β_2 are denoted before. The parameter d represent the rate of conversion death of hyphae, ρ^k is the branches, k positive number.
The Michaelis constant ρ_o is the value of ρ at which the hyphal death rate is half its maximum value of d.
A small ρ_o indicates high affinity, and a branching with a smaller ρ_o will approach d more quickly. Very high ρ values are required to approach d, which is reached only when ρ is high enough to branch the enzyme (Hein and Neimann, 1962).

3.11.3 Non- dimensionalisation

To facilitate the analysis of this system and to assist in its numerical integration, we non-dimensionalise the equations and numerically integrate of in terms of dimensionless quantities. To do so, we choose a reference time τ, a reference length scale $\bar{x}$ and reference scales for hyphal density, $\bar{\rho}$, and tip density, $\bar{n}$.
Since the definition $\rho(x,t)$ is the hyphal density in units of filament length per unit area, then the measure unit is $(L/L^2 = L^{-1})$. $n(x,t)$ is the tip density (number per unit area), then density then the measure unit is $(a/L^2 = aL^{-2})$, where a is positive number. v is representing the rate of extension of an apex at (x,t) in length per unit time, that is clear measure unit is $(L/T = LT^{-1})$ and d hyphal death or loss rate (length per unit time) *i.e* measure unit is $(L/T = LT^{-1})$. As above (see 3.4.1) we now, setting $\bar{x} = \tau v$, $\hat{d} = (\tau d/\rho_o)$, $\rho_o = \bar{\rho}$ and $(\bar{\rho}/\bar{n}) = \bar{x}$

and, making the choice $\alpha = (\alpha_2\tau^2 v)$ and $\bar{\rho} = (\alpha_2\tau v/\beta_2)$ becomes

$$\begin{aligned} \frac{\partial \rho^*}{\partial t^*} &= n^* - \frac{\hat{d}\rho^{*k}}{(1+\rho^{*k})}, \\ \frac{\partial n^*}{\partial t^*} &= -\frac{\partial n^*}{\partial x^*} + \alpha\rho^*(1-n^*). \end{aligned} \tag{3.29}$$

Using $\bar{n} = \alpha_2/\beta_2$ and dropping hats and stars, this leads to:

$$\begin{aligned} \frac{\partial \rho}{\partial t} &= n - \frac{d\rho^k}{(1+\rho^k)}, \\ \frac{\partial n}{\partial t} &= -\frac{\partial n}{\partial x} + \alpha\rho(1-n). \end{aligned} \tag{3.30}$$

3.11.4 Stability of uniform solutions

As first step, we look for uniform steady states of system (3.32), and therefore seek solutions of the algebraic equations $n - \frac{d\rho^k}{(1+\rho^k)} = 0$, $\alpha\rho(1-n) = 0$. Clearly, there are two steady states: $(0,0)$ and $(\sqrt[k]{\frac{1}{d-1}}, 1)$, where $d > 1$. Following standard procedures, it follows that $(0,0)$ is a saddle point and the point $(\sqrt[k]{\frac{1}{d-1}}, 1)$ is a stable node of the kinetic problem associated with (3.32).

3.11.5 Travelling wave solution

Many physically important nonlinear partial differential equations can be reduced to the nonlinear ordinary differential equations Yan-ze and Krishnan (2006) and thus we can reduce the system (3.32) to a set of two ordinary differential equation:

$$\begin{aligned} \frac{dP}{dz} &= \frac{-1}{c}[N - \frac{dP^k}{(1+P^k)}], \\ \frac{dN}{dz} &= \frac{1}{(1-c)}[\alpha P(1-N)], \quad c \neq 1, -\infty < z < \infty, \end{aligned} \tag{3.31}$$

The steady states of system (3.16) are again $(0,0)$ and $(\sqrt[k]{\frac{1}{d-1}},1)$. Hence the stability of the steady states depends on the value of c; $(0,0)$ is saddle point and $(\sqrt[k]{\frac{1}{d-1}},1)$ unstable node when $c>1$. $(0,0)$ is unstable node and $(\sqrt[k]{\frac{1}{d-1}},1)$ saddle point when $0<c<1$. $(0,0)$ is saddle point and $(\sqrt[k]{(\frac{1}{d-1}},1)$ stable node when $c<0$. (Fig .3.20a, b and c).

We seek bounded, non-negative solution of system (3.31). Fig. (3.20a) illustrates trajectories connecting in the (P,N) - plane, from the unstable node $(\sqrt[k]{\frac{1}{d-1}},1)$ to the saddle point $(0,0)$. This trajectory depends on value of c and α. c represent direction of this trajectory and value of α if it is small close to the line $P=N$ (null cline) and it is moving away when the value of α increase. $(0,0)$ and $(\sqrt[k]{\frac{1}{d-1}},1)$ are two intersection points for N and P null-clines. Two equilibria of system (3.31) is thus ensured. The potential for a heteroclinic trajectory representing a bounded travelling wave solution is established.

The equilibrium in positive (P,N) quadrant is such that $N\neq 0$ and $P\neq 0$ implying that the wave level at $z\to-\infty$ is $N\neq 0$ and $P\neq 0$. There are many interesting implications of hyphal death. Tip density in the interior of the colony is maintained at a nonzero level. Biologically, this means that, while old hyphae are weeded out, new growth is continually taking place so that the density level is regulated in the older sections colony, as well as at the expanding margin and a new rate constant is added to the parameter set that after rendering the equations dimensionless one parameter remain. Thus, the possibility of modulating growth is also created.

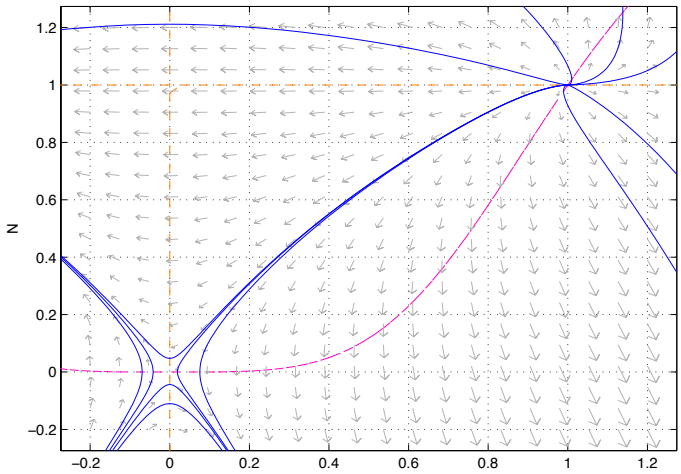

(a)

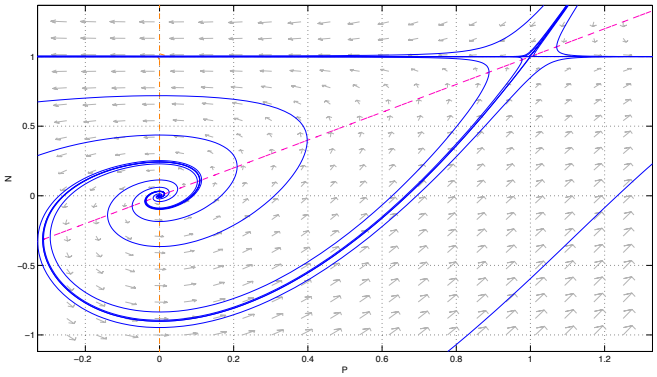

(b)

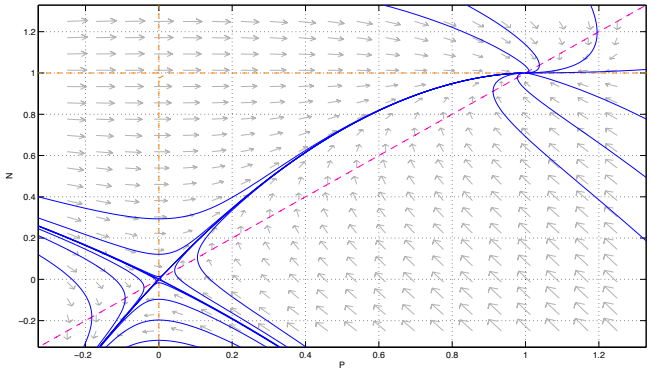

(c)

Figure 3.20: (a) The (P, N)- plane for ordinary differential equation $P' = \frac{-1}{c}[N - \frac{dP^k}{(1+P^k)}]$ and $N' = \frac{1}{(1-c)}[\alpha P(1-N)]$, here here $k = 4$, $\alpha = 2, d = 2$ and $c = 3$. The solid blue line corresponds to the model a trajectory connects the unstable node $(\sqrt[k]{\frac{1}{d-1}}, 1)$ to the saddle point $(0, 0)$. The dashed lines corresponds the model to the null-cline. (b) $c = 0.5$. (c) $c = -2$. Solutions are produced using MATLAB pplane7.

3.11.6 Numerical solution of the initial value problem

Using pdepe code in MATLAB. Solution to the system (3.32) for α, d and k values of $2, 2$ and 4, respectively, are illustrated in Fig .3.21(a). Fig. 3.22, details the relationship between c and α, and it illustrates that c is increasing when α an increasing function of α. Since $\alpha = (\alpha_2 v\tau^2)$, therefore, the wave speed increasing that is meaning the growth rate of fungi is increasing when the original α_2, v and $\tau = 1/\gamma_1$ are increasing. Biological mean, new growth is continually taking place, while old hyphae are eradication. The parameter α increase then the wavespeed c is increase, see Fig. 3.22. While the wave speed is not change or slightly change for changes of values of d, where we note that the profile of ρ increases when $d \to 1$, and it decreases when $d \to \infty$, see Fig. (3.23 a, b) when values of d are increase then the wavespeed c decrease, while when values of k are increase then the wavespeed c no change.

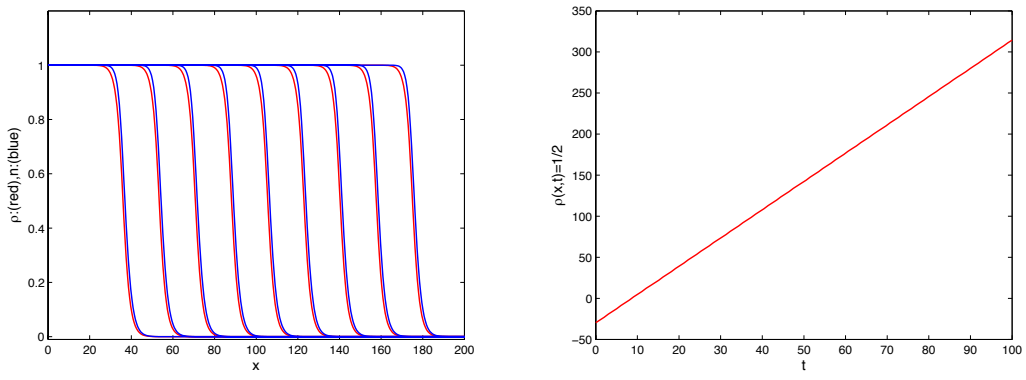

(a) (b)

Figure 3.21: (a) Solution to the system (3.32) with the parameters α, d and k taking values of $2, 2$ and 4, respectively. The time spacings: $10m$ where $m = 1, 2, ..., 9$. (b) The straight line represented the relation between t and the position of x is $\rho(x, t) = 1/2$ at above values of parameters, slope is representing wave speed $c = 3.441$.

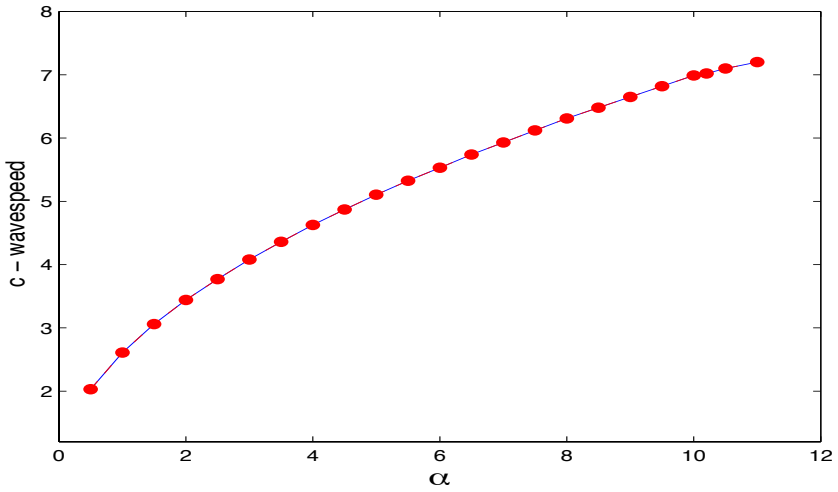

Figure 3.22: The relationship between α and wavespeed c, for parameter d and k are taken the values 2 and 4, respectively. That is clear when values of α are increase then the wavespeed c increase.

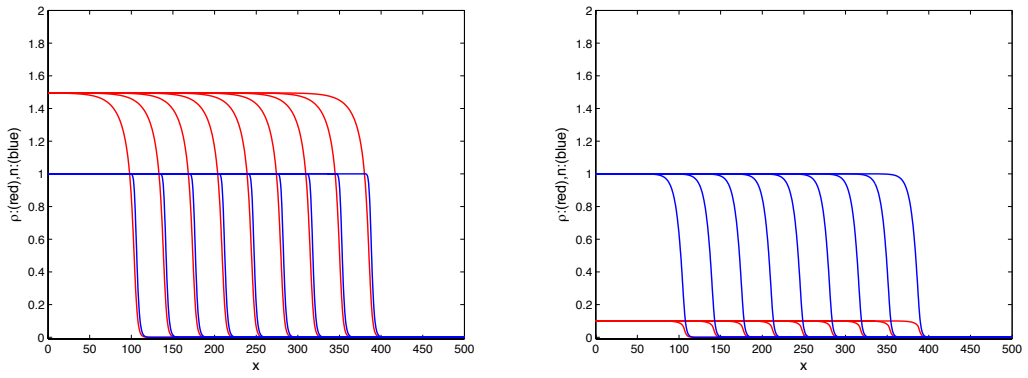

(a) (b)

Figure 3.23: Solution to the system (3.32) with the parameters α, d and k taking values of (a) $2, 1.2$ and 4, respectively. (b) $2, 10000$ and 4, respectively. Here the effect the parameters d on hyphal is very large for small value of d and maybe decays for large value of d. The time spacings: $10m$ where $m = 1, 2, ..., 9$. since $d = 1/\tau$, then the effect the parameters τ on hyphal is very small for large value of τ.

3.11.7 YHD: Dichotomous branches, tip-hyphae anastomoses

$$\begin{aligned} \frac{\partial \rho}{\partial t} &= n - \frac{d\rho^k}{(1+\rho^k)}, \\ \frac{\partial n}{\partial t} &= -\frac{\partial n}{\partial x} + \alpha n(1-\rho). \end{aligned} \tag{3.32}$$

As above Fig. (3.24a,b) and Fig. 3.25 shows the solution of (YHD) type with the parameters α, d and k taking values of (a) $2, 2$ and 4, respectively. we note here the relationship between α and wavespeed c is linearly and so for (YHD) type.

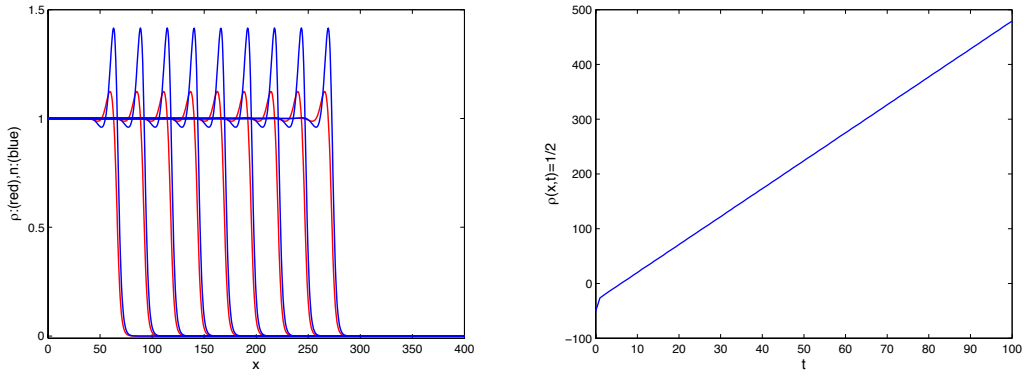

(a) (b)

Figure 3.24: Solution to the system of (YHD) type with the parameters α, d and k taking values of (a) $2, 2$ and 4, respectively. The time spacings: $10m$ where $m = 1, 2, ..., 9$. (b) The straight line represented the relation between t and the position of x is $\rho(x, t) = 1/2$ at above values of parameters, slope is representing wave speed $c = 5.1025$.

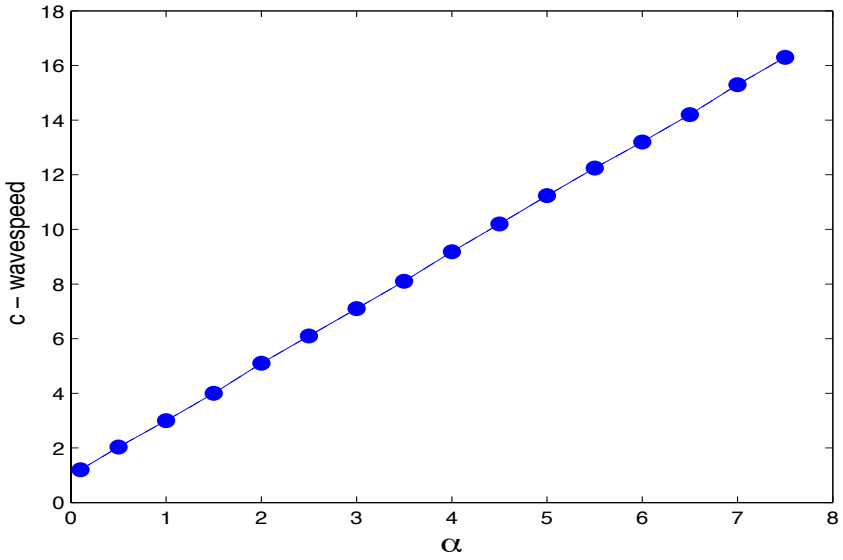

Figure 3.25: (c) The relationship between α and wavespeed c, for parameter d and k are taken the values 2 and 4, respectively. That is clear when values of α are increase then the wavespeed c increase.

Using similar techniques, we can illustrate or determine the wave speed for (FXD) and (YWD) at the same values of parameters, α, d and k taking values of $2, 2$ and 4, respectively.

Here, the wavespeed for FHD and FXD approximately equals $c = 3.441$ and 3.44 respectively. while the the wavespeed for YWD and YHD approximately equals $c = 5.0977$ and 5.102 respectively, see Fig. 3.26.

Table (3.6) illustrates the other biological types and the steady states that results from them. We noted the lateral branches, tip-hypha anastomoses FHD type and dichotomous, branches, tip-tip anastomoses YWD type have the same steady states $(0, 0)$ and $(\sqrt[k]{\frac{1}{d-1}}, 1)$. While the lateral branches, tip-tip anastomoses FXD type and dichotomous branches tip hyphae anastomoses YHD type have the same steady states $(0, 0)$ and $(1, \frac{d}{2})$.

Hence the stability of the steady states depends on the value of c; $(0, 0)$ is saddle point and $(\sqrt[k]{\frac{1}{d-1}}, 1)$ or $(1, \frac{d}{2})$ unstable node or spiral when $c > 1$. $(0, 0)$ is centre

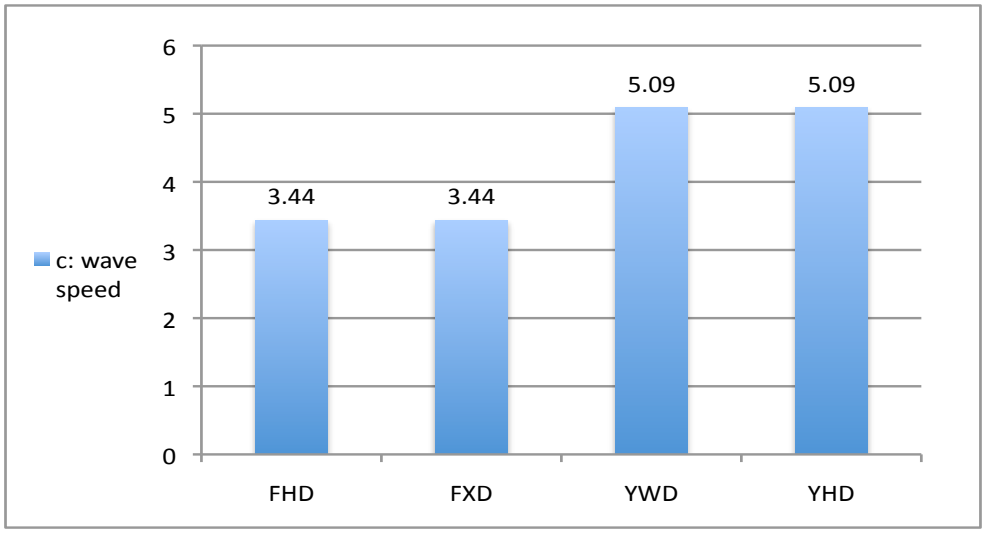

Figure 3.26: The chart represents wave speed c at the same values of α, d and k taking values of $2, 2$ and 4, respectively. It is clear the waves speed in FHD, FXD types are equal and YWD, YHD types are equal at the same values of α, d and k. The waves speed in YWD and YHD types large from FHD, FXD types at the same values of α, d and k.

or spiral and $(1, \frac{d}{2})$ or $\sqrt[k]{\frac{1}{d-1}}, 1)$ a saddle point when $0 < c < 1$. $(0, 0)$ is saddle point and $(\sqrt[k]{\frac{1}{d-1}}, 1)$ or $(1, \frac{d}{2})$ stable node and when $c < 0$.

From above information for this biological types there is travelling wave solution for $c > 0$.

To numerically integrate the propagation for phenotypes (FXD , YWD and YHD) types. We are sing the same technique as above for FHD and the same parameters α, d and k are taking values of $2, 2$ and 4, respectively, we noted the wavespeed $c \approx 3.44$ for FHD and FXD types, and the wavespeed $c \approx 5$ for YWD and YHD types. Fig. 3.26 illustrates FHD and FXD types have the wavespeeds are equals approximately $c = 3.44$, FHD and FXD types have the same wavespeeds at the same parameters and same values as above. That is clear, the waves speed in YWD and YHD types grater than YWD and YHD types at the same values of α, d and k.

Examining Table (3.6) for the system have two steady states, there is a trajectory

connecting these in the (P, N) - plane (a heteroclinic trajectory), these trajectory remains in the positive $(P, N))$ quadrant; and $(P^o, N^o) = (0, 0)$ is attractor for flow along the heteroclinic trajectory since it represents $z \to +\infty$ densities.

There are two interesting implications. The first is that tip density in the interior of the colony is maintained at nonzero level $(N \neq 0, P \neq 0)$.

Biological means that, while old hyphae are weeded out, new growth is continually taking place. so that the density level is regulated in the interior of the colony, as well as at the expanding margin.

For types has spiral, they are evident that density striation results when α is increased. Tip density which are essentially similar have peaks leading those of hyphae by approximately two dimensionless unit. The difference between high and low values of tip densities are also somewhat greater.

The density variations produced by these model fungi do not duplicate the hyphal density ring which may be precursors of sclerotai rings because they move as the colony grows, unlike the stationary striations of actual colonies. This is a result of our assumption that tips are constantly moving at a fixed growth rate. This assumption may not be accurate in some situations.

The second feature is that a new rate constant is added to the parameter set so that after rendering the equations dimensionless one parameter will remain.

The Table (3.6) shows the existence travelling wave solution for every type, that is satisfied when $c > 1$.

We can conclude the effect F and Y branching on the propagation of fungal colonies, where we get the Y type plus any other types still large from F plus the other types.

Table 3.6: Branching type with $d(\rho) = \frac{d\rho^k}{\rho_o + \rho^k}$

Biological Type	Symbol	Branching Rule σ $\sigma(\rho, n) = \sigma_1 - \sigma_2$	Dimensionless equation for propagation	Steady state $\bar{P}, \bar{N}$	Trevelling wave satisfied
Lateral branches tip-hypha anastomoses	FHD	$\sigma = \alpha_2\rho - \beta_2 n\rho$	$-cdP/dz = N - \frac{dP^k}{1+P^k}$ $(1-c)dN/dz = \alpha P(1-N)$	$(0,0)$ $(\sqrt[k]{\frac{1}{d-1}}, 1)$	all satisfied for all $c > 1$
Lateral branches with density limitation	FXD	$\sigma = \alpha_2\rho - \beta_3\rho^2$	$-cdP/dz = N - \frac{dP^k}{1+P^k}$ $(1-c)dN/dz = \alpha P(1-P)$	$(0,0)$ $(1, \frac{d}{2})$	all satisfied for all $c > 1$
Dichotomous branches, tip-tip anastomoses	YWD	$\sigma = \alpha_1 n - \beta_1 n^2$	$-cdP/dz = N - \frac{dP^k}{1+P^k}$ $(1-c)dN/dz = \alpha N(1-N)$	$(0,0)$ $(\sqrt[k]{\frac{1}{d-1}}, 1)$	all satisfied for all $c > 1$
Dichotomous branches tip - hyphae anastomoses	YHD	$\sigma = \alpha_1 n - \beta_2\rho n$	$-cdP/dz = N - \frac{dP^k}{1+P^k}$ $(1-c)dN/dz = \alpha N(1-P)$	$(0,0)$ $(1, \frac{d}{2})$	all satisfied for all $c > 1$

3.12 Discussion and Conclusion

The Chapter has studied modelling the propagation of fungal colonies. We illustrated σ's functions net creation of tips, see Table (3.1) which contain σ's functions, tip production or loss and parameters description. Combining branching with tip - loss provides the phenotypes see Table (3.2). We get four types: FHD, FXD, YWD and YHD. We studied the above types when $d(\rho) = d\rho^k$ using non- dimensionalisation, stability of uniform solutions, travelling wave solution and numerical solution of the initial value problem and using pdepe in MATLAB. Mathematically we focused on travelling wave solution because biologically, the behaviour of fungal growth mycelium is approximately the same behaviour of travelling wave solution (Edelstein, 1982). In these solutions, we showed the relationship between α and wavespeed c while keeping the parameter d and k fixed, the relationship between d and wavespeed c while keeping the parameter α and k fixed and the relationship between k and wavespeed c while keeping the parameter α and d fixed, where higher α values the propagation speed is large and slightly changes for parameter d and k. To avoid repeating the same previous technique, we made the table for each biological type to illustrate the properties for every one of them, see Table 3.3. Also it shows briefly the existence or absence of travelling wave, according to the conditions mentioned previously. We studied more complex phenotypes, see Table (3.5). Finally, We studied alternative hyphal death terms $d(\rho) = \frac{d\rho^k}{\rho_o^k + \rho^k}$ and we got the results by using the same previous techniques. From these results, the wave speeds in YWD and YHD types are larger than from FHD, FXD types at the same values of α, d and k. We can conclude the effect F and Y branching on the propagation of fungal colonies, where we get the Y type plus any other types still large from F plus the other types.

This term $d(\rho) = \frac{d\rho^k}{\rho_o^k + \rho^k}$ has two features that we wish to explain.

The first is the "delay" in hyphal death: for low values of ρ, the death rate is does to zero. This models, a resilience of the network to mild to no directs crowding.

The second feature is the saturation at the death rate. This could represent the situation where hyphal aggregates are formed at high densities.

The most notable feature is that only branching type and not the death or anastomosis terms affect colony expansion rate. The death and resulting or anastomosis terms simply control the biomass density.

Although these models have hyphal death, no account is taken of the process by while the by products of thus death are reused by the mycelium.

Recycling of hyphae appears to be an important facet of growth in certain situations see (Falconer et al., 2007, 2008). for detailed description of this process.

Chapter 4

Different Models for Tip Motion

4.1 Introduction

In this chapter we consider alternative flux J of hyphal tips for the first model, to investigate the effects of tip diffusion on the development of fungal networks. In the previous chapter, we illustrated some properties of system (3.3), and studied properties of simple branching types augmented with hyphal death.
Next, we reintroduce the kinetic terms d and $\sigma(\rho, n)$ and so study the system,

$$\begin{aligned} \frac{\partial \rho}{\partial t} &= |-D_n \frac{\partial n}{\partial x} + nv| - d(\rho), \\ \frac{\partial n}{\partial t} &= D_n \frac{\partial^2 n}{\partial x^2} - \frac{\partial (nv)}{\partial x} + \sigma(\rho, n). \end{aligned} \tag{4.1}$$

Now, if $d(\rho) = 0$, we will investigate results of two cases.

i. $D_n \neq 0$, $v \neq 0$: tip diffusion and convection,

ii. $D_n \neq 0$, $v = 0$: tip diffusion,

($D_n = 0$, $v \neq 0$: tip convection has been done already, see (Edelstein, 1982)). Furthermore, we will discuss the results where $d(\rho) \neq 0$, for the same cases for D_n and v.

4.2 Tip Diffusion and Convection when $d(\rho) = 0$

In this section, we will study $D_n \neq 0$, $v \neq 0$ when $d(\rho) = 0$. Here we consider one typical network architecture.

4.2.1 YH: Dichotomous branching, tip - hyphae anastomoses

The model system in this case is

$$\begin{aligned} \frac{\partial \rho}{\partial t} &= |-\epsilon \frac{\partial n}{\partial x} + nv|, \\ \frac{\partial n}{\partial t} &= \epsilon \frac{\partial^2 n}{\partial x^2} - \frac{\partial nv}{\partial x} + \alpha_1 n - \beta_2 n\rho, \end{aligned} \tag{4.2}$$

4.2.2 Non- dimensionalisation

To facilitate the analysis of this system and to assist in it is numerical integration, we non - dimensionalise the equations. To do so, we choose a reference time τ, a reference length scale $\bar{x}$ and reference scales for hyphal density, $\bar{\rho}$, and tip density, $\bar{n}$. Setting

$$\rho^* = \frac{\rho}{\bar{\rho}}, \quad n^* = \frac{n}{\bar{n}}, \quad t^* = \frac{t}{\tau}, \quad and, \quad x^* = \frac{x}{\bar{x}}, \tag{4.3}$$

and substituting into (4.2) yields

$$\begin{aligned}\frac{\partial \rho^*}{\partial t^*} &= |(\frac{\epsilon\tau\bar{n}}{\bar{\rho}\bar{x}})\frac{\partial n^*}{\partial x^*} + (\frac{\tau v\bar{n}}{\bar{\rho}})n^*|,\\ \frac{\partial n^*}{\partial t^*} &= (\frac{\epsilon\tau\bar{n}^2}{\bar{n}\bar{x}^2})\frac{\partial^2 n^*}{\partial x^{*2}} - (\frac{\tau v\bar{n}}{\bar{x}\bar{n}})\frac{\partial n^*}{\partial x^*} + (\frac{\alpha_1\tau\bar{n}}{\bar{n}})n^* - (\frac{\beta_2\tau\bar{\rho}\bar{n}}{\bar{n}})n^*\rho^*.\end{aligned} \tag{4.4}$$

Now, setting $\bar{x} = \tau v$ and $\bar{\rho}/\bar{n} = \bar{x}$, (4.4) becomes

$$\begin{aligned}\frac{\partial \rho^*}{\partial t^*} &= |(\frac{\epsilon}{\tau v})\frac{\partial n^*}{\partial x^*} + n^*|,\\ \frac{\partial n^*}{\partial t^*} &= (\frac{\epsilon}{\tau v})\frac{\partial^2 n^*}{\partial x^{*2}} - \frac{\partial n^*}{\partial x^*} + (\frac{\alpha_1\tau\bar{n}}{\bar{n}})n^* - (\frac{\beta_2\tau\bar{\rho}\bar{n}}{\bar{n}})n^*\rho^*,\end{aligned} \tag{4.5}$$

where $D_n = (\epsilon/\tau v^2)$ and on cancelling get,

$$\begin{aligned}\frac{\partial \rho^*}{\partial t^*} &= |D_n\frac{\partial n^*}{\partial x^*} + n^*|,\\ \frac{\partial n^*}{\partial t^*} &= D_n\frac{\partial^2 n^*}{\partial x^{*2}} - \frac{\partial n^*}{\partial x^*} + (\frac{\alpha_1\tau\bar{n}}{\bar{n}})n^* - (\frac{\beta_2\tau\bar{\rho}\bar{n}}{\bar{n}})n^*\rho^*,\end{aligned} \tag{4.6}$$

after dropping stars and chosen $\bar{\rho} = \alpha_1/\beta_2$, the system (4.7) becomes

$$\begin{aligned}\frac{\partial \rho}{\partial t} &= |D_n\frac{\partial n}{\partial x} + n|,\\ \frac{\partial n}{\partial t} &= D_n\frac{\partial^2 n}{\partial x^2} - \frac{\partial n}{\partial x} + \alpha n(1-\rho),\end{aligned} \tag{4.7}$$

where $\alpha = (\alpha_1\tau)$. System 4.7 has uniform steady states $(\rho,\ 0)$ given by the solution of the algebraic equations $n = 0$ and $\alpha n(1-\rho) = 0$. Fig. 4.1 illustrates the $(\rho,\ n)$ - plane, showing trajectories connects the points $(\rho,\ 0)$.

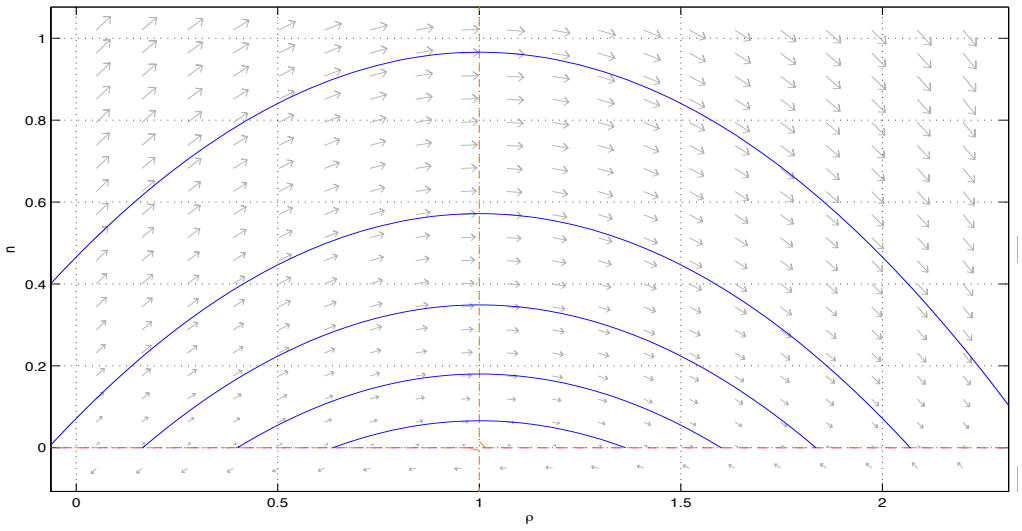

Figure 4.1: Phase plane $(\rho,\ n)$ of ODEs associated with Eq. 4.2. Red - dotted lines indicate the nullclines, exhibits a hetroclinic trajectory which remains in the positive $(\rho,\ n)$ quadrant. This describes the only "simple" fungi which could be successful at propagating. Note that a trajectories connects the points $(\rho,\ 0)$, for values $\alpha = 2$. Solutions are produced using MATLAB pplane7.

4.2.3 Travelling wave solution

We seek solution this as is standard $\rho(x,t) = P(z)$, and $n(x,t) = N(z)$, where $z = x - ct$. Here $P(z)$, $N(z)$ represent density profiles, and c can be interpreted as the rate of propagation of the colony. For these to be biologically meaningful we require P, N to be bounded, non - negative function of z and thus we can reduce the system (4.7) to a set of two ordinary differential equation:

$$\begin{aligned} -c\frac{dP}{dz} &= |-D_n\frac{dN}{dz} + N|, \\ -c\frac{dN}{dz} &= D_n\frac{d^2N}{dz^2} - \frac{dN}{dz} + \alpha N(1-P). \end{aligned} \tag{4.8}$$

Now set $\frac{dN}{dz} = U$, therefore $\frac{dU}{dz} = \frac{d^2N}{dz^2}$. The system (4.8) then becomes,

$$\begin{aligned} \frac{dP}{dz} &= \frac{-1}{c}[|-D_nU+N|], \\ \frac{dN}{dz} &= U, \\ \frac{dU}{dz} &= \frac{1}{D_n}[(1-c)U-\alpha N(1-P)]. \end{aligned} \tag{4.9}$$

System (4.9) has a line of uniform steady states points: $(P,\ 0,\ 0)$. Hetroclinic trajectory that remain in the positive $(P,\ N,\ U)$ quadrant. This describes the only "simple" fungi, which could be successful at propagating. Trajectories connects the points $(P,\ 0,\ 0)$, for values $c > 0,$ and $\alpha = 2$.

4.2.4 Numerical solution of initial value problem

For a better appreciation of the shapes of propagating solutions, numerical simulations were performed for the full PDE model, starting from some initial distribution, which resembled a tapering mycelial front (with $n,\ \rho \to 0$ for $z \to \infty$). The results are shown in Fig. (4.2a, b), which illustrates the distribution of tips in this phenotype. In type YH tips are maintained in a peak close to the margin of the colony. As this peak moves, depositing hyphae in its tracks, the mycelial front grows radially outwards in the interior of the colony, where hyphal density has attained its limiting value, see Fig. (4.2a, b).

Increasing D_n foe fixed α essentially selects for faster waves as the most stable solution for the system (4.2). These parameters thus provide the ability to modulate growth, to adapt to new situations. The grow is increasing when α is increasing. Since the growth parameter α has dependence on α_1 and τ. therefore the grow is increasing when α_1 is increasing, and the grow is increasing when τ is increasing and α_1 fixed.

Since the wavespeed c dependence on parameters D_n and α then, by linear model with nonpolynomial terms in MATLAB. Fig. 4.3(a), details the relationship between c and D_n, and it illustrates that c is increasing when D_n an increase function of D_n. Fig. 4.3(b) details the relationship between c and α, and it illustrates that c is increasing when α an increase of α.

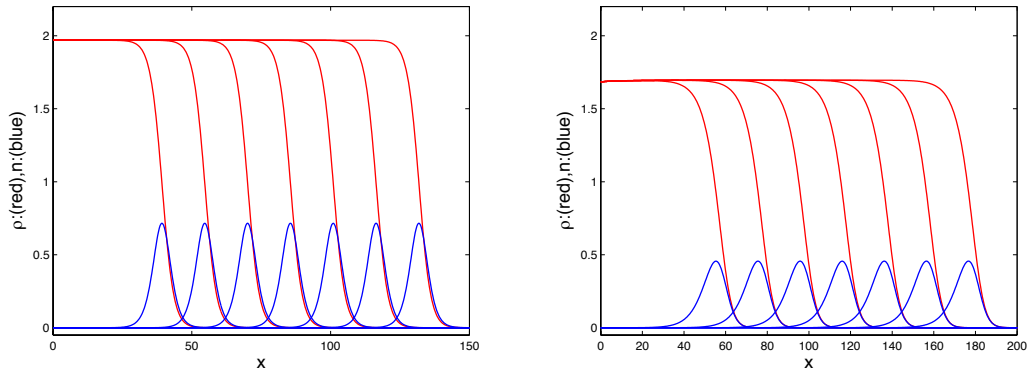

(a) (b)

Figure 4.2: Solution to the system (4.7) with the parameter D_n taking values of (a) 0.1 (b) 2, and the parameters α, v taking values $1, 1$ respectively. For higher D_n values the propagation speeds are larger. Fungi tend to concentrate their tips in a peaked distribution at the colony margin, where new growth takes place. (The wavespeed $c = 4.1946$ for $\alpha = v = 1$, $D_n = 0.1$ and $c = 6.328$ for $\alpha = 1$, $D_n = 2$). The time spacings: $10m$ where $m = 3, 4, ..., 9$.

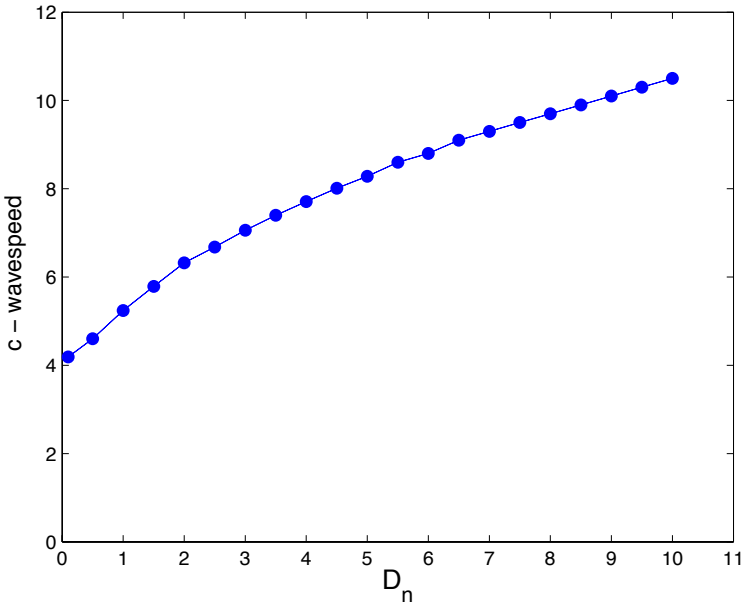

(a)

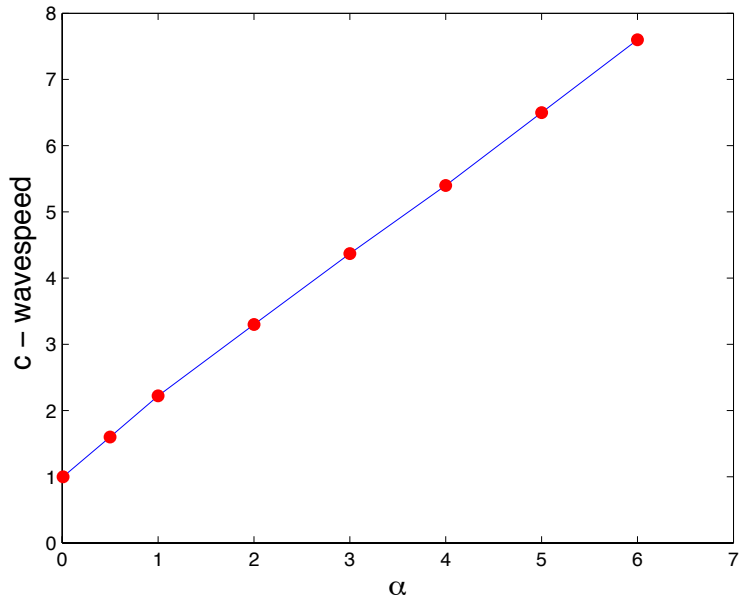

(b)

Figure 4.3: (a) The relation between wave speed c and diffusion D_n that is clear when D_n increases then the wave speed c increased, for fixed value of $\alpha = 1$. (b) The relation between wave speed c and parameter α that is clear when α increases then the wave speed c increases, for fixed parameter value of $D_n = 0.1$. Clearly this relation is linear relationship.

4.3 Tip Diffusion when $d(\rho) = 0$

The second case $D_n \neq 0$, $v = 0$, here we consider two typical network architectures.

4.3.1 FH: Lateral branching, tip - hypha anastomoses

The model system in this case is:

$$\begin{aligned} \frac{\partial \rho}{\partial t} &= |-\epsilon \frac{\partial n}{\partial x}|, \\ \frac{\partial n}{\partial t} &= \epsilon \frac{\partial^2 n}{\partial x^2} + \alpha_2 \rho - \beta_2 n \rho. \end{aligned} \tag{4.10}$$

As above, we non - dimensionalise the equations and after dropping stars and chosen $\bar{\rho} = \alpha_2 \tau v / \beta_2$, the system (4.10) becomes

$$\begin{aligned} \frac{\partial \rho}{\partial t} &= |D_n \frac{\partial n}{\partial x}|, \\ \frac{\partial n}{\partial t} &= D_n \frac{\partial^2 n}{\partial x^2} + \alpha \rho (1 - n), \end{aligned} \tag{4.11}$$

where $\alpha = (\alpha_2 \tau^2 v)$. Clearly, there are two uniform steady state $(0, n)$ and $(\rho, 1)$ given by the solution of algebraic equation $\alpha \rho (1 - n) = 0$.

4.3.2 Travelling wave solution

As above, let $\frac{dN}{dz} = U$ therefore $\frac{dU}{dz} = \frac{d^2N}{dz^2}$. We get the following system.

$$\begin{aligned} \frac{dP}{dz} &= \frac{-1}{c}[|-D_nU|], \\ \frac{dN}{dz} &= U, \\ \frac{dU}{dz} &= \frac{1}{D_n}[-cU - \alpha P(1-N)]. \end{aligned} \tag{4.12}$$

System (4.12) has two uniform steady states points: $(0, N, 0)$ has a one dimensional unstable node manifold and two dimensional centre manifold when $c > 0$. $(P, 1, 0)$ has a two dimensional unstable node manifold and one dimensional centre manifold when $c > 0$.

4.3.3 Numerical solution of initial value problem

Solutions to Eq. (4.11) for different values D_n, are illustrated in Fig. (4.4a, b). The profile of branching ρ arise when D_n increased. Increasing D_n fixed α essentially selects for faster waves as the most stable solution in the system (4.11). ($c = 0.599$ for $\alpha = 3$, $D_n = 0.1$ and $c = 3.66$ for $\alpha = 3$, $D_n = 2$). These parameters thus provide the ability to modulate growth to adapt to new situations.

In response to environmental stress of various kinds, a possible fungal strategy could be to increase the rate tip reorientation, D_n, while keeping α fixed. This would make the colony grow more quickly out of the hostile zone. Changing the rate of anastomosis, β_2, cannot alter the colony growth rate, while the fungal strategy could be to increase the rate of branching, α_2 and τ. This would make the colony grow more quickly out of the hostile zone, when D_n fixed. Altering α and fixed D_n essentially selects for faster waves as the most stable solution to the system (4.11). Fig. (4.4) and Fig. (4.5) shows hyphal distributions produced by

such colonies for values of D_n and α. It evident that the density of tips increases when D_n. Increasing D_n causes the biomass density to increase (whilst tip density remain unaltered). This is a result of the tips move effectively "following space" creating a denser mycelium. From these results the effects of diffusion on the development of fungal networks are clear. The branches have risen and the speed for values of D_n has increased. Fig. 4.5(a) shows, the relation between wave speed c and diffusion D_n that is clear when D_n is increased then the wave speed c increased. Fig. 4.5(b) shows, the relation between wave speed c and diffusion α it is clear that when α is increases then the wave speed c increased.

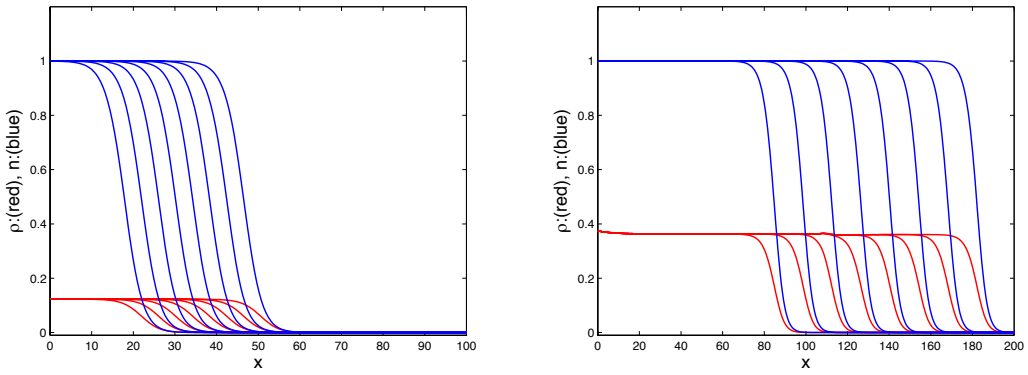

(a) (b)

Figure 4.4: Distance from the centre. Solution to the system (4.10) with the parameter D_n and α are taking values of (a) $0.1, 3$ (b) $1, 3$, respectively. For higher D_n and fixed α values the propagation speeds are larger. The time spacings: $10m$ where $m = 2, 3, ..., 9$.

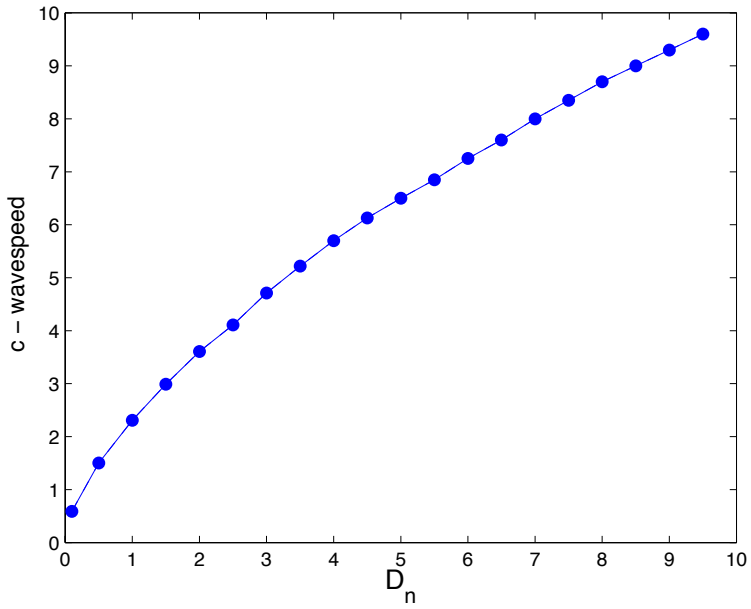

(a)

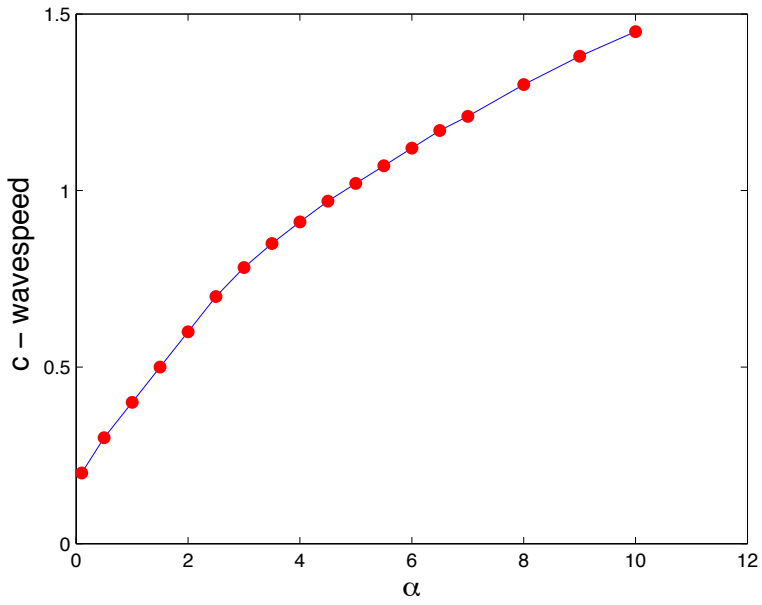

(b)

Figure 4.5: (a) The relation between wave speed c and tip diffusion D_n, that is clear when D_n increased then the wave speed c increased, for fixed parameter value of $\alpha = 3$. (b) The relation between wave speed c and tip parameter α, that is clear when α increased then the wave speed c increased, for fixed parameter value of $D_n = 0.5$.

4.3.4 YW: Dichotomous branching, tip - tip anastomoses

The model system in this case is:

$$\begin{aligned} \frac{\partial \rho}{\partial t} &= |-\epsilon \frac{\partial n}{\partial x}|, \\ \frac{\partial n}{\partial t} &= \epsilon \frac{\partial^2 n}{\partial x^2} + \alpha_1 n - \beta_1 n^2. \end{aligned} \tag{4.13}$$

As above, we non - dimensionalise the equations and after dropping stars and chosen $\bar{n} = (\alpha_1/\beta_1)$, the system (4.13) becomes

$$\begin{aligned} \frac{\partial \rho}{\partial t} &= |D_n \frac{\partial n}{\partial x}|, \\ \frac{\partial n}{\partial t} &= D_n \frac{\partial^2 n}{\partial x^2} + \alpha n(1-n), \end{aligned} \tag{4.14}$$

where $\alpha = (\alpha_1 \tau)$. The second equation of system (4.14) is

$$\frac{\partial n}{\partial t} = \alpha n(1-n) + D_n \frac{\partial^2 n}{\partial x^2}, \tag{4.15}$$

where α and D_n are positive parameters, which is classic equation suggested by (Fisher, 1937). It is the natural extension of the logistic growth population model when the population disperses via linear diffusion. This equation and it is travelling wave solution have been widely studied,(Fife, 1979; Kolmogroff et al., 1937; Bartton, 1986; Grindrod, 1996; Luther, 1906) discovered, investigation and analysis of travelling waves in chemical reactions. Showalter and Tyson (1987) put Luther's (1906) remarkable discovery and analysis of chemical wave in modern context. Luther obtained the wavespeed in terms of parameters associated with the reactions he was studying, see e.g. (Murray, 2002).

4.3.5 A Closer Look: Travelling Wave in one spatial dimension

In one spatial dimension, x, diffusion of a molecule with concentration $n(x,t)$ can be described as

$$\frac{\partial n}{\partial t} = D_n \frac{\partial^2 n}{\partial x^2} = D_n \Delta n.$$

In mathematical terms, $n(x,t)$ is a travelling wave that moves at constant speed c in the positive x - direction, if

$$n(x,t) = n(x-ct) = n(z), \quad z = x - ct.$$

z is referred to as wave variable. Now, PDE can be expressed as set of ODEs

$$n(x,t) = n(x-ct) = n(z), \quad z = x - ct.$$

can be rewritten as

$$\frac{\partial n}{\partial t} = -c\frac{dn}{dz},$$
$$\frac{\partial n}{\partial x} = \frac{dn}{dz}.$$

Partial differential equations in x and t therefore become sets of ordinary differential equations. To be physically realistic $n(z)$ has to be bounded for all z and non-negative. It can be shown that there are no physically realistic travelling wave solutions for reaction-diffusion equations of the form

$$n_t = f(n) + Dn_{xx}$$

if $f(n)$ is linear. However approximating can be made of the leading edge (Murray, 2002).In biological systems $f(n)$ is typically non-linear. To propagating wave solutions, we take this Example: logistic growth

$$\frac{dn}{dt} = n(1-n); \quad n(x,0) = \frac{1}{1+e^x}.$$

This equation can be solved to give

$$n(x,t) = \frac{ce^t}{1+ce^t}.$$

To satisfy the initial conditions we further require

$$n(x,0) = \frac{c}{1+c} = \frac{1}{1+e^x} \Rightarrow c = e^{-x}.$$

$$n_t = n(1-n); \quad n(x,0) = \frac{1}{1+e^x}$$

is thus solved by

$$n(x,t) = \frac{ce^{(t-x)}}{1+e^{(t-x)}}$$

If we set $z = t - x$ we thus have

$$n(z) = \frac{ce^z}{1+e^z}$$

If $z = x - t = \text{const}$ then the shape does not change, *i.e.* if $dx/dt = 1$. The shape of the wave thus does not change if one travels with the wave at speed 1. This wave depends on the initial conditions and is highly unstable. Consider the

Fisher equation

$$n_t = kn(1-n) + Dn_{xx}.$$

This equation can be non-dimensionalized by using $1/k$ as timescale and $\sqrt{D_n/k}$ as length gives the non-dimensionalized Fisher equation

$$n_t = n(1-n) + n_{xx}.$$

We write

$$n(x,t) = n(x-ct) = N(z), \quad z = x - ct, \quad c \geq 0,$$

therefore, we have

$$N^{''} + cN^{'} + N(1-N) = 0$$

Now; determine nullclines; determine steady states; determine stability of steady states and determine trajectories and phase vectors

$$N^{'} = P = 0$$
$$P^{'} = -cP - N(1-N) = 0$$

The N - nullcline is given by $P = 0$, the P - nullcline is given by $P = (-\frac{N(1-N)}{c})$. Steady states: $(N,\ P) = (0,\ 0)$ and $(N,\ P) = (1, 0)$. To determine the stability of the steady states we linearize the set of equations at these steady states $(N^*,\ P^*)$

and determine the eigenvalues of the Jacobian, and so.

$$J = \begin{bmatrix} 0 & 1 \\ -(1-2N^*) & -c \end{bmatrix}$$

$$\lambda_{\pm} = \frac{1}{2}(-tr(J) \pm \sqrt{tr(J)^2 - 4det(J)}).$$

Steady States: $(N,\ P) = (1,\ 0)$ saddle point, $(N,\ P) = (0,\ 0)$: stable node if $c \geq 2$, stable spiral if $c < 2$. Fisher Equation:

$$N^{'} = P$$
$$P^{'} = -cP - N(1-N)$$

Steady states: $(N,\ P) = (1,\ 0)$ saddle point and $(N,\ P) = (0,\ 0)$ stable node if $c \geq 2$. Phase plane trajectory:

$$\frac{P}{N} = \frac{-cP - N(1-N)}{P}$$

Since N can assume negative values if there is a stable spiral at $(N,\ P) = (0,\ 0)$ we require $c \geq 2$ for physically realistic travelling wave solutions.
For travelling waves to exist we require one stable node and one saddle.
Initial conditions: If $n(x,\ 0)$ has compact support,

$$n(x,\ 0) = n_o(x) \geq 0, \quad n_o(x) = \begin{cases} 1, & x \leq x_1, \\ 0, & x \geq x_2, \end{cases}$$

where $x_1 < x_2$ then we obtain travelling wave solutions with $c = c_{min} = 2$. For other initial data the solution critically depends on the behaviour of $n(x;0)$ as $x \to \pm\infty$. Consider the leading edge of the evolving wave where since n is small

$n_2 << n$ such that

$$n_t \sim n + n_{xx}, \quad n(x,\ 0) = Ae^{(-\alpha x)}, \quad \alpha > 0,$$

with solution

$$n(x,\ t) = Ae^{(-\alpha(x-ct))},$$

if $\alpha cn = n + \alpha^2 n, \quad i.e. \quad c = \frac{1}{\alpha} + \alpha$. The wave speed c depends on the initial conditions α.

Again, Eq. 4.14, clearly, there are two uniform steady state $(\rho,\ 0)$ and $(\rho,\ 1)$ given by the solution of algebraic equation $\alpha n(1-n) = 0$. It is clear Fig. 4.6 illustrates the $(\rho,\ n)$ - plane, showing trajectories from an unstable point $(\rho,\ 0)$ to the stable point $(\rho,\ 1)$.

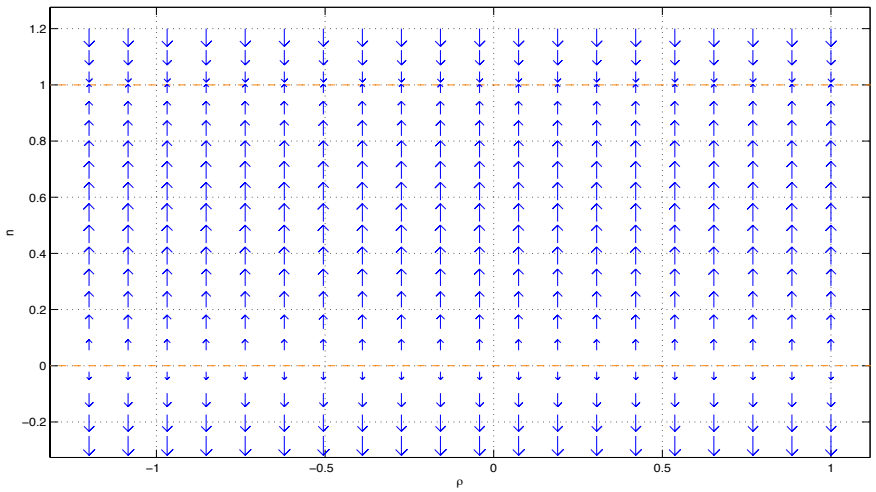

Figure 4.6: Phase plane $(\rho,\ n)$ of ODEs associated with Eq. 4.14. Red - dotted lines Indicate the nullclines: Note that a trajectories connects the point $(\rho,\ 0)$ to the point $(\rho,\ 1)$, for values $\alpha = 2$. Solutions are produced using MATLAB ode45.

4.3.6 Travelling wave solution

As above, we can reduce the system (4.14) to a set of two ordinary differential equations:

$$\begin{aligned} -c\frac{dP}{dz} &= |-D_n\frac{dN}{dz}|, \\ -c\frac{dN}{dz} &= D_n\frac{d^2N}{dz^2}+\alpha N(1-N), \end{aligned} \tag{4.16}$$

Let $\frac{dN}{dz}=U$ therefore $\frac{dU}{dz}=\frac{d^2N}{dz^2}$. Finally the system (4.16) becomes.

$$\begin{aligned} \frac{dP}{dz} &= \frac{-1}{c}[|-D_nU|], \\ \frac{dN}{dz} &= U, \\ \frac{dU}{dz} &= \frac{1}{D_n}[-cU-\alpha N(1-N)]. \end{aligned} \tag{4.17}$$

System (4.17) has two uniform steady states points: $(P,\ 0,\ 0)$ saddle point, when $c>0$.

$(P,\ 1,\ 0)$ the system has two dimensional unstable node manifold and one dimensional centre manifold when $c>0$.

4.3.7 Numerical solution of initial value problem

As above, two solutions to the Eq. (4.14) for α and D_n values of 2, 0.5 and 2, 1.5 respectively, are illustrated in Figure 4.7(a) and 4.7(b). Of these, the second propagates are considerably faster rate than the first with respect to the same normalised units. The profile of branching ρ is high when D_n increased. Altering D_n and fixed α essentially selects for faster waves as the most stable solution to the system (4.14). (The wavespeed $c=2.536$ for $\alpha=2$, $D_n=0.5$ and $c=3.533$ for $\alpha=2$, $D_n=1.5$). These parameters thus provide the ability

to modulate growth, to adapt to new situations.

The growth is increasing when α is increasing. Since the growth parameter α has dependence on α_1 and β_1. therefore the grow is increasing when α_1 is increasing, but the growth is decreasing when β_1 is increasing and α_1 fixed.

Since the wavespeed c dependence of the wave speed on parameter D_n then, by using MATLAB as above. Fig.(4.8(a)), details the relationship between c and D_n, and it illustrates that c is increasing when D_n an increase function of D_n. Fig.(4.8(b)), details the relationship between c and α, and it illustrates that c is increasing when α an increase.

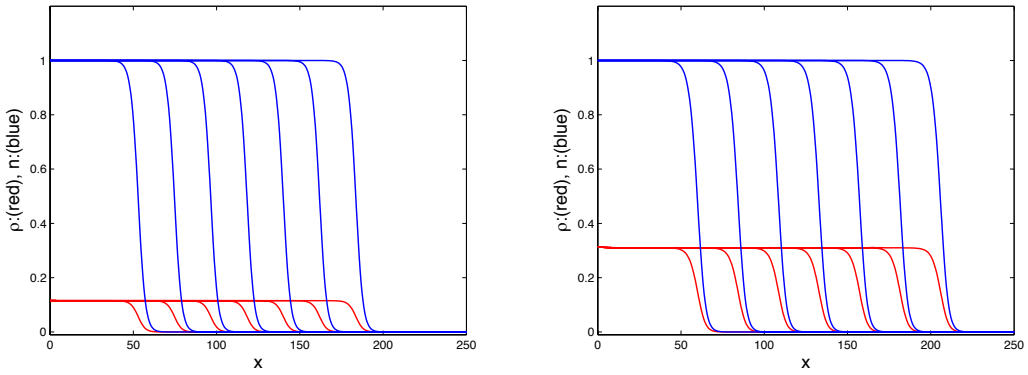

(a) (b)

Figure 4.7: Solution to the system (4.14) with the parameter α and D_n are taking values of (a) $2, 0.5$ (b) $2, 1.5$, respectively. For higher D_n and α values the propagation speeds are larger. The time spacings: $10m$ where $m = 3, 4, ..., 9$.

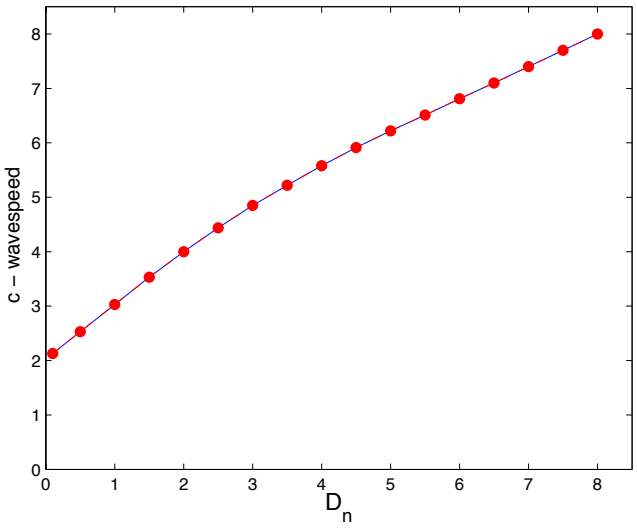

(a)

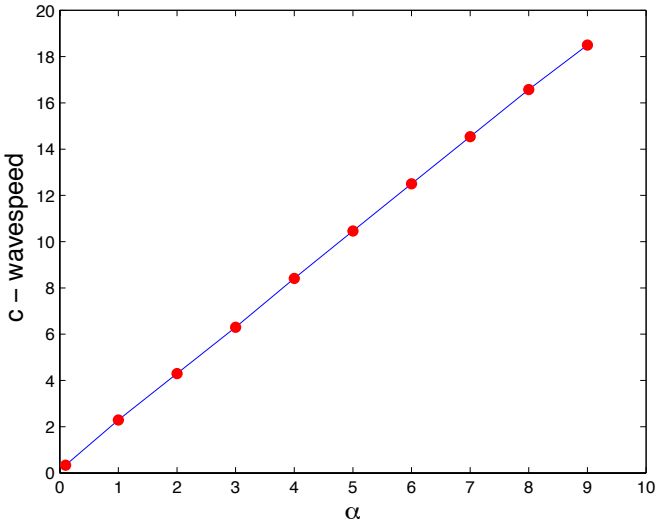

(b)

Figure 4.8: (a) The relation between wave speed c and diffusion D_n that is clear when D_n then the wave speed c increased at $\alpha = 2$. (b) The relation between wave speed c and the parameter α that is clear when α then the wave speed c increased at $D_n = 0.5$ and this relation is linear relationship.

Next sections we will discuss the cases for system (2.38) when $d = \gamma\rho$. The case $D_n = 0$, $v \neq 0$, when $d(\rho) \neq 0$ has been done already (see previous Chapter). There are no biological types give us biological realistic when $D_n \neq 0$, $v = 0$.

4.4 Tip Diffusion and Convection with $d(\rho) \neq 0$

There are many biological types give us biological realistic when $d(\rho) \neq 0$, $D_n \neq 0$ and $v \neq 0$. For examples below:

4.4.1 FH: Lateral branching, tip - hypha anastomoses

The model system in this case is:

$$\begin{aligned} \frac{\partial \rho}{\partial t} &= |\epsilon \frac{\partial n}{\partial x} + nv| - \gamma_1 \rho, \\ \frac{\partial n}{\partial t} &= \epsilon \frac{\partial^2 n}{\partial x^2} - \frac{\partial (nv)}{\partial x} + \alpha_2 \rho - \beta_2 \rho n, \end{aligned} \tag{4.18}$$

where $\rho(x,t)$, $n(x,t)$, v, γ_1, α_2, β_2,and ϵ are defined as above. Using the same technique in the last sections. To shows the relationship between parameters and wave speed c, The following steps we will study the properties for the system (4.18) with non-dimensionless, using $\bar{\rho} = (\alpha_2 v/\gamma_1\beta_2)$

$$\begin{aligned} \frac{\partial \rho}{\partial t} &= |D_n \frac{\partial n}{\partial x} + n| - \gamma_1 \rho, \\ \frac{\partial n}{\partial t} &= D_n \frac{\partial^2 n}{\partial x^2} - \frac{\partial n}{\partial x} + \alpha \rho (1 - n), \end{aligned} \tag{4.19}$$

where $\alpha = (\alpha_2 v/\gamma_1)$.

First step, we look for uniform steady states of system (4.19) *i.e.* we seek solution algebraic equations: $n - \rho = 0$, $\alpha\rho(1 - n) = 0$. There are two steady states: $(\rho, n) = (0, 0)$, $(1, 1)$. Following standard procedures it can be easily shown that $(0, 0)$ is a saddle point and $(1, 1)$ is a stable node of the kinetic problem associated with (4.19), see Figure (4.9).

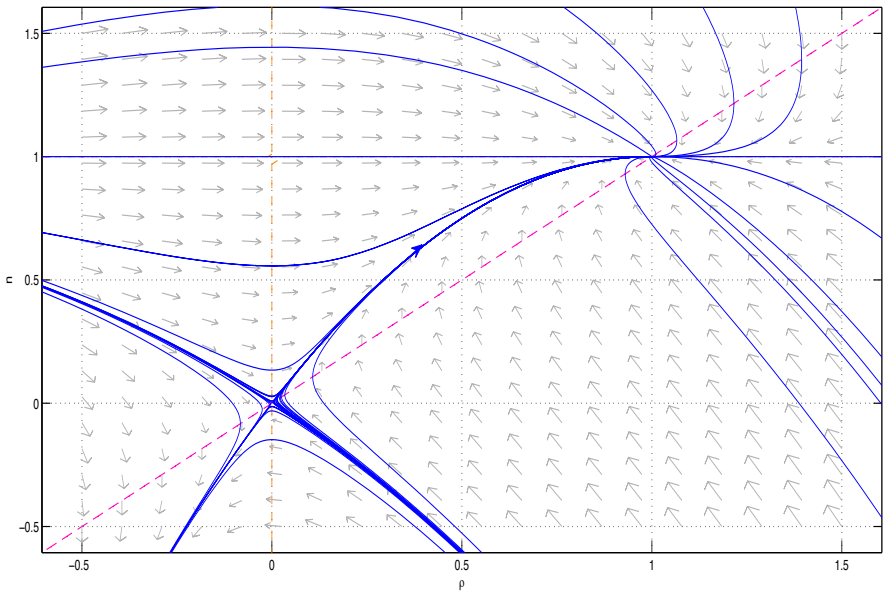

Figure 4.9: Phase plane (ρ, n) of ODEs associated with 4.19. Blue curves represented sample trajectories. Red-dotted lines Indicate the nullclines: Note that a trajectory connects the saddle point $(0, 0)$ to the stable node $(1, 1)$, for values $\alpha = 2$ and $D_n = 1$. Solutions are produced using pplane7.

We seek solution this as is standard $\rho(x, t) = P(z)$, and $n(x, t) = N(z)$, where $z = x - ct$. As above, we get

$$\begin{aligned} \frac{dP}{dz} &= \frac{-1}{c}[|-D\frac{dN}{dz} + N| - P], \\ \frac{dN}{dz} &= U, \\ \frac{dU}{dz} &= \frac{1}{D}[(1-c)U + \alpha P(1-N). \end{aligned} \tag{4.20}$$

System (4.20) has two steady states points $(0, 0, 0)$ and $(1, 1, 0)$. Their stability depends on the value of c.

When $c > 0$, $(0, 0, 0)$ the system has two dimensional unstable node manifold and one dimensional stable node manifold and $(1, 1, 0)$ unstable node.
When $c > 0$, $(0, 0, 0)$ the system has two dimensional unstable node manifold and one dimensional stable node manifold and $(1, 1, 0)$ unstable node.
When $c < 0$, $(0, 0, 0)$ the system has two dimensional unstable node manifold and one dimensional stable node (when $1 > 4\alpha c$) or spiral manifold (when $1 < 4\alpha c$), and at $(1, 1, 0)$ the system has two dimensional unstable node manifold and one dimensional stable node manifold.
The solution of system (4.19) clearly depends on parameters D_n and α. In particular, the values of these parameters effects the wave speed. We show, below the effect each parameter has on the wave speed.

1- The Diffusion coefficient , D_n.

Two solutions to the system (4.19) for $[D, \alpha] = [0.001, 1]$ and $[1, 1]$ respectively are illustrated in Fig. (4.10a, b). Of these, the second propagates at a considerably faster rate than the first with respect to same normalized units. Altering D_n essentially selects for faster waves as the most stable solutions to the system (4.19). This parameter thus modulates the growth rate. Fig. 4.10(c). illustrates that c is increasing when D_n increase, for higher D_n values the propagation speed is large.

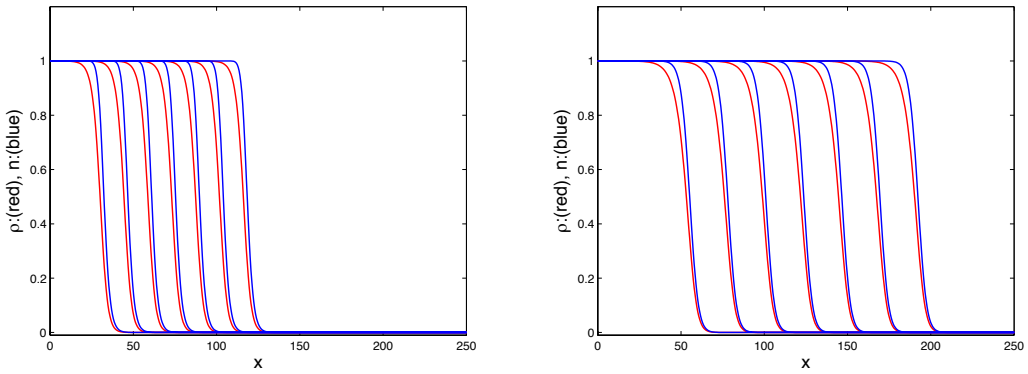

(a) (b)

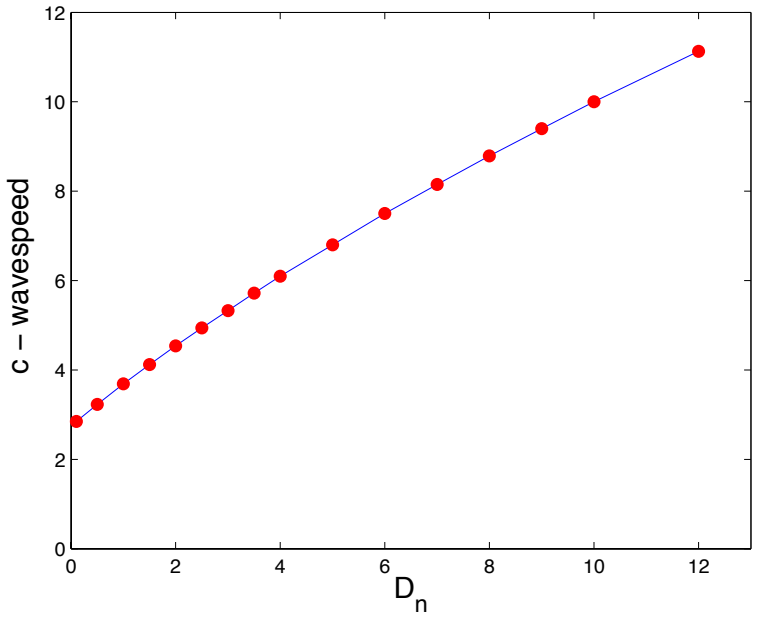

(c)

Figure 4.10: Solution to the system (4.18) with the parameters taking values of (a) α=2 and D_n= 0. 1 (b) α=2 and D_n= 2. For higher D_n values the propagation speed is larger. The time spacings: $10m$ where $m = 3, 4, ..., 9$.($c = 2.85$ for $D_n = 0.1$ and $c = 4.54014$ for $D_n = 2$). (c) The relation between c and D_n where α=2. Here we note that when diffusion D_n is increasing then wavespeed c still increasing

2- The parameter coefficient , α.

Two solution to the system (4.19) for $[D, \alpha] = [0.5, 0.5]$ and $[0.5, 5]$ respectively are illustrated in Fig. (4.11a, b). Of these, the second propagates at a considerably faster rate than the first with respect to same normalized units $\bar{\rho}$. Altering α essentially selects for faster waves as the most stable solutions to the system (4.18). ($c = 1.91024$ for $\alpha = 0.5$ and $c = 4.97$ for $\alpha = 5$). This parameter thus modulates the growth rate.

Fig. 4.12. illustrates that c is increasing when α increase, for higher α values the propagation speed is large. Since $\alpha = (\alpha_2 v/\gamma_1^2)$, that is mean α is increase when the parameter α_2 increase and fixed another parameters v and γ_1, similarly for the parameter v when fixed another parameters α_2 and γ_1, but α is decrease when the parameter γ_1 increase and fixed another parameters v and α_2.

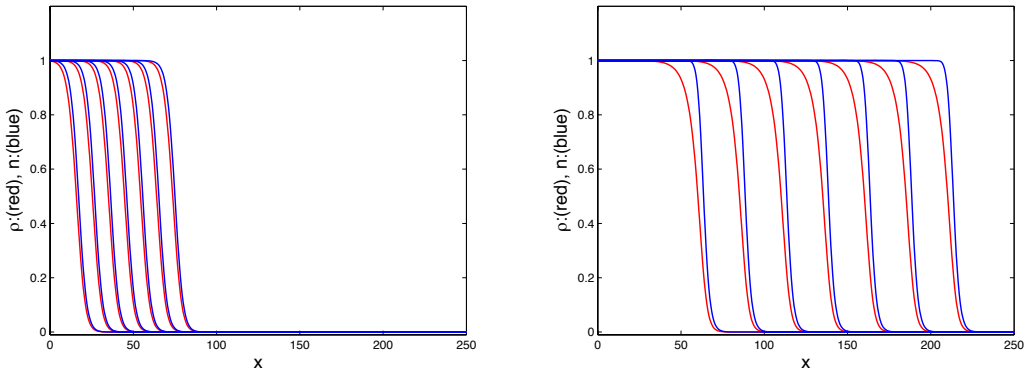

(a) (b)

Figure 4.11: Solution to the system (4.18) with the parameters are taking values of (a) α=0.5, and D_n= 0.5. (b) α= 5 and D_n= 0.5. For higher D_n values the propagation speed is large.($c = 1.91024$ for $\alpha = 0.5$ and $c = 4.97$ for $\alpha = 5$). The time spacings: $10m$ where $m = 3, 4, ..., 9$.

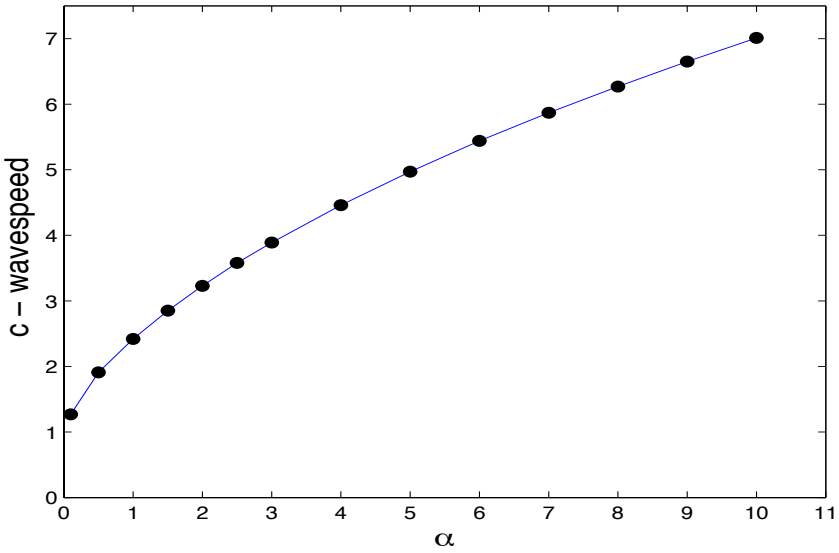

Figure 4.12: (c) The relation between c and α where D_n=0.5. Here we note that when diffusion α is increasing then wavespeed c still increasing.

4.4.2 FX: Lateral branches with density limitation

The model system in this case

$$\begin{aligned} \frac{\partial \rho}{\partial t} &= |\epsilon \frac{\partial n}{\partial x} + nv| - \gamma_1 \rho, \\ \frac{\partial n}{\partial t} &= \epsilon \frac{\partial^2 n}{\partial x^2} - \frac{\partial (nv)}{\partial x} + \alpha_2 \rho - \beta_3 \rho^2. \end{aligned} \tag{4.21}$$

As above $\bar{\rho} = (\alpha_2/\beta_3)$, we have the system

$$\begin{aligned} \frac{\partial \rho}{\partial t} &= | - D_n \frac{\partial n}{\partial x} + n| - \rho, \\ \frac{\partial n}{\partial t} &= D_n \frac{\partial^2 n}{\partial x^2} - \frac{\partial n}{\partial x} + \alpha \rho (1 - \rho). \end{aligned} \tag{4.22}$$

where $\alpha = (\alpha_2 v/\gamma_1^2)$. This single parameter represent the rate of hyphal per unit length hypha per unit time. As a first step, we look for uniform steady states of system (4.22) i.e seek solution of $n - \rho = 0$, $\alpha\rho(1 - \rho) = 0$. Therefore there are two steady state: $(0, 0)$ and $(1, 1)$. Following standard procedure it can be

easily show that $(0,0)$ is a saddle point and $(1,1)$ is a stable spiral of the kinetic problem associated with (4.22).

As above section, we get

$$\begin{bmatrix} P' \\ N' \\ U' \end{bmatrix} = \begin{bmatrix} \frac{-1}{c}[|-U+N|-P] \\ U \\ (1-c)U+\alpha P(1-P) \end{bmatrix} \tag{4.23}$$

System (4.23) has two steady states points $(0,0,0)$ and $(1,1,0)$. Their stability depends on the value of c.

When $c>0$ and $1 \geq 4\alpha c$, $(0,0,0)$ has a two-dimensional unstable manifold and a one-dimensional stable manifold and $(1,1,0)$ is an unstable node. $(0,0,0)$ has a two-dimensional unstable manifold and a one-dimensional stable manifold and $(1,1,0)$ has a two-dimensional unstable spiral manifold and a one-dimensional stable manifold when $1<4\alpha c$.

When $c<0$, $(0,0,0)$ has a two-dimensional stable spiral manifold and one-dimensional unstable node, $(1,1,0)$ has a two-dimensional unstable manifold and a one-dimensional stable manifold. Here we can not show there is a trajectory connecting these in the (P,N,U) plane, therefore we go to numerical solution of initial value problem.

4.4.3 Numerical solution of initial value problem

Two solution to the system (4.22) for fixed $D_n = 0.001$ and α values of 0.5 and 2.5 are illustrated in Fig. (4.13a, b). Of these, the second propagates at a considerably faster rate than the first. Altering D_n essentially selects for faster waves as the most stable solutions to the system (4.22). (The wave speed $c = 2.23$ for $D_n = 0.1$ and $c = 4.55$ for $D_n = 2$ with fixed $\alpha = 2$). This parameter thus

provides the ability to modulate growth, so as to adapt to new situations, see Fig. 4.13.

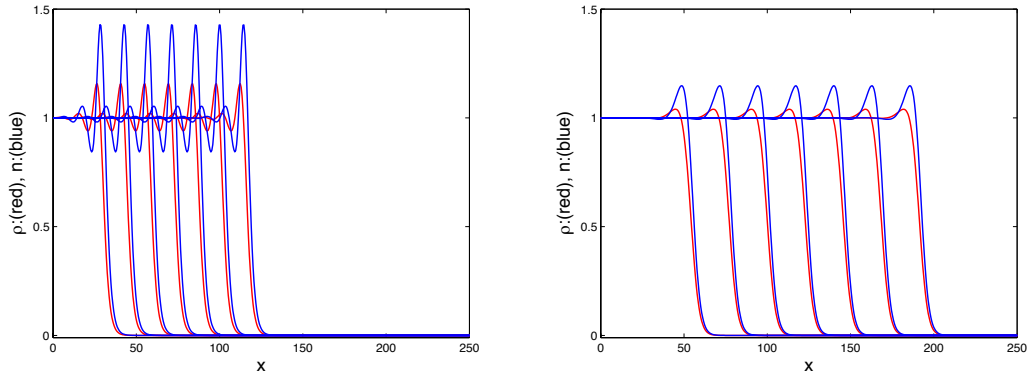

(a) (b)

Figure 4.13: Solution to the system (4.22) for type FXD with the parameters, $\alpha = 2$ D_n taking values of (a) 0.1 and (b) 2. Units of density and distance are normalized $\bar{\rho}$. The time spacings: $10m$ where $m = 3, 4, ..., 9$.

Altering α essentially selects for faster waves as the most stable solutions to the system (4.22). (The wave speed $c = 1.9189$ for $\alpha = 0.5$ and $c = 4.9719$ for $\alpha = 5$ with fixed $D_n = 0.5$). This parameter thus provides the ability to modulate growth, so as to adapt to new situations, see Fig. 4.14.

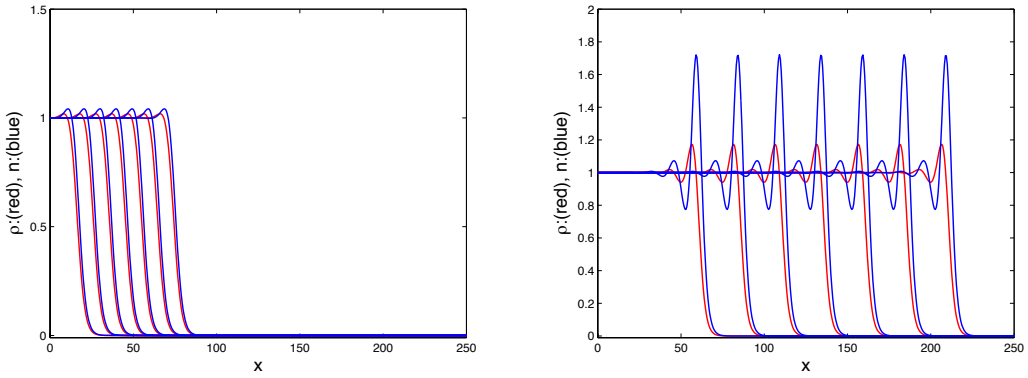

(a) (b)

Figure 4.14: Solution to the system (4.22) for type FXD with the parameters, $D_n = 0.5$ α taking values of (a) 0.5 and (b) 5. Units of density and distance are normalized $\bar{\rho}$. (c) For higher α values the propagation speed is large. The time spacings: $10m$ where $m = 3, 4, ..., 9$.

Fig. 4.14. illustrates that c is increasing when α increase, for higher α values the propagation speed is large, $\alpha = (\alpha_2 v/\gamma_1^2)$ that is mean α is increase when the parameter α_2 increase and fixed another parameters v and γ_1, similarly for the parameter v when fixed another parameters α_2 and γ_1, but α is decrease when the parameter γ_1 increase and fixed another parameters v and α_2.

From Fig. 4.13 and Fig. 4.14, we notes that when D_n increase then the profile of tips and branching approach to stable node while α increase then the profile of tips and branching increase to stable spiral (more complicated).

Fig. 4.15 illustrates that c is increasing when D_n increase, for higher D_n values the propagation speed is large and c is increasing when α increase, for higher α values the propagation speed is large.

Note also, the increasing α increases the number and size of the oscillation behind the leading edge. These oscillations represent (moving) bends of higher biomass and tip density. The size is number of oscillation is determined by the linear theory discussed above.

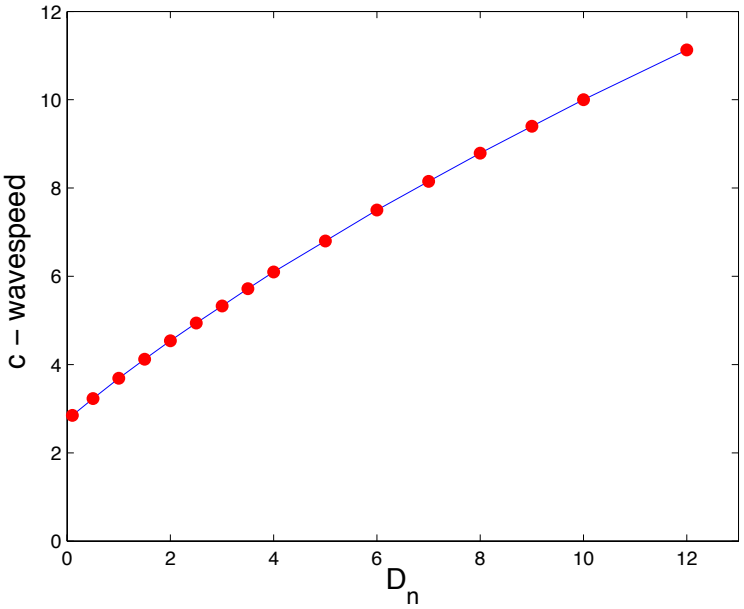

(a)

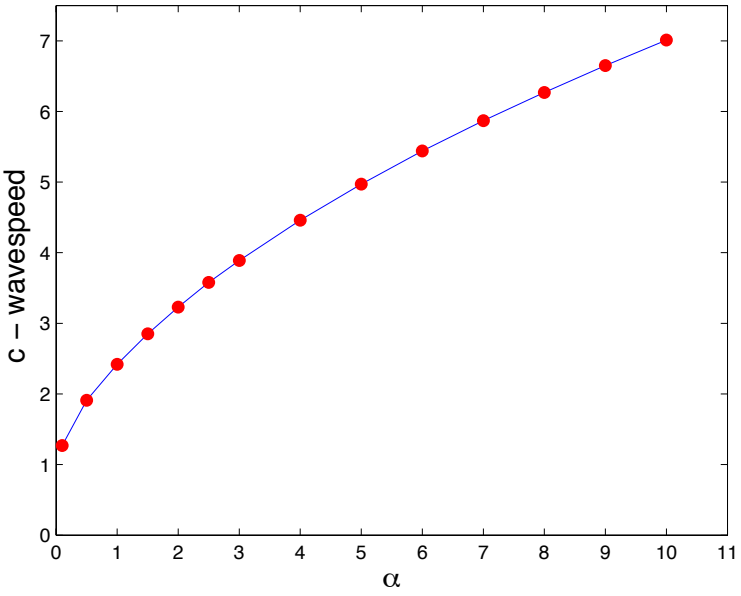

(b)

Figure 4.15: (a) The relation between D_n and speed where $\alpha = 2$. Here we note that when diffusion D_n is increasing then wavespeed c still increasing. (a) The relation between α and speed where $D_n = 0.5$. Here we note that when diffusion α is increasing then wavespeed c still increasing

4.5 Conclusion and Discussion

Hyphal death clearly eliminates excess accumulation in the colony interior so that growth can be more evenly distributed. The wavespeed c is increasing when values of diffusion D_n is increase. For examples, Fig. 4.16, illustrated the wavespeed is increasing when values for α and D_n are take the same values for every type branches. We note that the rate of wavespeed for YHD and YWD types are faster than the rate for FHD and FXD types for the value at the same values of α and D_n. So as this figure illustrated the wavespeed is increasing when values for α and D_n are fixed for every type branches.

From the Figures above we can clarify that the wavespeed c for the branches types FHD, FXD, YWD and YHD at the same values of α, D_n. Therefore now we can say the effect of diffusion on wave speed is that the value of diffusion increases when the wavespeed c is increases.

Table (4.1) illustrates the other biological types and the steady states that results from them. We noted the lateral branches, tip-hypha anastomoses FHD type; the lateral branches, tip-tip anastomoses FXD type; dichotomous, branches, tip-tip anastomoses YWD type have the same steady states; and dichotomous branches tip hyphae anastomoses YHD type have the same steady states $(0, 0, 0)$ and $(1, 1, 0)$. Hence the stability of the steady states depends on the value of c; $(0, 0, 0)$ is saddle point and $(1, 1, 0)$ unstable node or spiral when $c > 1$. $(0, 0, 0)$ is centre or spiral and $(1, 1, 0)$ saddle point when $0 < c < 1$. $(0, 0)$ is saddle point and $(1, 1, 0)$ stable node and when $c < 0$. From above information for this biological types there is travelling wave solution are satisfies for $c > 0$.

Examining Table (4.1) for the system have two steady states, there is a trajectory connecting these in the (P, N, U) - coordinates (a heteroclinic trajectory), these trajectory remains in the positive (P, N, U) quadrant; and $(P^o, N^o, U^o) = (0, 0, 0)$ is attractor for flow along the heteroclinic trajectory since it represents $z \to +\infty$ densities. There are two interesting implication of hyphal death. The first is that tip density in the interior of the colony is maintained at nonzero level ($N \neq 0, P \neq 0$ and $U \neq 0$).

Biological mean the old hyphae are weeded out, new growth is continually taking place. so that the density level is regulated in the (Edelstein, 1982) of the colony, as well as at the expanding margin.

The Table (4.1) shows the existence of a travelling wave solution for every type, that is satisfied when $c > 1$.

We can conclude the effect F and Y branching on the propagation of fungal colonies, where we get the Y type plus any other types still large from F plus the other types.

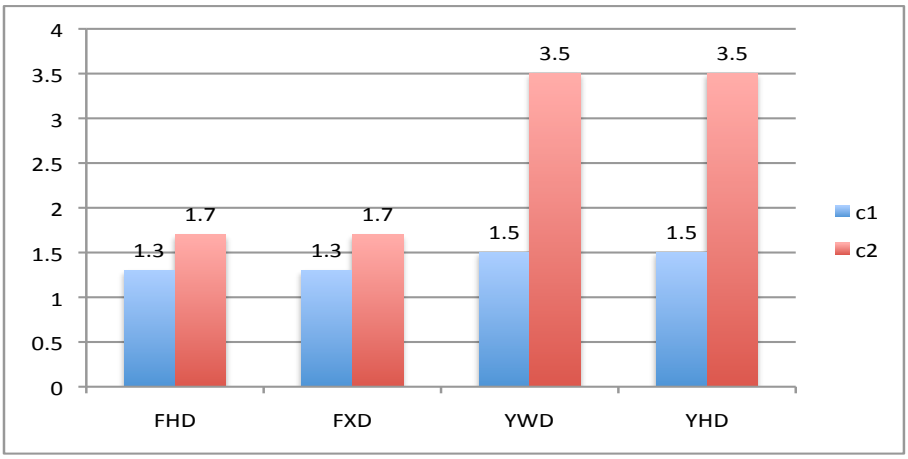

Figure 4.16: The chart represents wave speed c at the value of $D_n = 0.2$ and $\alpha = 0.5$ and $D_n = 1$, $\alpha = 2$ that represented c_1 and c_2 respectively. It is clear the wave speeds in FHD, FXD types approximately are equal and YWD, YHD types are equal at the value of D_n. The waves speed in YWD, YHD types larger than from FHD and FXD types at the same values of D_n and α. Apical branching produce fast growth.

Table 4.1: Simple branching type, tip diffusion and convection with $d = \gamma_1 \rho$

Biological Type	Symbol	Branching Rule σ	Choice of scales	Dimensionless equation for propagation	Steady state	Traveling wave
Lateral branches tip-hypha anastomoses with diffusion	FHD	$\sigma = \rho(\alpha_2 - \beta_2 n)$	$\bar{n} = \alpha_2/\beta_2$ $\tau = 1/\gamma_1$ $\bar{\rho} = \alpha_2 v/\gamma_1\beta_2$	$dP/dz = \frac{-1}{c}[N - P]$ $dU/dz = (1-c)U + \alpha P(1-N)$ $dN/dz = U$	$(0,0,0)$ $(1,1,0)$	all satisfied for $c > 0$
Lateral branches with density limitation with diffusion	FXD	$\sigma = \rho(\alpha_2 - \beta_3 \rho)$	$\bar{\rho} = \alpha_2/\beta_3$ $\tau = 1/\gamma_1$ $\bar{n} = \alpha_2\gamma_1/v\beta_3$	$dP/dz = \frac{-1}{c}[N - P]$ $dU/dz = (1-c)U + \alpha P(1-P)$ $dN/dz = U$	$(0,0,0)$ $(1,1,0)$	all satisfied for $c > 0$
Dichotomous branches, tip-tip anastomoses with diffusion	YWD	$\sigma = n(\alpha_1 - \beta_1 n)$	$\bar{n} = \alpha_1/\beta_1$ $\tau = 1/\gamma_1$ $\bar{\rho} = v\alpha_1/\gamma_1\beta_1$	$dP/dz = \frac{-1}{c}[N - P]$ $dU/dz = (1-c)U + \alpha N(1-N)$ $dN/dz = U$	$(0,0.0)$ $(1,1,0)$	all satisfied for$c > 0$
Dichotomous branches tip - hyphae anastomoses with diffusion	YHD	$\sigma = n(\alpha_1 - \beta_2 \rho)$	$\bar{\rho} = \alpha_1/\beta_2$ $\tau = 1/\gamma_1$ $\bar{n} = \alpha_1\gamma_1/v\beta_2$	$dP/dz = \frac{-1}{c}[N - P]$ $dU/dz = (1-c)U + \alpha N(1-P)$ $dN/dz = U$	$(0,0,0)$ $(1,1,0)$	all satisfied for $c > 0$

Chapter 5

The Effects of Substrate on The Development of Fungal Networks

5.1 Introduction

Boswell et al. (2002) derived a model of mycelial growth which combines elements from the models of Edelstein - Keshet *et al.* and Davidson *et al.*, and reformulated the manner in which certain processes are modelled. In particular, they reconsidered the mechanisms that may be responsible for substrate translocation and develop models appropriate for 2-D geometries.

In this chapter, we will study, modelling the effects of substrate on the development of fungal networks. The main aim in this Chapter is to ascertain the role of substrate in the model.

Their models consist of a system of partial differential equations where the variables denote hyphal density, tip density and concentration of a growth - limiting substrate.

A series of papers by Davidson et al. (1996), Davidson (1998), Davidson and Olsson (2000) provide a description of growth by focussing on the macroscopic development of fungal mycelium. In (Davidson, 1998), the system was considered to comprise three main elements: a biomass density, an internal substrate concentration and an external substrate concentration, and translocation was assumed to occur by diffusion alone. Fungal growth and subsequent substrate depletion was modelled by a system of reaction - diffusion equations, where the flux and reaction terms were chosen to represent important qualitative features associated with mycelial growth. In Davidson and Olsson (2000), an active translocation mechanism was introduced where the flux of material was modelled via a convection term (where the velocity is substrate dependent) directed towards the edge of the fungal colony. The results of this model are in good qualitative and quantitative agreement with a set of experiments on out-growth of *Arthrobotrys superba* in nutrient - free environment (Persson et al., 2000).

5.1.1 Modelling

The model consider the fungal mycelium as a continuous distribution consisting of three components:

$\rho(x,t)$, $n(x,t)$ are define as before, s denotes the interaction of a nutrient source or substrate.

Now

$$\frac{\partial \rho}{\partial t} = \underbrace{f_\rho(\rho, n, s)}_{\text{new hyphae - inactivated hyphae}}, \tag{5.1a}$$

$$\frac{\partial n}{\partial t} = -\frac{\partial}{\partial x}\underbrace{J_n(\rho, n, s)}_{\text{tip migration}} + \underbrace{f_n(\rho, n, s)}_{\text{branching- anastomosis}}, \tag{5.1b}$$

$$\frac{\partial s}{\partial t} = -\frac{\partial}{\partial x}\underbrace{J_s(\rho, n, s)}_{\text{diffusion}} + \underbrace{f_s(\rho, n, s)}_{\text{-uptake}}, \tag{5.1c}$$

where J and f denote the flux (migration) and reaction (creation/loss) terms, respectively. The hyphal length created per unit time is absolute value of the tip flux: $|J_n|$ where

$$f_\rho = |J_n(\rho, n, s)| - d\rho, \tag{5.2}$$

we assume that unit length hyphal branching rate depends on s as it brown that substrate availability and turgor pressure play important roles in remediating branching (Gruhn et al., 1992); we assume it is a linear relationship. We take the per unit length branching rate to be $\alpha_2 s$, where α_2 non negative and define before. Now let us define the total rate of loss of tips by mathematical symbol $\beta_2 n\rho$, where β_2 is non negative and define as before. So that f_n take this form

$$f_n = \sigma(\rho, n, s) = \alpha_2 \rho s - \beta_2 n\rho. \tag{5.3}$$

Let f_s the rate the substrate is used. The uptake modelled by kn where k is a positive constant.

The fungi uses substrate in a number of ways: uptake, maintenance, transaction and growth. The term f_s, which corresponding to the rate of substrate depletion from the environment, should take a similar form to the uptake term specified above, as

$$f_s = -kn, \tag{5.4}$$

where k non - negative constant.

We note that this term would allow substrate to become regulative. However, as will be shown later, $n \to 0$ as $s \to 0$ and therefore this problematic case does not arise.

Hyphal growth is impossible in the absence of substrate supply and to include this essential feature, let us assume that the speed of tip movement is proportional to the amount of the substrate at the tip. In this case, the tip flux take the form

$$J_n = |-D_n \frac{\partial n}{\partial x} + vsn|, \tag{5.5}$$

where v some positive constant and D_n tip diffusion and it is non - negative constant. The next, the substrate is suppose to diffuse in a standard Fickian manner, that is,

$$J_s = -D_s \frac{\partial s}{\partial x}, \tag{5.6}$$

where D_s is a non - negative constant.

Therefore, the system we will consider takes the form

$$\begin{aligned}
\frac{\partial \rho}{\partial t} &= |-D_n \frac{\partial n}{\partial x} + vns| - d(\rho), \\
\frac{\partial n}{\partial t} &= D_n \frac{\partial^2 n}{\partial x^2} - \frac{\partial (vns)}{\partial x} + \alpha_2 \rho s - \beta_2 n \rho, \\
\frac{\partial s}{\partial t} &= D_s \frac{\partial^2 s}{\partial x^2} - kn,
\end{aligned} \tag{5.7}$$

In the following sections, we will study effects that explain including substrate has on the modelling of colony growth. We will study properties of simple branching types with $d(\rho) = 0$ with convection or with diffusion and convection, of tips as examples.

5.2 FHS: Lateral Branching, Tip - Hypha Anastomoses with Substrate

The model system in this case is

$$\begin{aligned}
\frac{\partial \rho}{\partial t} &= |-D_n \frac{\partial n}{\partial x} + vns|, \\
\frac{\partial n}{\partial t} &= D_n \frac{\partial^2 n}{\partial x^2} - \frac{\partial (vns)}{\partial x} + \alpha_2 \rho s - \beta_2 n \rho, \\
\frac{\partial s}{\partial t} &= D_s \frac{\partial^2 s}{\partial x^2} - kn,
\end{aligned} \tag{5.8}$$

where $\rho(x,t)$, $n(x,t)$, v, α_2 and β_2, are define above, $s(x,t)$ is substrate, and k is constant.

To clarify the effect of parameters on the wave speed c therefore, we will study the system (5.8) without non - dimensionalising. We will study and plot the relation between wave speed c and each parameter in turn.

To studying lateral branching, tip - hypha anastomoses with the substrate with

convection, let us assume $v \neq 0$, D_n, $D_s = 0$. Therefore the system (5.8) becomes

$$\begin{aligned} \frac{\partial \rho}{\partial t} &= nvs, \\ \frac{\partial n}{\partial t} &= -\frac{\partial (vns)}{\partial x} + \alpha_2 \rho s - \beta_2 n \rho, \\ \frac{\partial s}{\partial t} &= -kn. \end{aligned} \tag{5.9}$$

5.2.1 Stability of uniform solutions

As a first step, we look for uniform steady states of system (5.9), and thus seek solutions of the algebraic equations

$$nvs = 0, \quad \rho(\alpha_2 s - \beta_2 n) = 0, \quad \text{and} \quad -kn = 0.$$

Clearly, there are two lines of biologically relevant steady states: $(\rho_o, 0, 0)$ and $(0, 0, s_o)$, for (non-negative) constants ρ_o and s_o.

Now, the Jacobian associated with system (5.9) at $(\hat{\rho}, \hat{n}, \hat{s})$ is

$$J = \begin{bmatrix} 0 & v\hat{s} & v\hat{n} \\ \alpha_2 \hat{s} - \beta_2 \hat{n} & -\beta_2 \hat{\rho} & \alpha_2 \hat{\rho} \\ 0 & -k & 0 \end{bmatrix},$$

and hence at $(\rho_o, 0, 0)$,

$$J = \begin{bmatrix} 0 & 0 & 0 \\ 0 & -\beta_2 \rho_o & \alpha_2 \rho_o \\ 0 & -k & 0 \end{bmatrix},$$

eigenvalues are λ_1=0, $\lambda_2 = \frac{-\beta_2\rho_o+\sqrt{{\beta_2}^2\rho_o^2-4\alpha_2 k\rho_o}}{2}$ and $\lambda_3 = \frac{-\beta_2\rho_o-\sqrt{{\beta_2}^2\rho_o^2-4\alpha_2 k\rho_o}}{2}$ with the corresponding eigenvectors,

$$\overrightarrow{e_1} = \begin{bmatrix} 1 \\ 0 \\ 0 \end{bmatrix}, \quad \overrightarrow{e_2} = \begin{bmatrix} 0 \\ \lambda_2/k \\ 1 \end{bmatrix}, \quad \text{and} \quad \overrightarrow{e_3} = \begin{bmatrix} 0 \\ \lambda_3/k \\ 1 \end{bmatrix}.$$

The ode assaulted with (5.9) has one dimensional centre manifold and two dimensional stable manifold.

When $\rho_o \geq (\frac{4\alpha_2 k}{\beta_2^2})$, the stable component is given by a stable node, if $\rho_o < (\frac{4\alpha_2 k}{\beta_2^2})$ it is a stable focus.

The Jacobain at $(0, 0, s_o)$ is

$$J = \begin{bmatrix} 0 & vs_o & 0 \\ \alpha_2 s_o & 0 & 0 \\ 0 & -k & 0 \end{bmatrix},$$

which has eigenvalues $\lambda_1 = 0$, $\lambda_2 = \sqrt{\alpha v} s_o$ and $\lambda_3 = -\sqrt{\alpha v} s_o$, with the corresponding eigenvectors,

$$\overrightarrow{e_1} = \begin{bmatrix} 0 \\ 0 \\ 1 \end{bmatrix}, \quad \overrightarrow{e_2} = \begin{bmatrix} -\frac{sv}{k} \\ -\frac{\lambda_2}{k} \\ 1 \end{bmatrix}, \quad \text{and} \quad \overrightarrow{e_3} = \begin{bmatrix} -\frac{sv}{k} \\ -\frac{\lambda_3}{k} \\ 1 \end{bmatrix}.$$

Therefore $(0, 0, s_o)$ is a saddle point .

5.2.2 Travelling wave solution

As above we seek solutions of the for $P(z), N(z), S(z)$, where $z = x - ct$. Thus we can reduce the system (5.9) to a set of three ordinary differential equation:

$$\begin{aligned}
\frac{dP}{dz} &= -\frac{1}{c}[vNS], \\
\frac{dN}{dz} &= \frac{1}{(vS-c)}[-\frac{kv}{c}N^2 + P(\alpha_2 S - \beta_2 N)], \quad vS \neq c, \\
\frac{dS}{dz} &= \frac{k}{c}N.
\end{aligned} \tag{5.10}$$

As above we can find steady states for the system (5.10). Therefore we have two lines of steady states $(P_o, 0, 0)$ and $(0, 0, S_o)$. Now, the Jacobian associated with system (5.10) at $(\hat{P}, \hat{N}, \hat{S})$ is

$$J = \begin{bmatrix} 0 & -\frac{v\hat{S}}{c} & -\frac{v\hat{N}}{c} \\ \frac{(\alpha_2\hat{S}-\beta_2\hat{N})}{(v\hat{S}-c)} & \frac{\frac{-2kv\hat{N}}{c}-\beta_2\hat{P}}{(v\hat{S}-c)} & -\frac{v[\frac{-kv\hat{N}^2}{c}+\hat{P}(\alpha_2\hat{S}-\beta_2\hat{N})]}{(v\hat{S}-c)^2} + \frac{\alpha_2\hat{P}}{(v\hat{S}-c)} \\ 0 & \frac{k}{c} & 0 \end{bmatrix}.$$

Therefore the Jacobain at $(P_o, 0, 0)$ is

$$J_{(P_o,0,0)} = \begin{bmatrix} 0 & 0 & 0 \\ 0 & \frac{\beta_2 P_o}{c} & -\frac{\alpha_2 P_o}{c} \\ 0 & \frac{k}{c} & 0 \end{bmatrix},$$

which has eigenvalues λ_1=0, $\lambda_2 = \frac{P_o\beta_2 + \sqrt{P_o^2\beta_2^2 - 4P_o\alpha_2 k}}{2c}$ and $\lambda_3 = \frac{P_o\beta_2 - \sqrt{P_o^2\beta_2^2 - 4P_o\alpha_2 k}}{2c}$ with the corresponding eigenvectors,

$$\overrightarrow{e_1} = \begin{bmatrix} 1 \\ 0 \\ 0 \end{bmatrix}, \quad \overrightarrow{e_2} = \begin{bmatrix} 0 \\ c\lambda_2/k \\ 1 \end{bmatrix}, \quad \text{and} \quad \overrightarrow{e_3} = \begin{bmatrix} 0 \\ c\lambda_3/k \\ 1 \end{bmatrix}.$$

Thus system (5.10) has one dimensional centre manifold and two dimensional unstable manifold. When $P_o \geq (4\alpha_2 k/\beta_2^2)$ the unstable component is given by an unstable node, if $P_o < (4\alpha_2 k/\beta_2^2)$ it is an unstable. When $P_o \geq (4\alpha_2 k/\beta_2^2)$ the unstable component is given by a unstable node, if $P_o < (4\alpha_2 k/\beta_2^2)$ it is a stable focus, when $c < 0$.

The Jacobain at $(0, 0, S_o)$ is

$$J_{(0,0,S_o)} = \begin{bmatrix} 0 & \frac{-vS_o}{c} & 0 \\ \frac{\alpha_2 S_o}{(vS_o - c)} & 0 & 0 \\ 0 & \frac{k}{c} & 0 \end{bmatrix},$$

which has eigenvalues λ_1=0, $\lambda_2 = \frac{\sqrt{\alpha_2 cv(c-vS_o)}S_o}{c(c-vS_o)}$ and $\lambda_3 = -\frac{\sqrt{\alpha_2 cv(c-vS_o)}S_o}{c(c-vS_o)}$, with the corresponding eigenvectors,

$$\overrightarrow{e_1} = \begin{bmatrix} 0 \\ 0 \\ 1 \end{bmatrix}, \quad \overrightarrow{e_2} = \begin{bmatrix} -sv/k \\ c\lambda_2/k \\ 1 \end{bmatrix}, \quad \text{and} \quad \overrightarrow{e_3} = \begin{bmatrix} -sv/k \\ c\lambda_3/k \\ 1 \end{bmatrix}.$$

$(0, 0, S_o)$ is saddle point when $c > vS_o$, $c > 0$, and it is an stable focus when $0 < c < vS_o$. This point is a saddle when $c < 0$. Here when fixed c then eigenvalues λ real positive $\forall\ 0 \leq S_o < c$, and as $S_o \to c$, $\lambda \to \infty$. From this analysis we have:

i. Fixed c. no biological realistic travelling waves exists with $vS_o > c$.

ii. For any gives S_o any biological realistic travelling waves that exists must have $c > vS_o$.

The condition on the wave corresponding to the initial value problem are

$$(P(z), N(z), S(z)) \to (P_o, 0, 0) \quad as \quad z \to -\infty,$$
$$(P(z), N(z), S(z)) \to (0, 0, S_o) \quad as \quad z \to +\infty$$

Since P_o, N_o and S_o represent concentrations, we are only concerned with biologically relevant non - negative solution.

Two equilibria of system (5.10) is thus ensured. Provided conditions: there is a trajectory of system (5.10) connecting these in the (P, N, S) space and this trajectory remains in the positive (P, N, S) quadrant, are also met. The potential for a heteroclinic trajectory representing a bounded travelling wave solution is established.

The equilibrium in positive (P, N, S) quadrant is such that $N \neq 0$, $P \neq 0$ and $S \neq 0$ implying that the wave level at $z \to -\infty$ is $N \neq 0$, $P \neq 0$ and $S \neq 0$.

5.2.3 Numerical solution of initial value problem

In order to extend the analysis conducted above we solved the initial value problem numerically, as described using MATLAB "pdepe".

The numerical results reveal that a wave front forms from the initial data and, as expected, the ρ, n and s wave fronts interact due to the autocatalytic coupling. These fronts persist for suitable parameter choices. The solution of system (5.9) depends on parameters α_2, β_2, v, and k. We choose the values for these parameters such that the above the condition for stability are satisfied. Fig. 5.1 shows the solution type obtained for $\alpha = 0.4$, β=1.265, $v = 1$, $k = 0.5$. This figure confirms that the wave front connects the unstable uniform steady state $(\rho_o, 0, 0)$ to the stable uniform steady state $(0, 0, s_o)$, (here $\rho_o = 1$ and $s_o = 1$).

Fig. 5.1 illustrates profile of the branching, tips and substrate. The travelling

wave moves from left to right. Fig. 5.2 illustrates the relation between time t and $\rho(x,t) = 1/2$, that helps us to clearly the slope is straight line conferring that the front moves with constant speed.

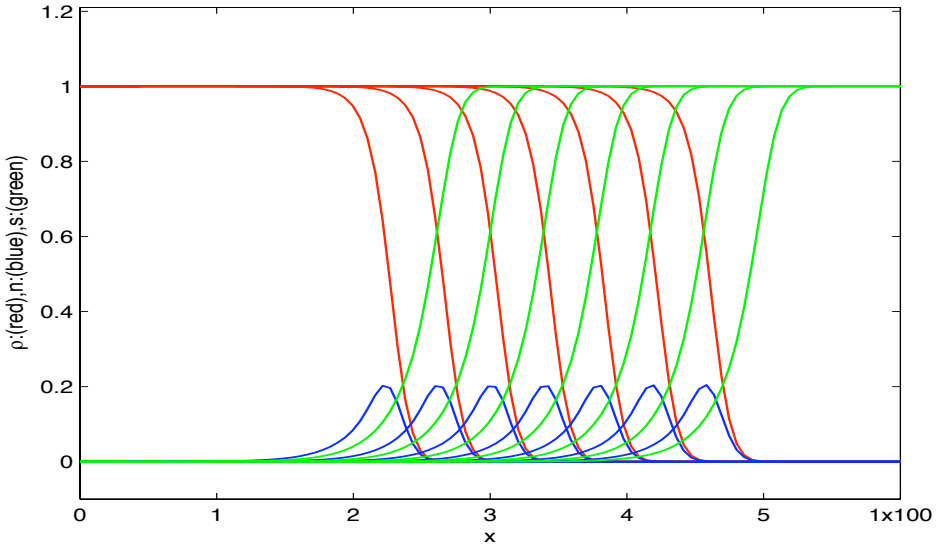

Figure 5.1: Right travelling wave solution of the system (5.9): (red) is ρ, (blue) is n and (green) is s, with parameters taking values as (α =0.4, β=1.265, v =1, k =0.5. The time spacings: 30,40,50,60,70,80,90,100.

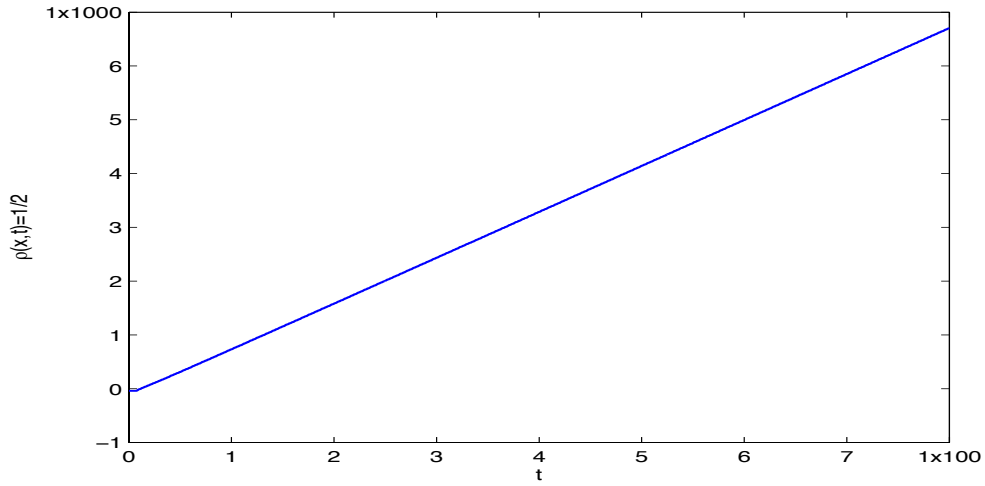

Figure 5.2: The relation between time t and $\rho(x,t) = 1/2$. Here the slope produces a value for $(c = 8.3175)$.

5.2.4 The effects of parameters on the solution behaviour

The solution of system (5.9) depends on parameters α_2, β_2, v, and k. The values of these parameters effect the wave speed. We will study the effects or properties of each parameter in turn, as below:

1 - The effects of α_2 on the solution behaviour

There are two solutions to the system (5.9) for the above values of parameters which are illustrated in Fig. (5.3a, b). Of these, the second propagates at a considerably faster rate than the first with respect to the same normalized unit. The solution of the system (5.9) for $\alpha_2 = 1.5$, $\beta_2 = 4$, $v = 1$, and $k = 0.5$ produces wave speed $(c = 3.060272)$. However, the value $\alpha_2 = 5$ with fixed other parameters produces wave speed $(c = 5.11689)$. From Fig. (5.3 a, b), we note the profile of variable n (blue) is highs when the value of the parameter α_2 increases. As solution in Fig. 5.4 illustrates the wave speed increases with α_2.

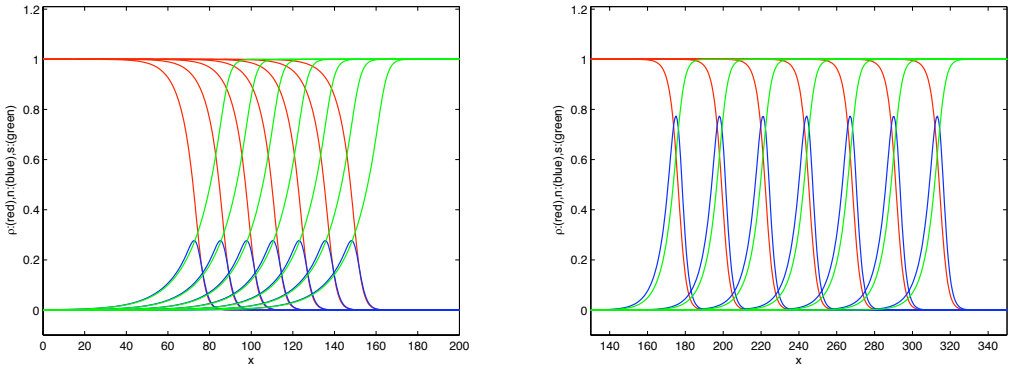

(a) (b)

Figure 5.3: Solution of PDEs system (5.9) for type FHS with the parameters α_2, β_2, v, k. taking values of (a) $\alpha_2 = 1.5$, $\beta_2 = 4$, $v = 1$, $k = 0.5$ and (b) $\alpha_2 = 5$, $\beta_2 = 4$, $v = 1$, $k = 0.5$. For α_2 values the propagation speed is larger. The time spacings: 30,40,50,60,70,80,90,100.

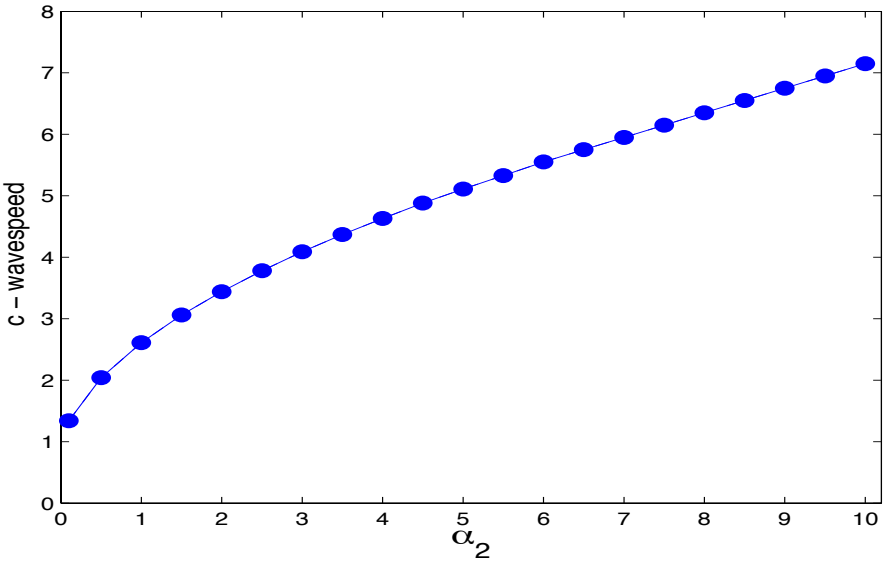

Figure 5.4: The relation between the parameter α_2 and waves speed c, where c evaluate from slope as above Fig. (5.2), when $\rho = 1/2$. The parameters taking fixed values β_2=4, v =1, k =0.5 and change values α_2. For α_2 values the propagation speed is larger.

2 - The effects of β_2 on the solution behaviour

Changing the rate of anastomosis, β_2, can not alter the colony growth rate. From Fig. (5.5a, b), we note the profile of variable n (blue) lower when the value of the parameter β_2 increasing. The wave speed for ρ and s is $c = 2.613$ for all values of β_2. Fixed values parameters α_2, v, and k are taken $1, 1, 0.5$ respectively and we change values of β_2=1.5 and 4. See Fig. (5.5a, b). Here we get values of wave speed $c = 2.613$ or slightly change. That is clear the wave speed no change for varying parameter β_2 values or the change almost slight.

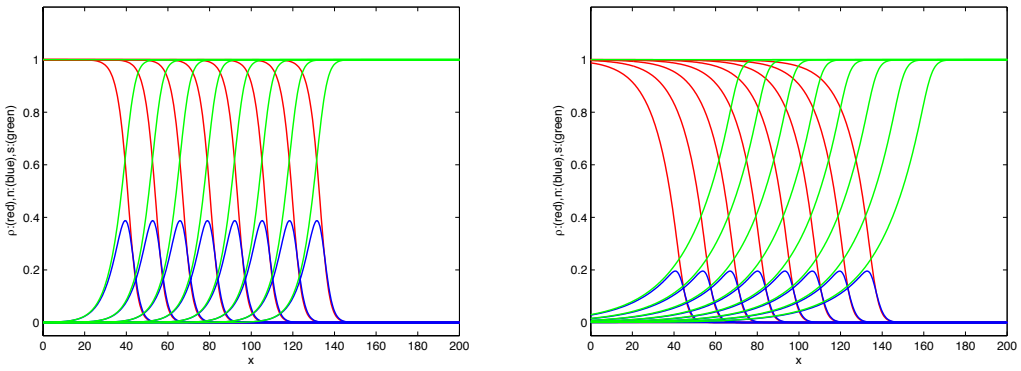

(a) (b)

Figure 5.5: Solution PDEs system (5.9) for type FHS with the parameters α_2, β_2, v, k. taking values of (a) α_2 =1, β_2= 1.5, v =1, k =0.5 and (b) α_2 =1, β_2=4, v =1, k =0.5. Here the wave speed was $c = 2.613$. The time spacings: 30,40,50,60,70,80,90,100.

3 - The effects of v on the solution behaviour

The similar methods as above. Fig. 5.6 illustrate the relation between the parameter v and wave speed c. In this case fixed the values of parameters α_2, β_2, and k are taken the values $1, 4, 0.5$ and change values of v. Afterwards evaluate the slopes for each case. Therefore, the v values the propagation speed is larger. Here, the relation between the parameter v and wave speed c is linearly, see Fig. 5.6.

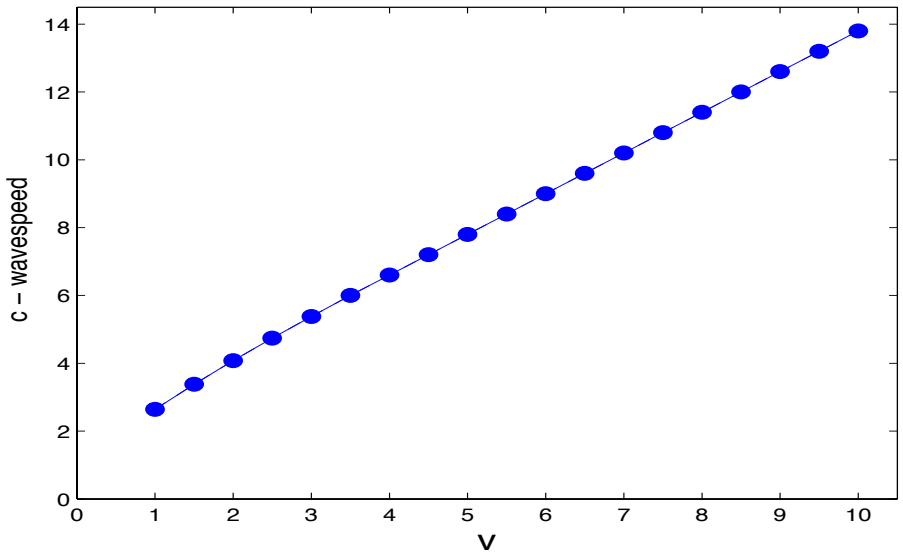

Figure 5.6: The relation between the parameter v and waves speed c, where c evaluate from slope as above, when $\rho = 1/2$. The parameters taking fixed values α_2=1, β_2 = 4, k =0.5 and change values v. For v values the propagation speed is larger.

4 - The effects of k on the solution behaviour

The wave speed slightly decreases when the values of the parameter k increases. The profile of tips n and branching ρ are decrease when values k increased, see Fig. (5.7a, b). We fixed the values of parameters α_2, β_2, and v are taken the values $1, 7, 1$ and change values of k such that satisfies the condition as above regarding the existence of travelling waves. From Fig. (5.7a, b), we note the profile of variable ρ (red) decrease when value of the parameter k increasing.

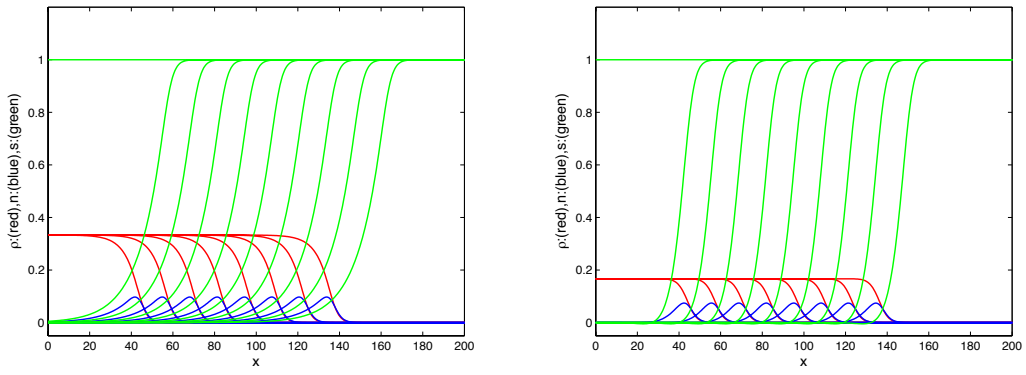

(a) (b)

Figure 5.7: Solution PDEs system (5.9) for type FHS with the parameters α_2, β_2, v, k. taking values of (a) $\alpha_2 = 1, \beta_2 = 7, v = 1$ and $k = 1.5$ and (b) $\alpha_2 = 1, \beta_2 = 7, v = 1$ and $k = 3$. Here, we note that the profile of tips n and branching ρ are reduced when values k increased. The time spacings: 30,40,50,60,70,80,90,100.

5.3 Lateral Branching, Tip - Hypha Anastomoses with Substrate (FHS), with Convection and Diffusion

We now assume $v \neq 0$, $D_n \neq 0$ and $D_s \neq 0$, therefore the system (5.8) becomes

$$\begin{aligned} \frac{\partial \rho}{\partial t} &= |-D_n \frac{\partial n}{\partial x} + vns|, \\ \frac{\partial n}{\partial t} &= D_n \frac{\partial^2 n}{\partial x^2} - \frac{\partial (nvs)}{\partial x} + \alpha_2 \rho s - \beta_2 n \rho, \\ \frac{\partial s}{\partial t} &= D_s \frac{\partial^2 s}{\partial x^2} - kn. \end{aligned} \tag{5.11}$$

Where $\rho(x,t)$, $n(x,t)$, v, α_2 and β_2, $s(x,t)$, and k are define above, $D_n \neq 0$ and $D_s \neq 0$ are diffusion for tips and substrate respectively. Previously, we focused on the effects of parameters on the development of fungal networks.

The solution of system (5.11) is dependent on parameters α_2, β_2, v, k, D_n and D_s. A previous section we showed the effects of the parameters on the solution behaviour of each parameter in turn. Next stage we will shows effects the diffusion D_n and D_s on the solution behaviour as below:

1 - The effects of D_n on the solution behaviour

There are two solutions to the system (5.11) for the above values of parameters which are illustrated in Fig. (5.8a, b). The solution of the system (5.11) for α_2, β_2, v, k, D_n and D_s values are taken $1, 4, 1, 0.5, 0.2$ and 0.2 respectively produces wave speed ($c = 2.77$). However, the value $D_n = 5$ with fixed other parameters produces wave speed ($c = 5.37$). Fig.(5.9) illustrates the relation between the parameter D_n and wave speed c where that is very clear when this parameter increases then the wave speed is increasing.

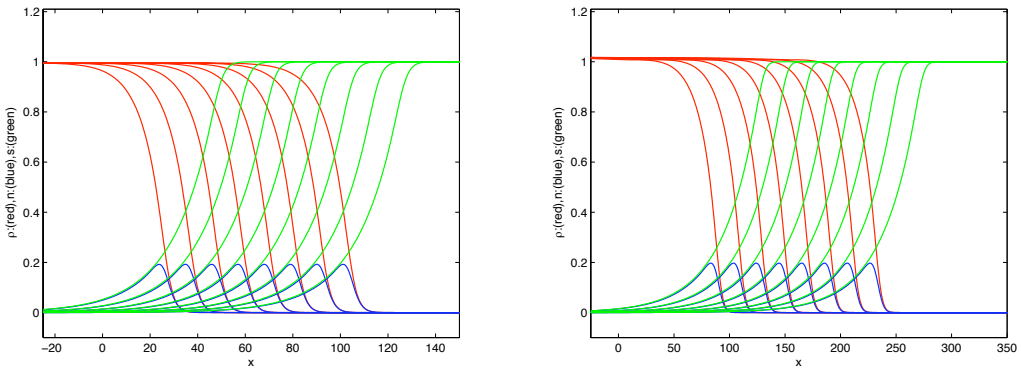

(a) (b)

Figure 5.8: Solution PDEs system (5.11) for type FHS with the parameters α_2, β_2, v, k, D_n and D_s. taking values of (a) α_2 =1, β_2=4, v =1, k =0.5, D_n= D_s=0.2 and (b) α_2 =1, β_2=4, v =1, k =0.5, D_n = 3, D_s=0.2. Here the wave speed in (a) $c = 2.77$ and in (b) $c = 5.37$. For D_n values the propagation speed is large. The time spacings: 30,40,50,60,70,80,90,100.

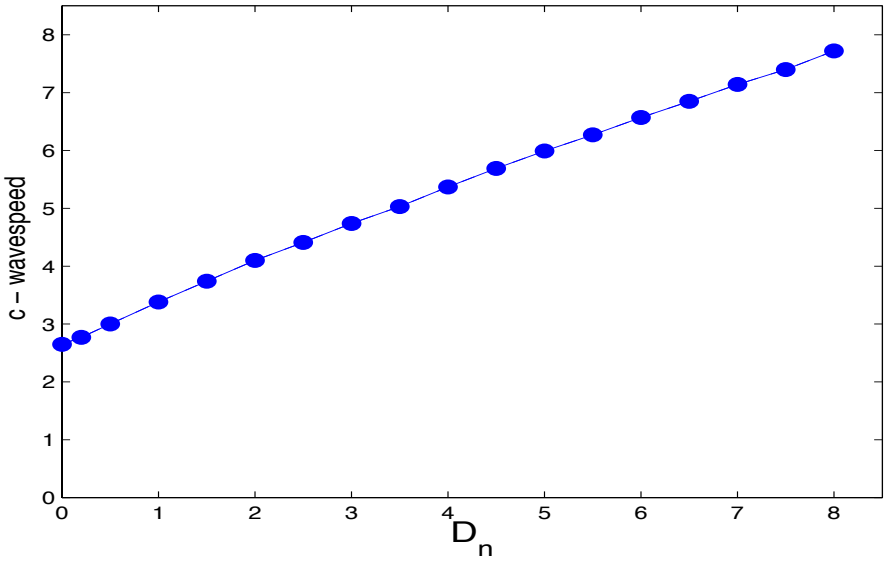

Figure 5.9: The relation between the parameter D_n and waves speed c, where c evaluate from slope as above. The parameters taking fixed values $\alpha_2 = 1$, $\beta_2 = 4$, $v = 1$, $k = 0.5$, $D_s = 0.2$ and change values D_n. For D_n values the propagation speed is larger.

2 - The effects of D_s on the solution behaviour

The parameter D_s does not alter the distribution for substrate. The wave speed no change for values D_s increasing. The solution of the system (5.11) for α_2, β_2, v, k, D_n and D_s values are taken $1, 4, 1, 0.5, 0.2$ and 0.01 respectively produces wave speed ($c = 2.1369$). However, the value $D_s = 0.5$ with fixed other parameters produces wave speed ($c = 2.1378$). We note the profile of variables ρ and s no change when value of the parameter D_s increases, see Fig. (5.10).

Fig. (5.11) illustrated the relation between the parameter D_s and wave speed c where that is clear the wave speed no change when the values of the parameter D_s increases.

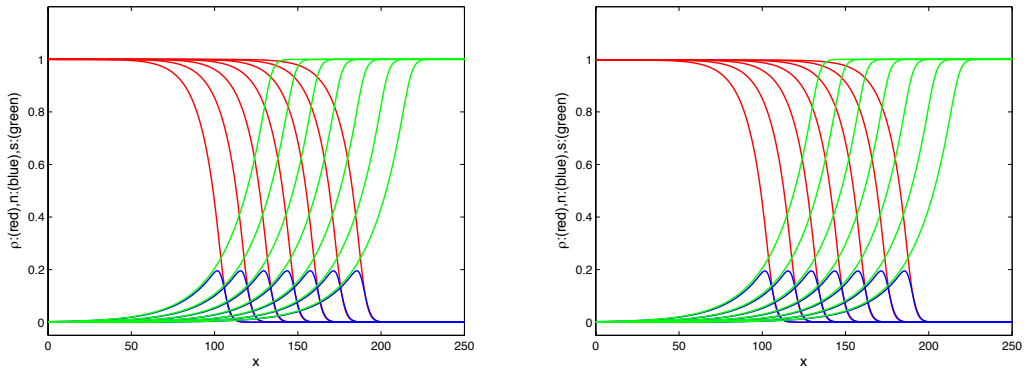

(a) (b)

Figure 5.10: Solution PDEs system (5.11) for type FHS with the parameters α_2, β_2, v, k, D_n and D_s. taking values of α_2 =1, β_2=4, v =1, k =0.5, D_n = 0.2 (a) $D_s = 0.01$. (b) $D_s = 0.5$. The time spacings: 30,40,50,60,70,80,90.

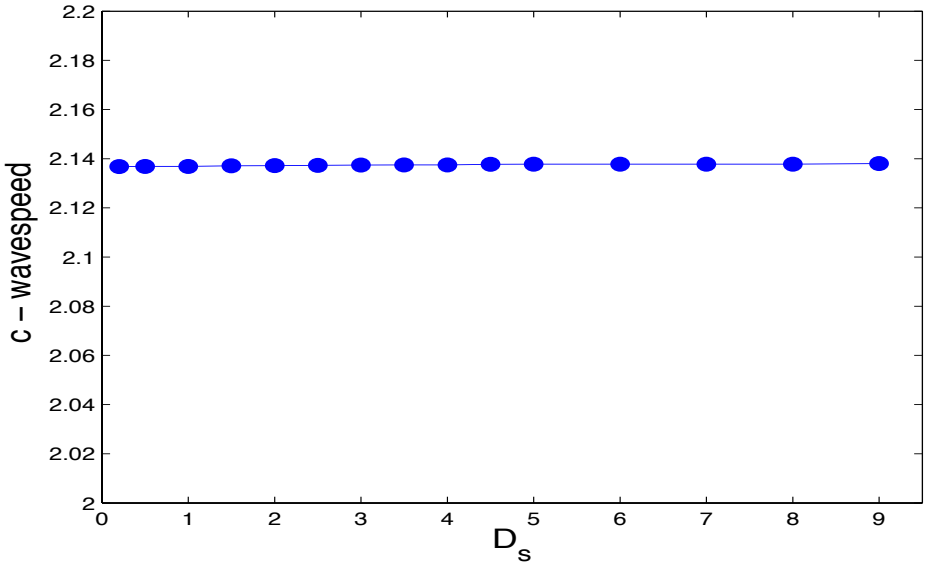

Figure 5.11: The relation between the parameter D_s and waves speed c, where c evaluate from slope as above, when $\rho = 1/2$. The parameters taking fixed values α_2=1, β_2 = 4, k =0.5, D_n=0.2 and change values D_s. For D_s values the propagation speed is no change.

3 - The effects of substrate on the solution behavior

To determine, the relation between change of s_o and the wave speed c. We will vary values of substrate s_o. System (5.11) has two steady states $(\rho_o, 0, 0)$ and $(0, 0, s_0)$, therefore we can change the position of ρ_o or s_o, such that this change preserves above conditions for stability. Fig. (5.12a, b and c) illustrated the relation between the parameter s_o and waves speed c, where c represented wave speed $\approx$ slpoe of the straight line represented the line which connected between mid point for profile of branching or substrate.

The parameters α_2, β_2 , k, D_n and D_s are fixed values and change values s_o. For s_o values the propagation speed is almost linearly dependent on s_o.

In Fig. 5.12(a), we take the values of parameters are $\alpha_2 = 1$, $\beta_2 = 4$, $v = 1$, $k = 0.5$, $D_n = 0.2$ and $D_s = 0.2$, the value of $s_o = 0.5$ if $x \to +\infty$ and $s_o = 0$ if $x \to -\infty$. Since the change in value of s_o effect on initial conditions of ρ_o and n_o, we notes $\rho_o = 0.25$ if $x \to -\infty$ and $\rho_o = 0$ if $x \to +\infty$ see Fig.5.12(a). We take the values of parameters as above, and change

$$s_o = \begin{cases} 2, & \text{if} \quad x \to +\infty, \\ 0, & \text{if} \quad x \to -\infty. \end{cases}$$

As above

$$\rho_o = \begin{cases} 4, & \text{if} \quad x \to -\infty, \\ 0, & \text{if} \quad x \to +\infty, \end{cases}$$

see Fig.5.12(b). n_o is increasing slightly. Fig.5.12(c) illustrated, the relation between the parameter s_o and waves speed c. For s_o values the propagation speed for substrate is increased. As S_o increases we see; Faster speed, wider colony periphery, more tips and more biomass.

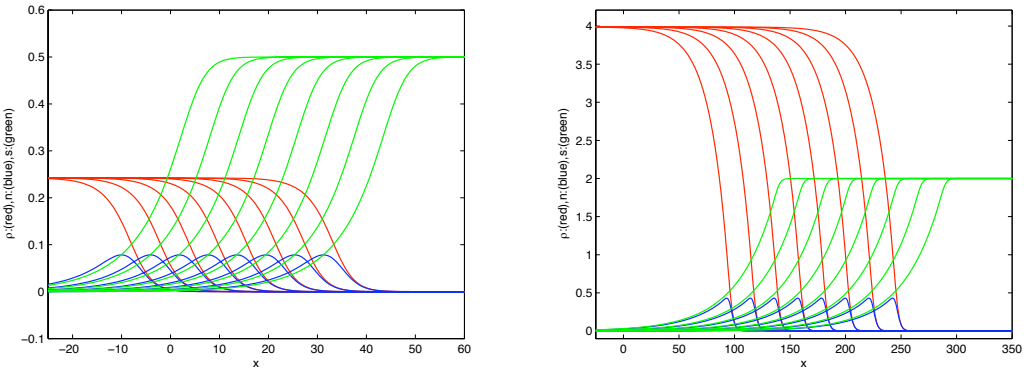

(a) (b)

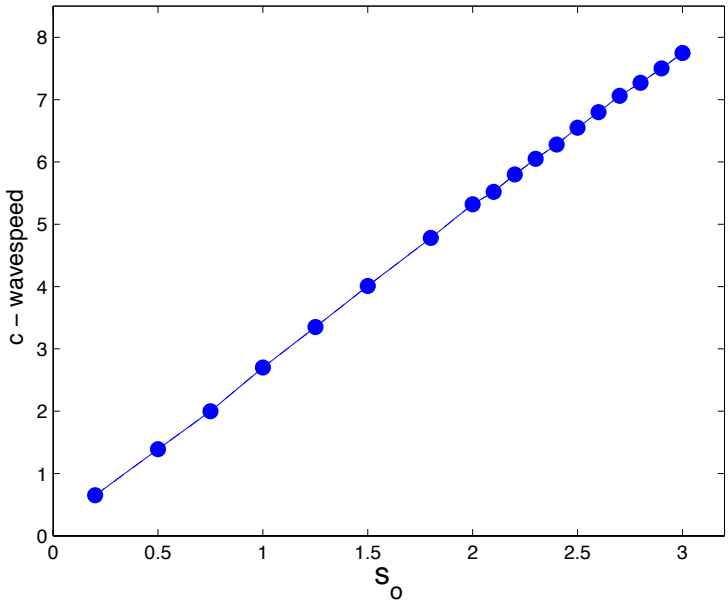

(c)

Figure 5.12: Solution PDEs system (5.11). Here change s_o (a) $s_o = 0.5$. (b) $s_o = 2$. The parameters $\alpha_2 = 1$, $\beta_2 = 4$, $v = 1$, $k = 0.5$, $D_n = 0.2$ and $D_s = 0.2$ are fixed values and change values s_o. The time spacings: 30,40,50,60,70,80,90,100. (c) The relation between the parameter s_o and waves speed c. For s_o values the propagation speed for substrate is increased.

5.4 Discussion and Conclusion

In this Chapter, we added the substrate to the system 3.3 in Chapter 3 and the system 4.1 in Chapter 4. We focused on the case when $d(\rho) = 0$

To clarify the effect of parameters on the wave speed c therefore, we studied the above systems (5.8) and (5.11) without non - dimensionalise. We illustrated the relation between wave speed c and each parameter in turn. So we studied lateral branching, tip - hypha anastomoses with the substrate with convection when $v \neq 0$, $D_n, D_s = 0$ for systems (5.8) and $v \neq 0$, $D_n \neq 0$ and $D_s \neq 0$ for systems (5.11). The parameters $\alpha_2, \beta_2, v, k, D_n$ and D_s affected the wave speed as follows: In lateral branching, tip - hypha anastomoses with substrate (FHS), with convection. For α_2 values the propagation speed is larger; β_2 can not alter the colony growth rate and we noted, the profile of tips n lows when values β_2 increased; For v values the propagation speed is larger and this relation is linear. The wave speed slightly decreases when the values of parameter k increases and we noted the profile of branching decreased when the value of the parameter k increasing. While, in the lateral branching, tip - hypha anastomoses with substrate (FHS), with convection and diffusion, we focused on the effect of D_n and D_s on wave speed, where D_n values the propagation speed is larger. We used numerical solution to show it. Biologically, the growth of fungi for branching or tips should be need energy (Persson et al., 2000).

Fungi generally obtain carbon by breaking down and absorbing surrounding materials. Fig. 5.12(c) illustrated the relation between the parameter s_o (energy) and waves speed c. For s_o values the propagation speed for substrate is increased. We could repeat this changes with other models including $d(\rho) \neq 0$. For $d(\rho) = 0$, we note that the tip density goes to zero behind the wave front and the biomass density is constant. It may be that certain applications require the inclusion of hyphal death and reuse term (see e.g. Falconer et al. (2007)). This constitutes interesting future work.

Chapter 6

2-Dimensional Spatially Extended Fungal Growth Model

Previous chapters illustrated that a 1-dimensional spatial domain can be a useful modelling tool in certain circumstance (*e*.g. modelling long, thin regions). Normally. The growth of many mycelia is approximately planar for example on surfaces, in Petri dies, etc, we would expect (planar) spatial domain to be in 2 - dimension. In this chapter, we consider the following 2-D spatially extended fungal growth system:

$$\begin{aligned} \frac{\partial \rho}{\partial t} &= [(nv_1)^2 + (nv_2)^2]^{\frac{1}{2}} - d(\rho), \\ \frac{\partial n}{\partial t} &= -(\frac{\partial nv_1}{\partial x} + \frac{\partial nv_2}{\partial y}) + \sigma(\rho, n), \end{aligned} \tag{6.1}$$

and fungal growth system with substrate

$$\begin{aligned}
\frac{\partial \rho}{\partial t} &= [(nv_1 s)^2 + (nv_2 s)^2]^{\frac{1}{2}} - d(\rho), \\
\frac{\partial n}{\partial t} &= -(\frac{\partial (nv_1 s)}{\partial x} + \frac{\partial (nv_2 s)}{\partial y}) + \sigma(\rho, n, s), \\
\frac{\partial s}{\partial t} &= -f_s,
\end{aligned} \tag{6.2}$$

where $v = (v_1, v_2)$ is vector and $(x, y) \in \Psi \subseteq \mathbb{R}^2$, for some set Ψ. In this chapter, we will devote our effort to rescale space in the systems (6.1) and (6.2), this operation will helpful to skip computational error on the boundary. We will study many cases from types of branching, and different values for parameters

6.1 Laplacian in Polar Coordinates

All the boundary-value problems that have been considered so far have been expressed in terms of rectangular coordinates. We would naturally try to describe the problem in polar coordinates, cylindrical coordinates, or spherical coordinates, respectively.

We know the relationship between Cartesian coordinates and polar coordinates gives at this form:

$$\begin{aligned}
x &= r\cos\theta, \\
y &= r\sin\theta,
\end{aligned}$$

where

$$\begin{aligned}
r &= \sqrt{x^2 + y^2}, \\
\theta &= tan^{-1}(\frac{y}{x}).
\end{aligned}$$

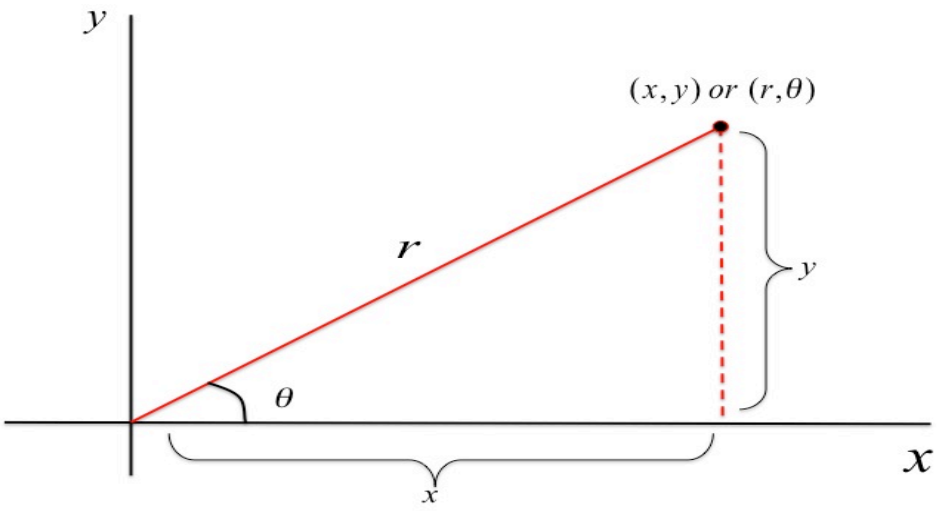

Figure 6.1: Polar coordinates of a point (x, y) are (r, θ)

See Fig. 6.1. The first pair of equation transform polar coordinates (r, θ) into rectangular coordinates (x, y); the second pair of equations enable us to transform rectangular coordinates into polar coordinates. These equations also make it possible to convert the two - dimensional Laplacian of function u,

$$\nabla^2 u = \frac{\partial^2 u}{\partial x^2} + \frac{\partial^2 u}{\partial y^2},$$

into polar coordinates. Using Chain Rule and show that

$$\frac{\partial u}{\partial x} = \frac{\partial u}{\partial r}\frac{\partial r}{\partial x} + \frac{\partial u}{\partial \theta}\frac{\partial \theta}{\partial x} = \cos\theta \frac{\partial u}{\partial r} - \frac{\sin\theta}{r}\frac{\partial u}{\partial \theta}$$

$$\frac{\partial u}{\partial y} = \frac{\partial u}{\partial r}\frac{\partial r}{\partial y} + \frac{\partial u}{\partial \theta}\frac{\partial \theta}{\partial y} = \sin\theta \frac{\partial u}{\partial r} + \frac{\cos\theta}{r}\frac{\partial u}{\partial \theta}$$

$$\begin{aligned}\frac{\partial^2 u}{\partial x^2} = \cos^2\theta \frac{\partial^2 u}{\partial r^2} - \frac{2\sin\theta\cos\theta}{r}\frac{\partial^2 u}{\partial r \partial \theta} + \frac{\sin^2\theta}{r^2}\frac{\partial^2 u}{\partial \theta^2} \\ + \frac{\sin^2\theta}{r}\frac{\partial u}{\partial r} + \frac{2\sin\theta\cos\theta}{r^2}\frac{\partial u}{\partial \theta},\end{aligned} \tag{6.3}$$

$$\begin{aligned}\frac{\partial^2 u}{\partial y^2} &= \sin^2\theta\frac{\partial^2 u}{\partial r^2} + \frac{2\sin\theta\cos\theta}{r}\frac{\partial^2 u}{\partial r\partial\theta} + \frac{\cos^2\theta}{r^2}\frac{\partial^2 u}{\partial\theta^2} \\ &+ \frac{\cos^2\theta}{r}\frac{\partial u}{\partial r} - \frac{2\sin\theta\cos\theta}{r^2}\frac{\partial u}{\partial\theta}.\end{aligned} \tag{6.4}$$

Now, adding (6.3) and (6.4) and simplifying yield the Laplacian of u in polar coordinates:

$$\nabla^2 u = \frac{\partial^2 u}{\partial r^2} + \frac{1}{r}\frac{\partial u}{\partial r} + \frac{1}{r^2}\frac{\partial^2 u}{\partial\theta^2},$$

that is mean

$$\frac{\partial^2 u}{\partial x^2} + \frac{\partial^2 u}{\partial y^2} = \frac{\partial^2 u}{\partial r^2} + \frac{1}{r}\frac{\partial u}{\partial r} + \frac{1}{r^2}\frac{\partial^2 u}{\partial\theta^2}. \tag{6.5}$$

We will concentrate only on boundary value problems involving Laplace's equation in polar coordinates (zero - flux boundary conditions):

$$\frac{\partial^2 u}{\partial r^2} + \frac{1}{r}\frac{\partial u}{\partial r} + \frac{1}{r^2}\frac{\partial^2 u}{\partial\theta^2} = 0 \tag{6.6}$$

6.2 Radially Symmetric Solutions

Hence, the Laplacian in polar coordinates can be written as

$$\begin{aligned}\frac{\partial n}{\partial x} + \frac{\partial n}{\partial y} &= \frac{1}{r}\frac{\partial(rn)}{\partial r} = \frac{\partial n}{\partial r} + \frac{n}{r}, \\ \frac{\partial^2 n}{\partial x^2} + \frac{\partial^2 n}{\partial y^2} &= \frac{\partial^2 n}{\partial r^2} + \frac{1}{r}\frac{\partial n}{\partial r} + \frac{1}{r^2}\frac{\partial^2 n}{\partial\theta^2}.\end{aligned} \tag{6.7}$$

We seek radially symmetric solutions, i.e. solutions for which $n(r,\theta) = n(r)$ and hence $\frac{\partial n}{\partial \theta} = \frac{\partial^2 n}{\partial \theta^2} = 0$. Therefore, using (6.7), the systems (6.1) and (6.2) become

$$\begin{aligned} \frac{\partial \rho}{\partial t} &= [(nv_1)^2 + (nv_2)^2]^{\frac{1}{2}} - d(\rho), \\ \frac{\partial n}{\partial t} &= -\frac{\partial (nv)}{\partial r} - \frac{(nv)}{r} + \sigma(\rho, n) \end{aligned} \tag{6.8}$$

and fungal growth system with substrate

$$\begin{aligned} \frac{\partial \rho}{\partial t} &= [(nv_1 s)^2 + (nv_2 s)^2]^{\frac{1}{2}} - d(\rho), \\ \frac{\partial n}{\partial t} &= -\frac{\partial (nvs)}{\partial r} - \frac{(nvs)}{r} + \sigma(\rho, n, s) \\ \frac{\partial s}{\partial t} &= -f_s(\rho, n, s), \end{aligned} \tag{6.9}$$

let us assuming that $v = v_1 = v_2$, for $(r,t) \in \mathbb{R}^+ \times \mathbb{R}^+$. To ensure symmetry at $r = 0$, we require that $\frac{\partial n}{\partial r} = 0$. We would expect a similar condition to hold at $r = \infty$. Since, for reasonable solutions we expect n_r to be bounded, for r sufficiently large, (6.8) and (6.9) can therefore be approximated large r by the system

$$\begin{aligned} \frac{\partial \rho}{\partial t} &= nv - d(\rho), \\ \frac{\partial n}{\partial t} &= -\frac{\partial (nv)}{\partial r} + \sigma(\rho, n) \end{aligned} \tag{6.10}$$

and fungal growth system with substrate

$$\begin{aligned} \frac{\partial \rho}{\partial t} &= nsv - d(\rho), \\ \frac{\partial n}{\partial t} &= -\frac{\partial (nsv)}{\partial r} + \sigma(\rho, n, s) \\ \frac{\partial s}{\partial t} &= -f_s(\rho, n, s) \end{aligned} \tag{6.11}$$

Thus, we would expect solutions of (6.8) and (6.9) to be well-approximated by solutions to (6.10) and (6.11), for large r in any case.

In Chapters 3,4 and 5, we discussed traveling wave extensively for types of branching and that were biological realistic.

Firstly, we study the system:

$$\begin{aligned} \frac{\partial \rho}{\partial t} &= nv - d(\rho), \\ \frac{\partial n}{\partial t} &= -\frac{\partial (nv)}{\partial x} + \sigma(\rho, n). \end{aligned} \tag{6.12}$$

where $\rho(x,t)$, $n(x,t)$, v, $d(\rho)$ and $\sigma(\rho,n)$ are defined above.

In Chapter 3, section 3.4, we studied the travelling wave for the type of branching which are biologically realistic.

Next sections, we will study radially symmetric solutions for the following types: FHD: Lateral branches tip-hyphae anastomoses; FXD: Lateral branches with density limitation; YWD: Dichotomous branches, tip-tip anastomoses and YWD: Dichotomous branches, tip-hyphae anastomoses. We will study properties of each type in turn. Furthermore we will study fungal growth system with substrate.

6.2.1 FHD: Lateral Branching Tip - Hypha Anastomoses Plus Hyphal Death

We know the model system (1-D) is

$$\begin{aligned} \frac{\partial \rho}{\partial t} &= n - \rho, \\ \frac{\partial n}{\partial t} &= -\frac{\partial n}{\partial x} + \alpha\rho(1-n). \end{aligned} \tag{6.13}$$

where $\alpha = (\alpha_2 v/\gamma_1^2)$. This single parameter represent the rate of hyphal per unit length hypha per unit time. We know the subroutines in pdepe code in MATLAB which take this form: **sol = pdepe (m, pdefun, icfun, bcfun, xmesh, tspan)**, where **m**: a parameter corresponding to the symmetry of the problem. **m** can be slab = 0, cylindrical = 1, or spherical = 2.

Therefore Fig. 6.2(a) illustrate solution to the system (6.13) with the parameter α taking value of 2, here **m**=0 while Fig. 6.2(b) illustrate solution to the system (6.13) with the parameter α taking value of 2, here **m**=1. It can be seen from Fig. 6.2(c) that the speed of the right travelling waves of problem 1-D is greater than the speed of radially symmetric solutions. This is due to the slowing effect of the $(\frac{1}{r}u_r)$ term. If diffusion is combined with an convection process, this provides a mechanism for maintaining a slow speed wave, for similar problem, see (Leung et al., 2008). We noticed also from Fig. 6.2(c) that blue and red lines appear straight, which reflect approximately constant speed in both cases. Using COMSOL, we solved system (6.1) on a square domain $-50 \leq x, y \leq 50$ and used zero flux boundary condition for all simulations presented.

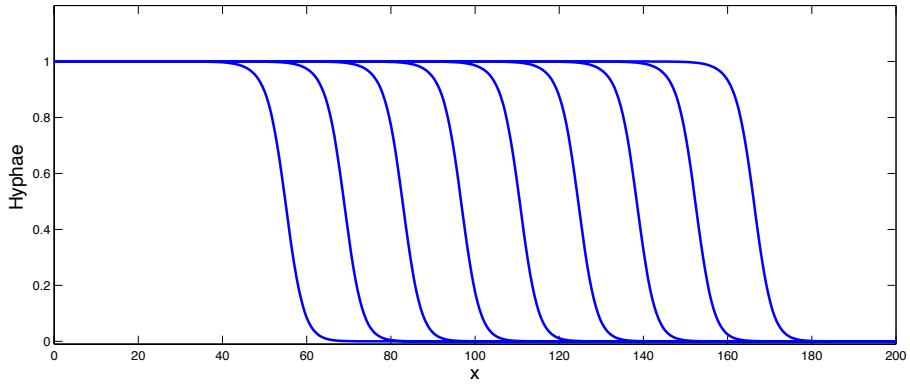

(a)

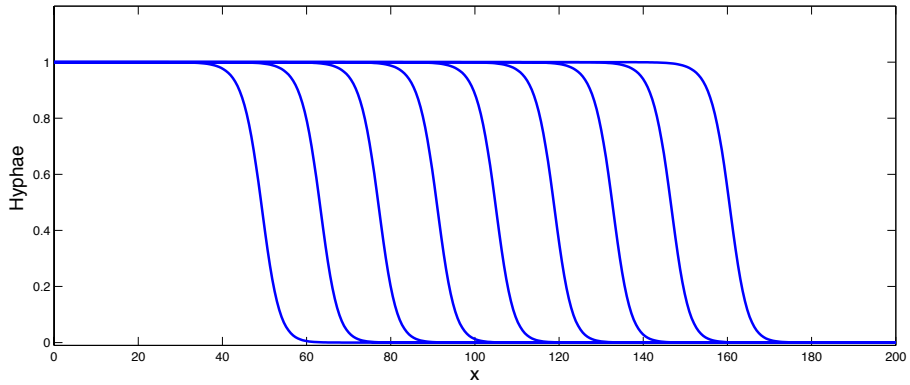

(b)

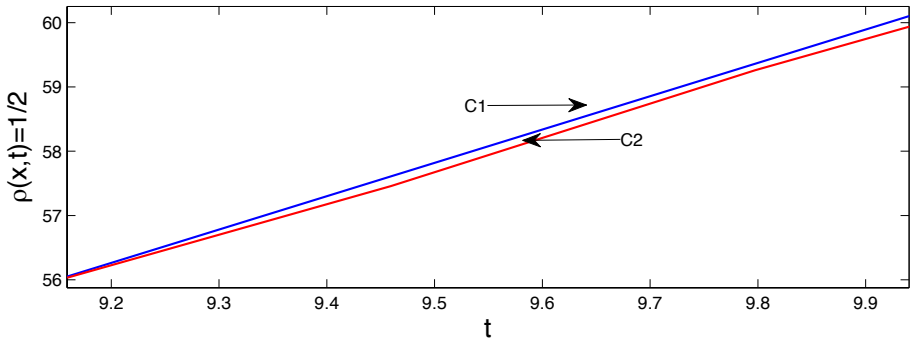

(c)

Figure 6.2: Solution to the system (6.13) with the parameter α and D_n taking value of $2, 1$ (a) one - dimensional and (b) radially - symmetric. The time spacings: $10m$ where $m = 1, 2, ..., 9$. (c) The blue line (c_1: c_{1-D}) represents the position of the front of 1-D problem (6.13) and the red line (c_2: c_{r-s}) the position of the front for radially symmetric solution of (6.13).

In previous chapters, we discussed the existence of a travelling wave in 1-D using above parameter α. We observed many different behaviours on the competition rate on the above parameters. We know the uniform steady states of system (6.13) has two steady states: $(0, 0)$ and $(1, 1)$, because the solutions of the algebraic equations $n - \rho = 0$, $\alpha\rho(1 - n) = 0$. That means the speed of hyphal density ρ and tip density n have similar behaviour. Therefore we refer to one of them in 2-D see as shown in Fig. 6.3 and Fig. 6.4.

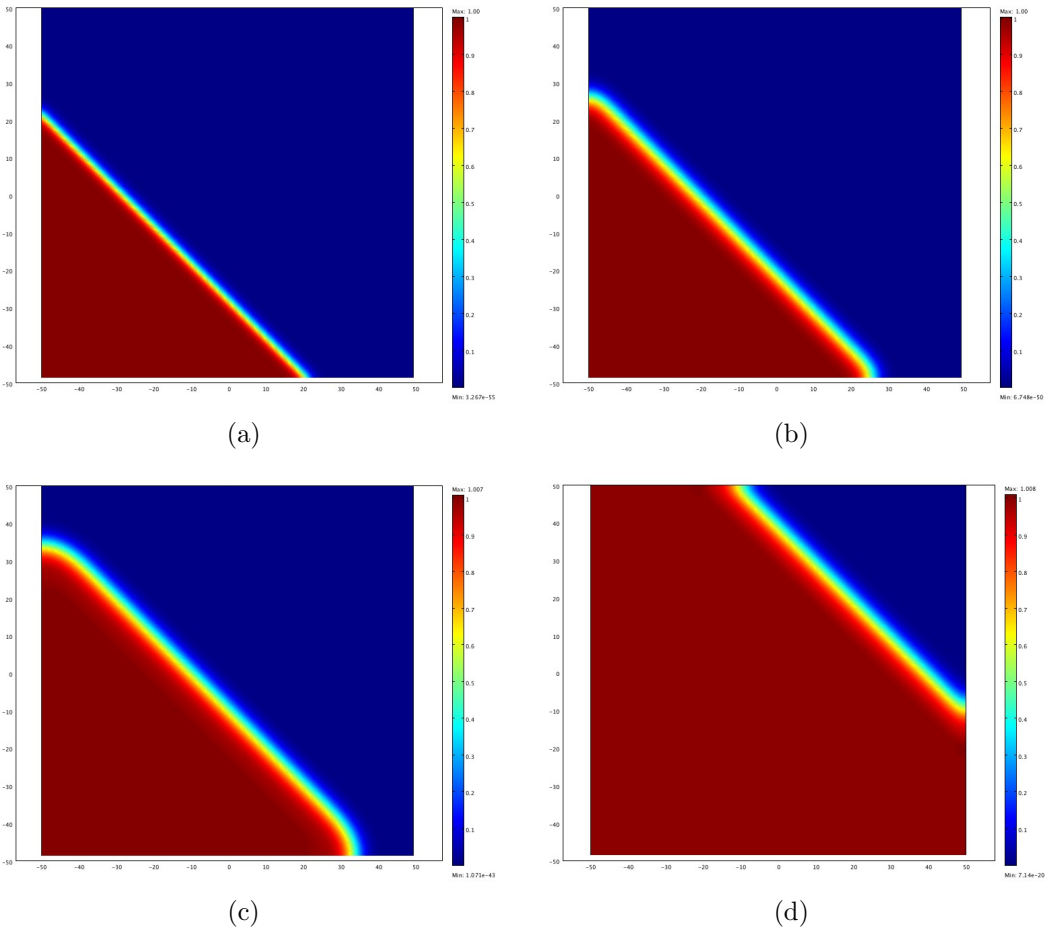

(a) (b)

(c) (d)

Figure 6.3: Right travelling wave solution for the system 6.1 when $\sigma = \alpha\rho(1-n)$. (a) the biomass density, $n(x, t)$ at $t = 1$; (b) the biomass density, $n(x, t)$ at $t = 5$; (c) the biomass density, $n(x, t)$ at $t = 10$; (d) the biomass density, $n(x, t)$ at $t = 30$;. Parameter values are $\alpha = 2$.

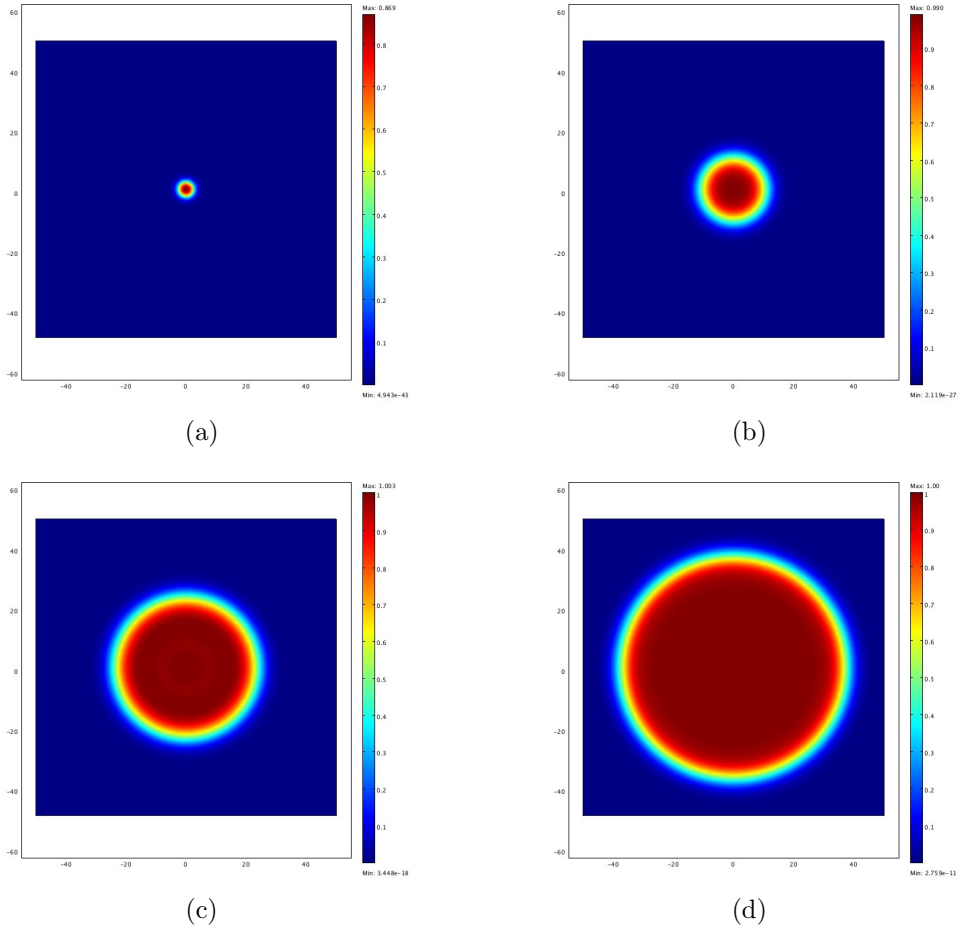

(a) (b)

(c) (d)

Figure 6.4: Two-dimensional solution of system 6.10 when $\sigma = \alpha\rho(1-n)$. (a) the biomass density, $n(x,t)$ at $t = 1$; (b) the biomass density, $n(x,t)$ at $t = 10$; (c) the biomass density, $n(x,t)$ at $t = 20$; (d) the biomass density, $n(x,t)$ at $t = 30$;. Parameter values are $\alpha = 2$.

Fig. 6.4 illustrates the biomass and hyphal density distributions in the all cases. The radial symmetry of both distributions is evident. Notice that the biomass and hyphal density distributions start extending see Fig. 6.4(a, b, c), and it is still extending outward close to the periphery Fig. 6.4,(d), with no change in the centre. These results are therefore consistent with both the experimental observations described directly above and those of the previous chapters. Again we see that growth in initially uniform conditions induces radial expansion of biomass accompanied by an expanding annulus of hyphal density positioned close to the edge of the biomass distribution. Here, clearly the biomass distribution of tips or branching to has "smoothed out" the initial similarity in the tips or branching concentration.

6.2.2 FXD: Lateral Branches with Density Limitation Plus Hyphal Death

The model system in this case is

$$\begin{aligned} \frac{\partial \rho}{\partial t} &= n - \rho, \\ \frac{\partial n}{\partial t} &= -\frac{\partial n}{\partial x} + \alpha\rho(1-\rho). \end{aligned} \tag{6.14}$$

Where α are defined before. As above, Fig. 6.5(a) illustrate solution to the system (6.14) with the parameter α taking value of 2 and $m = 0$ while Fig. 6.5(b) illustrate solution to the system (6.13) with the parameter α taking value of 2 and $m = 1$. It can be seen from Fig. 6.5(c) that the speed of the right travelling waves of problem 1-D is greater than the speed of radially symmetric solutions.

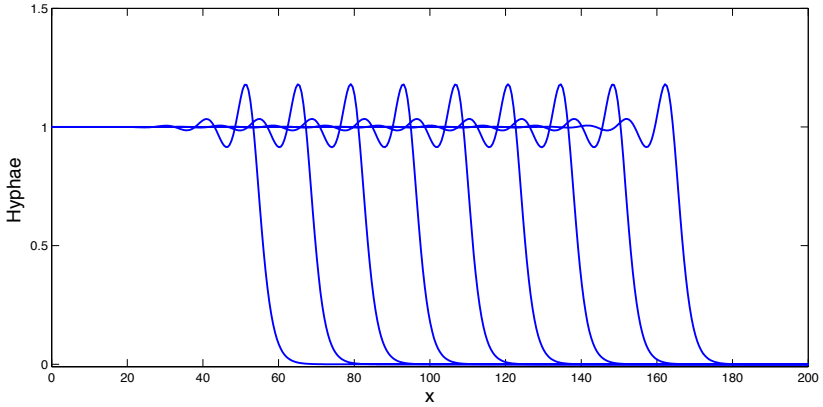

(a)

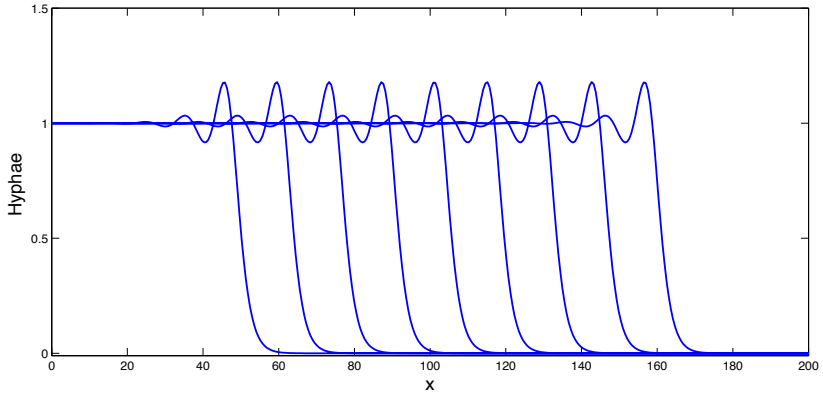

(b)

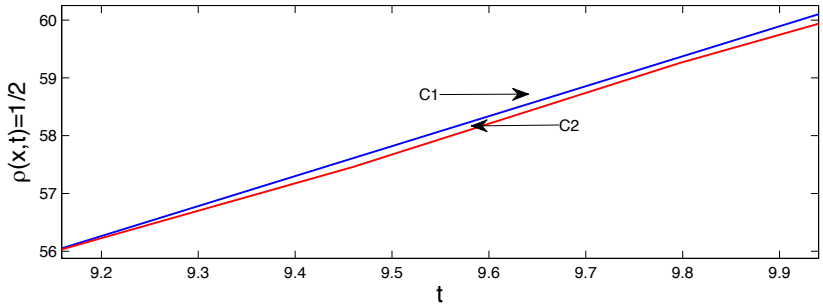

(c)

Figure 6.5: Solution to the system (6.14) with the parameter α taking value of 2 (a) (a) one - dimensional and (b) radially - symmetric. The time spacings: $10m$ where $m = 1, 2, ..., 9$. (c) The blue line (c_1: c_{1-D}) represents the position of the front of 1-D problem (6.13) and the red line (c_2: c_{r-s}) the position of the front for radially symmetric solution of (6.13).

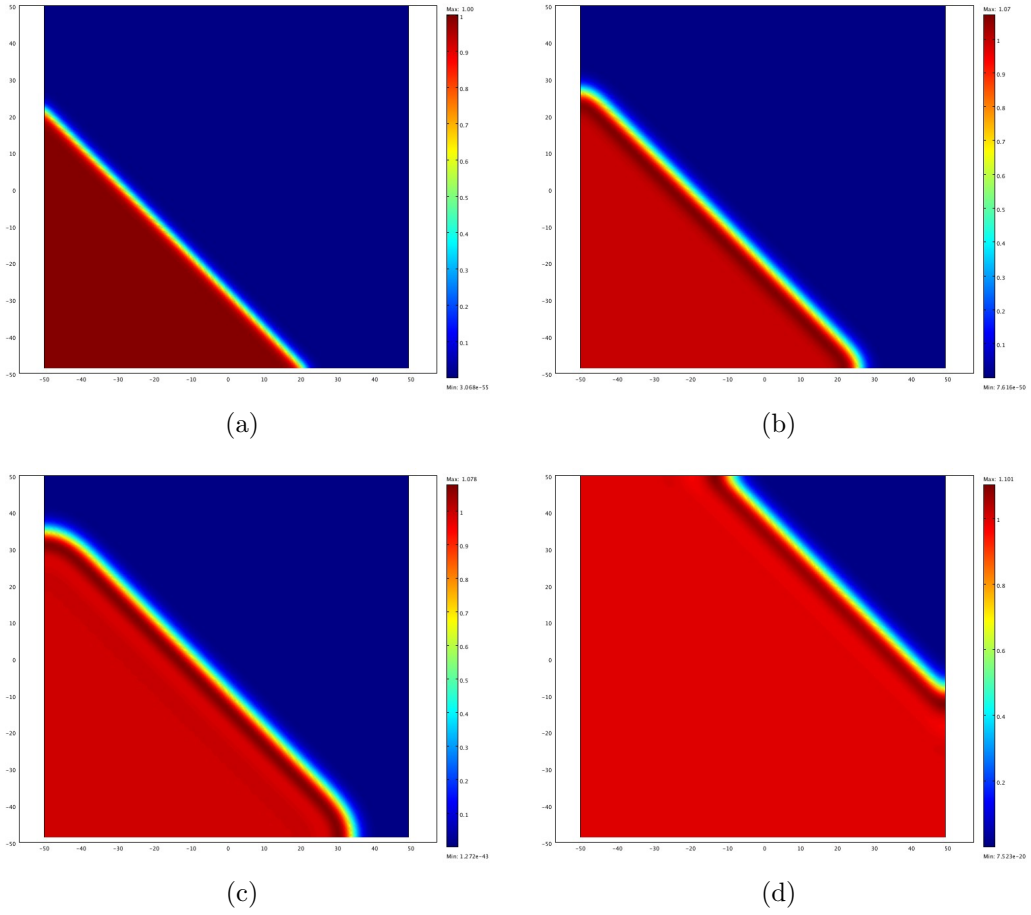

Figure 6.6: Right travelling wave solution for the system 6.1 when $\sigma = \alpha\rho(1-\rho)$, (a) the biomass density, $n(x,t)$ at $t = 1$; (b) the biomass density, $n(x,t)$ at $t = 5$; (c) the biomass density, $n(x,t)$ at $t = 10$; (d) the biomass density, $n(x,t)$ at $t = 30$;. Parameter values are $\alpha = 2$.

We are interested here in additional behaviour that may arise from setting the problem in 2-D. To begin we used planar initial data for ρ (n is identically the opposite), as shown in Fig. 6.6.

Fig. 6.7 illustrates the biomass and hyphal density distributions in the all cases. The radial symmetry of both distributions is evident. Notice that the biomass and hyphal density distributions is start extending see Fig. 6.7(a, b, c), and it is still outward close to the periphery Fig. 6.7,(d), Tip or branching density striations result when α increases. Tip or branching densities which are essentially

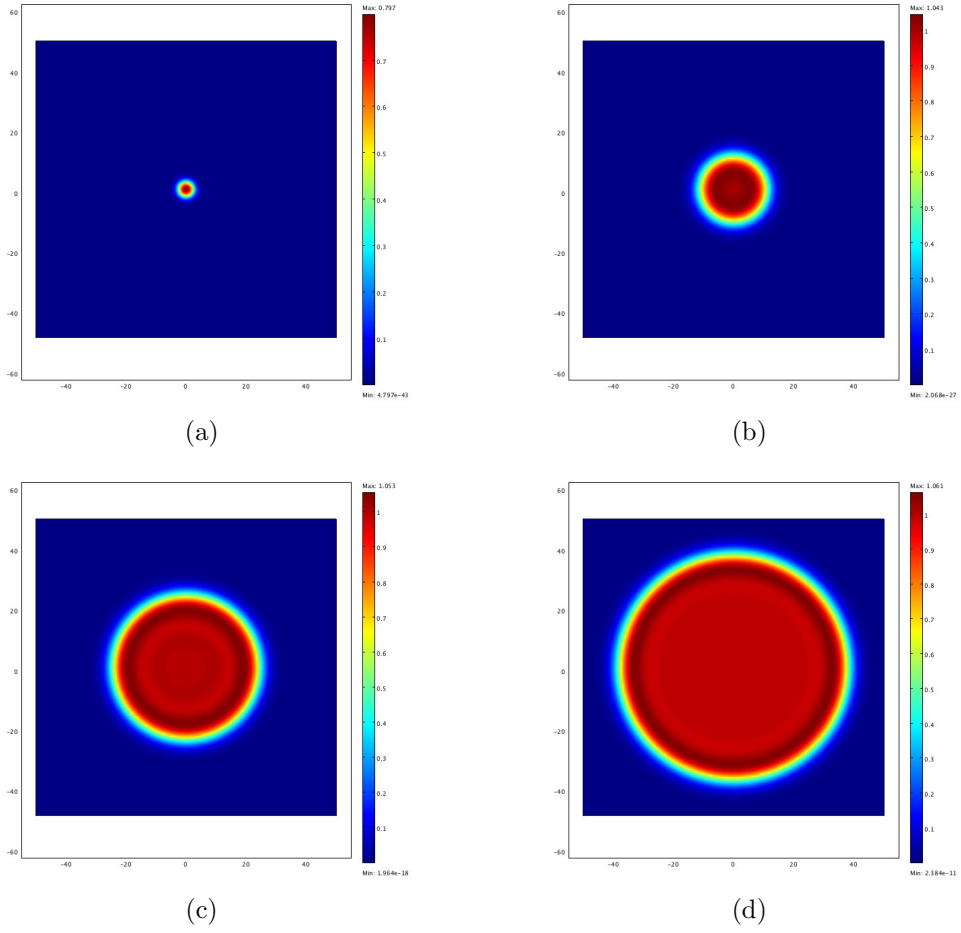

Figure 6.7: Two-dimensional solution of system 6.10 when $\sigma = \alpha\rho(1-\rho)$.(a) the biomass density, $n(x,t)$ at $t = 1$; (b) the biomass density, $n(x,t)$ at $t = 10$; (c) the biomass density, $n(x,t)$ at $t = 20$; (d) the biomass density, $n(x,t)$ at $t = 30$;. Parameter values are $\alpha = 2$.

similar have peaks leading those of hyphae by approximately two dimensionless units. This difference between high and low values of tip or branching density are also somewhat greater, that is clear from the dark red ring see Fig. 6.7.

These results are therefore consistent with both the experimental observations described directly above and those of the previous chapters.

Again we see that growth in initially uniform conditions induces radial expansion of biomass accompanied by an expanding annulus of hyphal density positioned

close to the edge of the biomass distribution. Here, clearly the biomass distribution of tips or branching to has "oscillation" similar to the tips and branching concentration.

Previously, it is clear the wave speeds in FHD, FXD types approximately are equal. Here the same behaviour, we note the profiles in Fig. 6.4(a, b, c, d) and Fig. 6.7(a, b, c, d) are equal at the same values of α.

6.2.3 YWD: Dichotomous Branches, Tip-tip Anastomoses Plus Hyphal Death

The model system in this case is

$$\begin{aligned} \frac{\partial \rho}{\partial t} &= n - \rho, \\ \frac{\partial n}{\partial t} &= -\frac{\partial n}{\partial x} + \alpha n(1-n). \end{aligned} \tag{6.15}$$

This type is completely similar to the behavior of solution of the FHD-type, while it different of the speed, where the waves speed in YWD types larger than from FHD type at the same values of α see Fig. 6.8(a, b, c, d) and Fig. 6.9(a, b, c, d).

6.2.4 YHD: Dichotomous Branches, Tip-tip Anastomoses Plus Hyphal Death

The model system in this case is

$$\begin{aligned} \frac{\partial \rho}{\partial t} &= n - \rho, \\ \frac{\partial n}{\partial t} &= -\frac{\partial n}{\partial x} + \alpha n(1-\rho). \end{aligned} \tag{6.16}$$

This type is completely similar to the behavior of solution of the FXD-type, while it different of the speed, where the waves speed in YHD types larger than from FXD type at the same values of α see Fig. 6.10(a, b, c, d) and Fig. 6.11(a, b, c, d).

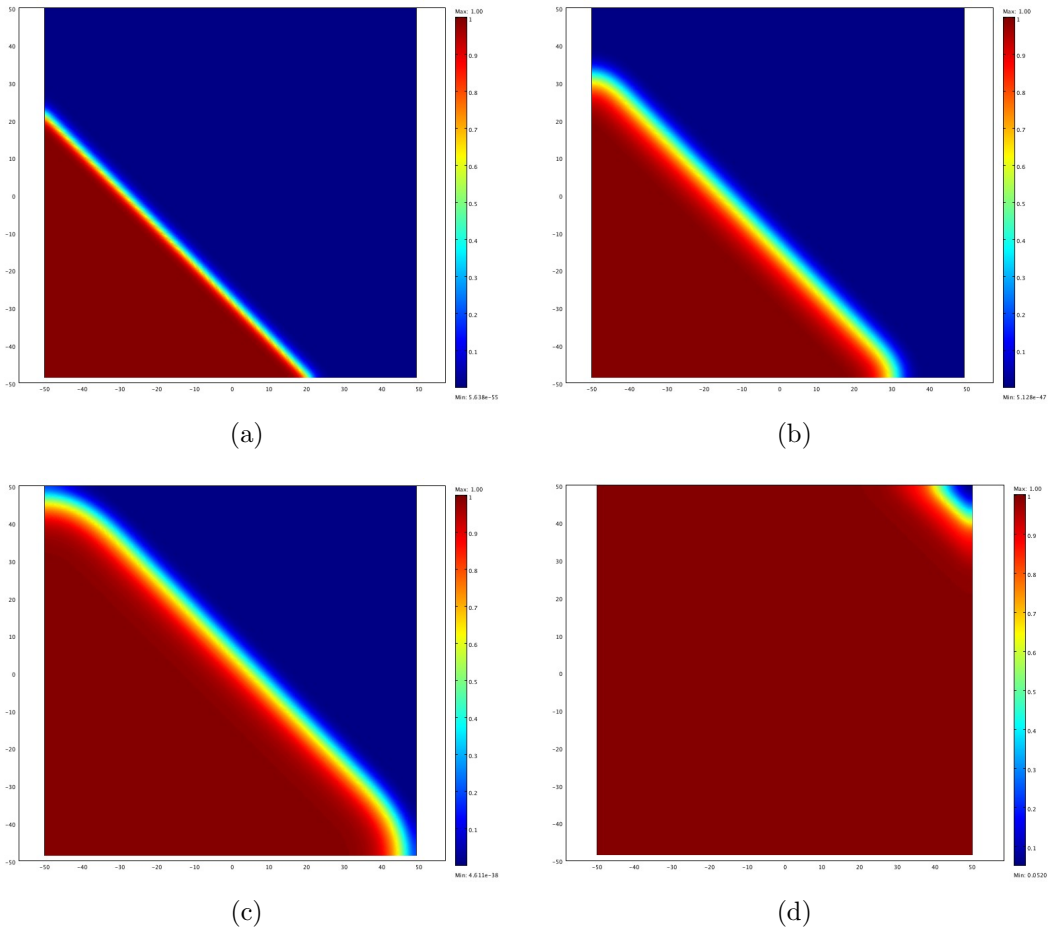

(a) (b)

(c) (d)

Figure 6.8: Right travelling wave solution for the system 6.1 when $\sigma = \alpha n(1-n)$. (a) the biomass density, $n(x,t)$ at $t = 1$; (b) the biomass density, $n(x,t)$ at $t = 10$; (c) the biomass density, $n(x,t)$ at $t = 20$; (d) the biomass density, $n(x,t)$ at $t = 30$;. Parameter values are $\alpha = 2$.

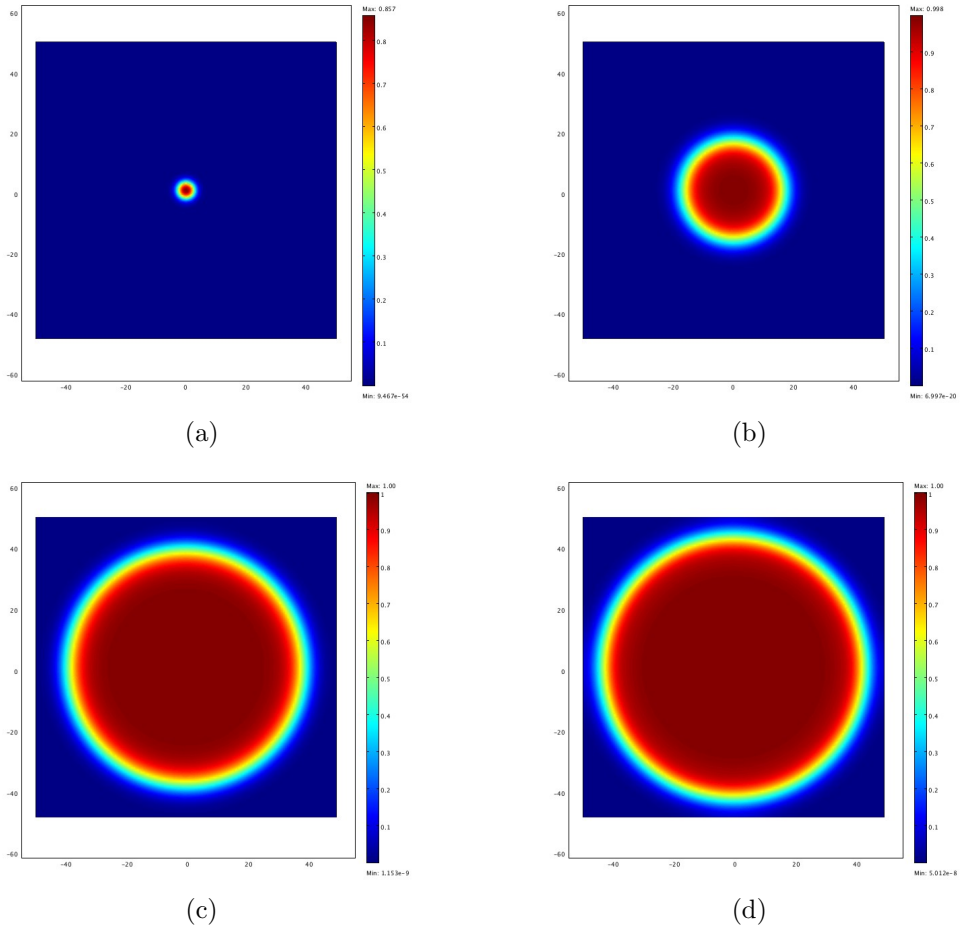

(a) (b)

(c) (d)

Figure 6.9: Two-dimensional solution of system 6.10 when $\sigma = \alpha n(1-n)$. (a) the biomass density, $n(x,t)$ at $t = 1$; (b) the biomass density, $n(x,t)$ at $t = 10$; (c) the biomass density, $n(x,t)$ at $t = 20$; (d) the biomass density, $n(x,t)$ at $t = 30$;. Parameter values are $\alpha = 2$.

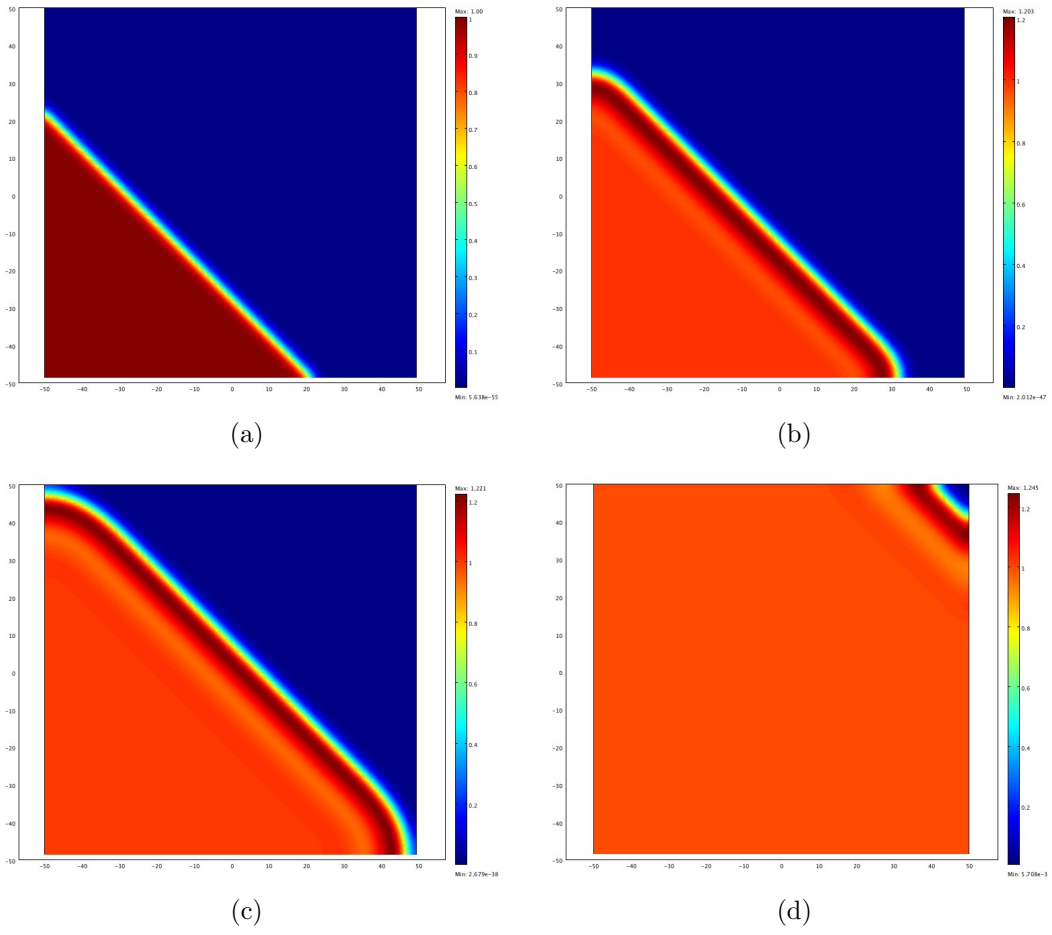

(a) (b)

(c) (d)

Figure 6.10: Right travelling wave solution for the system 6.1 when $\sigma = \alpha n(1-\rho)$. (a) the biomass density, $n(x,t)$ at $t = 1$; (b) the biomass density, $n(x,t)$ at $t = 10$; (c) the biomass density, $n(x,t)$ at $t = 20$; (d) the biomass density, $n(x,t)$ at $t = 30$;. Parameter values are $\alpha = 2$.

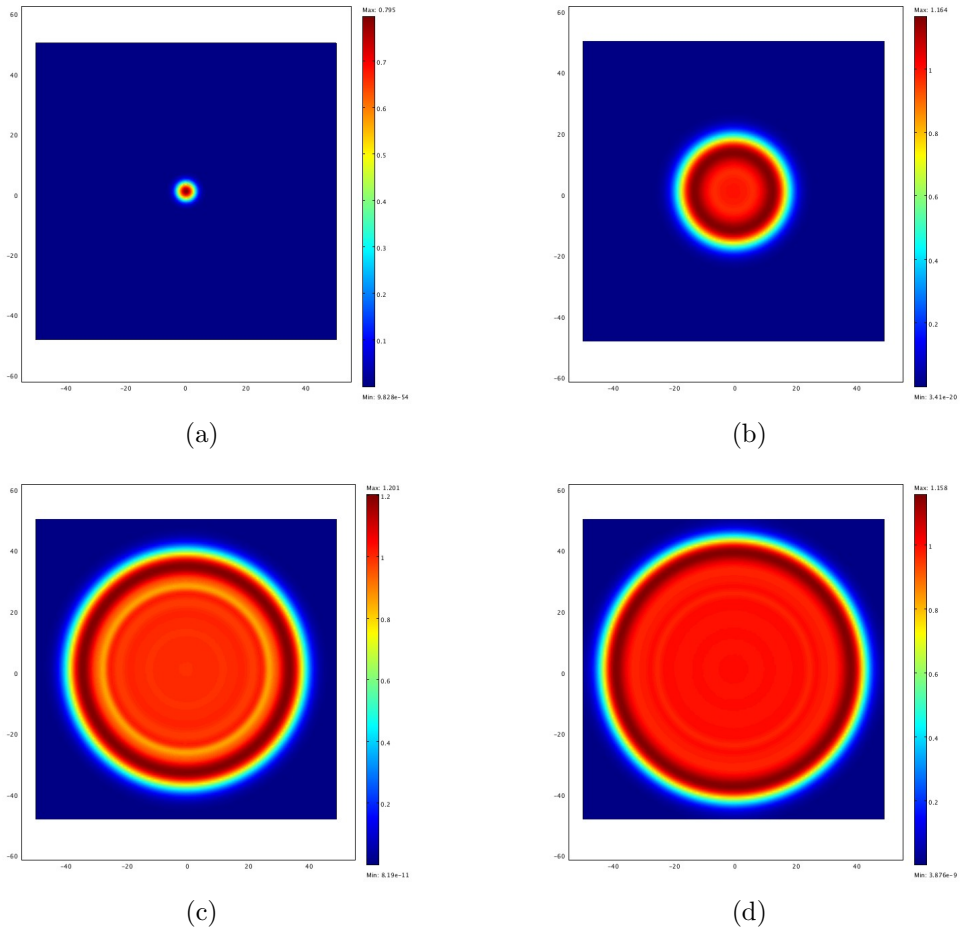

(a) (b)

(c) (d)

Figure 6.11: Two-dimensional solution of system 6.10 when $\sigma = \alpha n(1-\rho)$. (a) the biomass density, $n(x,t)$ at $t = 1$; (b) the biomass density, $n(x,t)$ at $t = 10$; (c) the biomass density, $n(x,t)$ at $t = 20$; (d) the biomass density, $n(x,t)$ at $t = 30$;. Parameter values are $\alpha = 2$. Increasing t introduces density striation as well as increasing propagation speed.

Note these oscillations represent moving bends of higher biomass and tip density. The size is number of oscillation is determined by the linear theory discussed above.

The density variations produced by these model. they move as the colony grows. This is a result of our assumption that tips are constantly moving at a fixed growth rate.

6.3 Comparison between types of branching

In the previous chapters (1-D), we showed that the wave speed in FHD, FXD types are equal and YWD, YHD types are equals at the same value of D_n and α. The waves speed in YWD, YHD types are larger than from FHD and FXD types for the same values of α, see Fig. 6.12

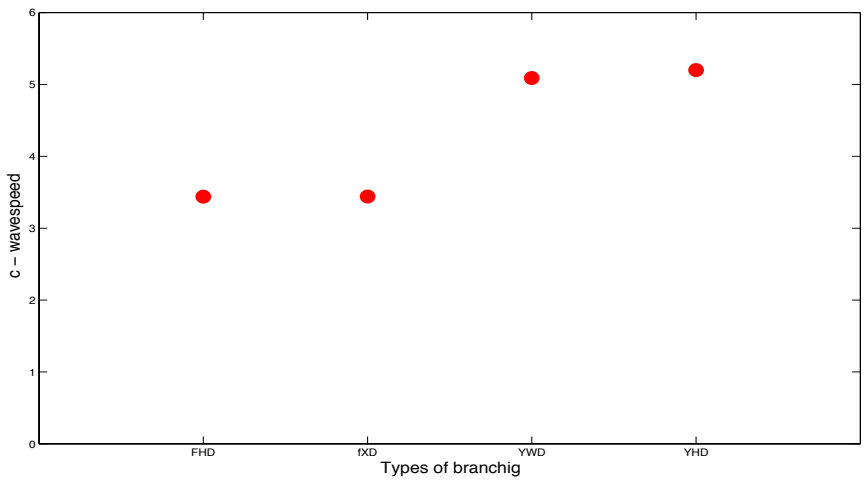

Figure 6.12: The chart represents wave speed c at the same value of α. It is clear the wave speed in FHD, FXD types are equal and YWD, YHD types are equals at the same value of α. The waves speed in YWD, YHD types are larger than from FHD and FXD types for the same values of α. Here $\alpha = 2$.

To Comparison between the types of branching:

i. FHD: Lateral branches tip-hyphae anastomoses;

ii. FXD: Lateral branches with density limitation;

iii. YWD: Dichotomous branches, tip-tip anastomoses;

iv. YHD: Dichotomous branches, tip-hyphae anastomoses

at the same values of α and time t. Fig. 6.13 and Fig. 6.14 illustrate, clearly, that the speed in FHD, FXD types are equal and YWD, YHD types are equals at the same value α and time t. The speed in YWD, YHD types are larger than from FHD and FXD types for the same values of α and time t.

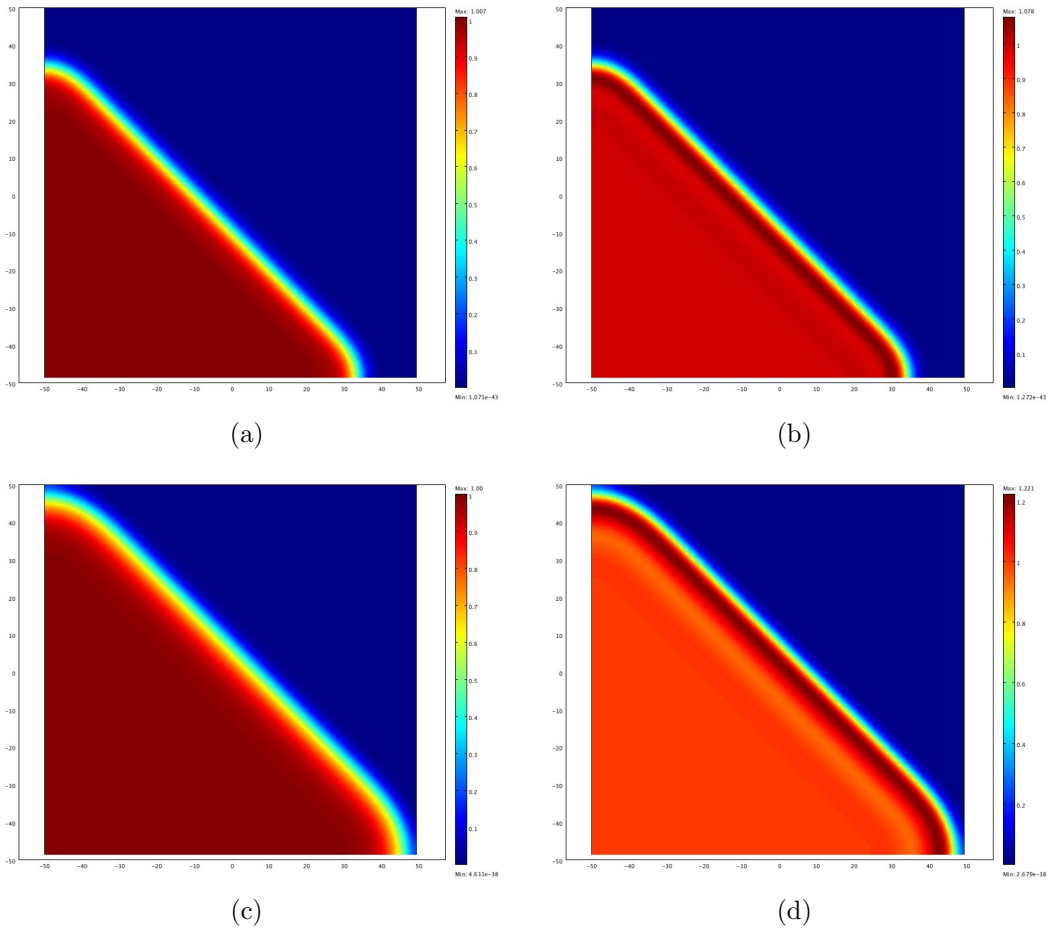

(a) (b)

(c) (d)

Figure 6.13: Right travelling wave solution for the system 6.1: (a) the biomass density, $n(x,t)$ for FHD type; (b) the biomass density, $n(x,t)$ for FXD type; (c) the biomass density, $n(x,t)$ for YWD type and (d) the biomass density, $n(x,t)$ for YHD type. Parameter values are $\alpha = 2$ and $t = 10$.

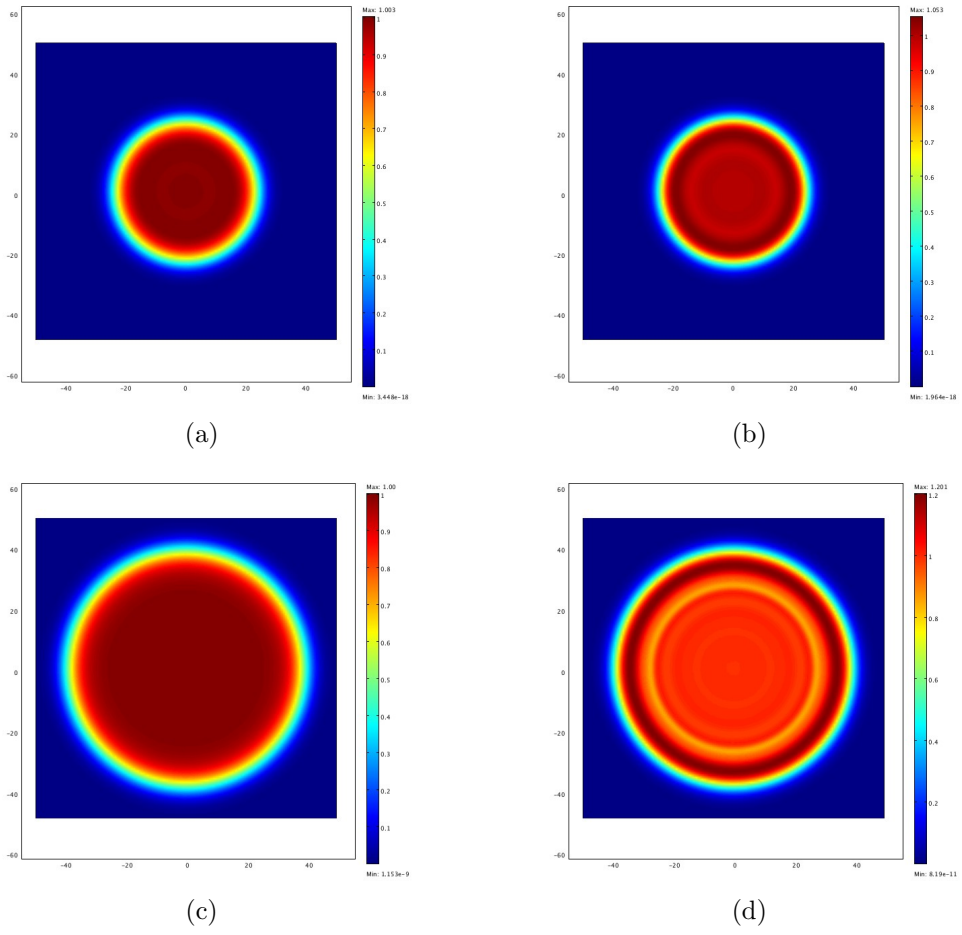

(a) (b)

(c) (d)

Figure 6.14: Two-dimensional solution of system 6.10: (a) the biomass density, $n(x,t)$ for FHD type; (b) the biomass density, $n(x,t)$ for FXD type; (c) the biomass density, $n(x,t)$ for YWD type and (d) the biomass density, $n(x,t)$ for YHD type. Parameter values are $\alpha = 2$ and $t = 15$.

6.4 Further Examples

In the previous sections, we illustrated the behaviors of the branching types in 2-D by use COMSOL. We solved systems (6.13, 6.14, 6.15, 6.16) on a square domain $-50 \leq x, y \leq 50$ and used zero flux boundary condition for all simulations presented. In this section, we can solve systems (6.13, 6.14, 6.15, 6.16) on a square domain $-50 \leq x, y \leq 0$ and $0 \leq x, y \leq 50$ and used zero flux boundary condition for all simulations presented. Initial conditions represent equally speed inoculation site.

Using the same techniques and at the same values of parameters α, we note the same behaviours. Then we can apply this technique on the FHD, FXD, YWD and YHD types.

Here, we solve two types FHD and FXD. For lateral branches tip-hyphae anastomoses we note that the biomass and hyphal density distributions start extending see Fig. 6.15(a, b, c), outward close to the periphery Fig. 6.15,(d), with no change in the centre. These results are therefore consistent with both the experimental observations described directly above and those of the previous sections.

The same previous techniques, we solved FXD type, we note hyphal densities which are essentially similar and have peaks leading those of hyphae by approximately two dimensionless units. This difference between high and low values of hyphal density are also somewhat greater, that is clear from the dark red ring see Fig. 6.16. Notice that the biomass and hyphal density distributions is start extending with oscillation, see Fig. 6.16(a, b, c), and it is still outward close to the periphery Fig. 6.16,(d). Finally, we can illustrate YHD and YHD types as the asme techniques as above, see Fig. 6.17 and Fig. 6.18.

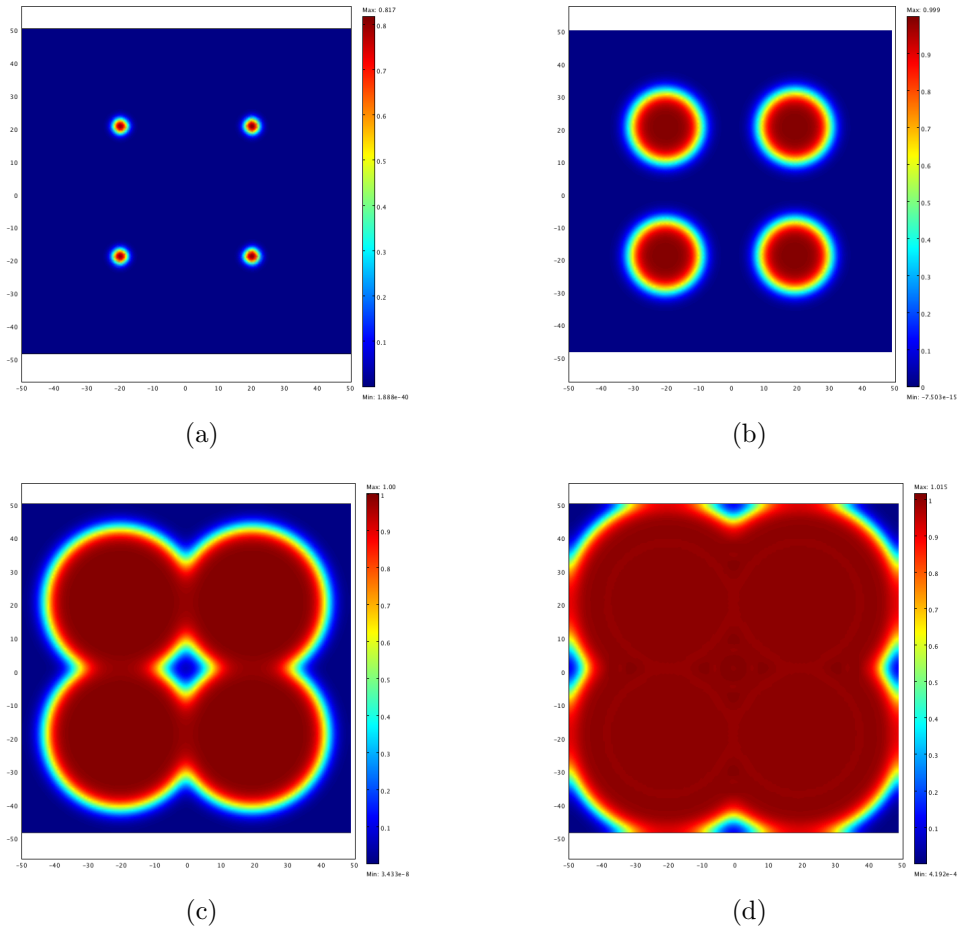

(a) (b)

(c) (d)

Figure 6.15: Two-dimensional solution of system 6.10 “FHD type” when $\sigma = \alpha\rho(1-n)$.(a) the biomass density, $n(x,t)$ at $t = 1$; (b) the biomass density, $n(x,t)$ at $t = 10$; (c) the biomass density, $n(x,t)$ at $t = 20$; (d) the biomass density, $n(x,t)$ at $t = 30$;. Parameter values are $\alpha = 2$.

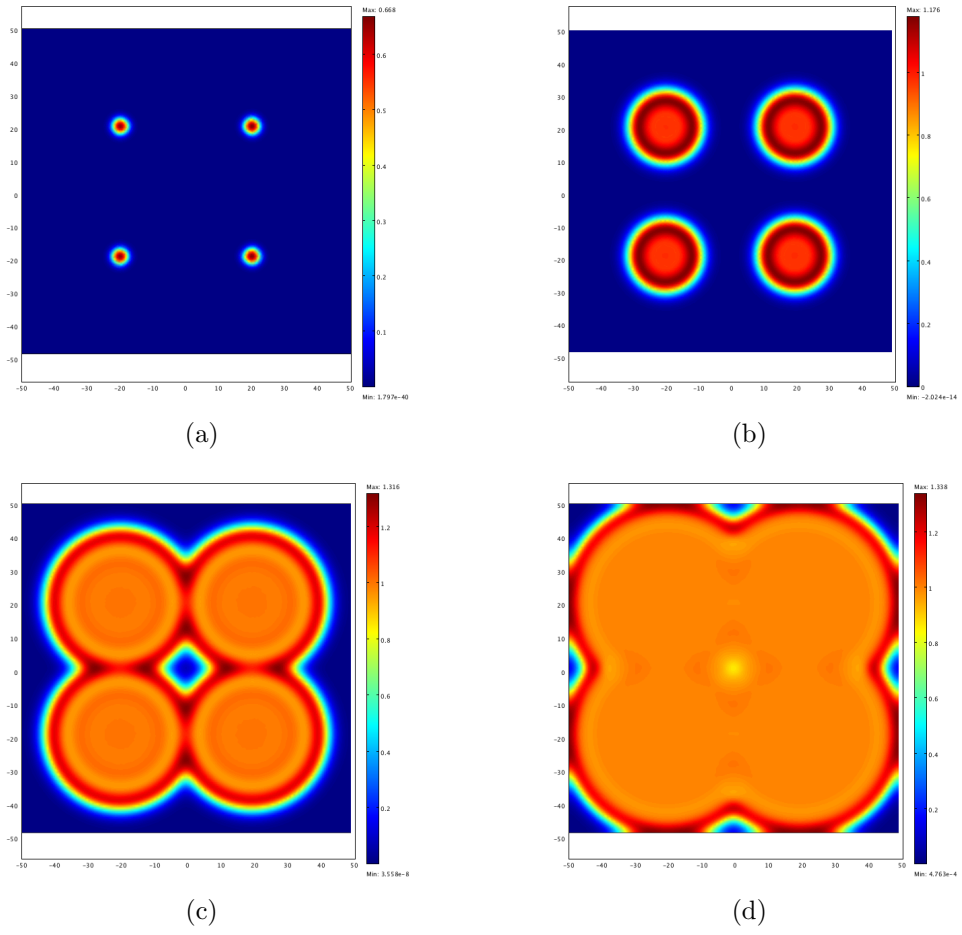

(a) (b)

(c) (d)

Figure 6.16: Two-dimensional solution of system 6.10 "FXD type" when $\sigma = \alpha\rho(1-\rho)$. (a) the biomass density, $n(x,t)$ at $t = 1$; (b) the biomass density, $n(x,t)$ at $t = 10$; (c) the biomass density, $n(x,t)$ at $t = 20$; (d) the biomass density, $n(x,t)$ at $t = 30$;. Parameter values are $\alpha = 2$.

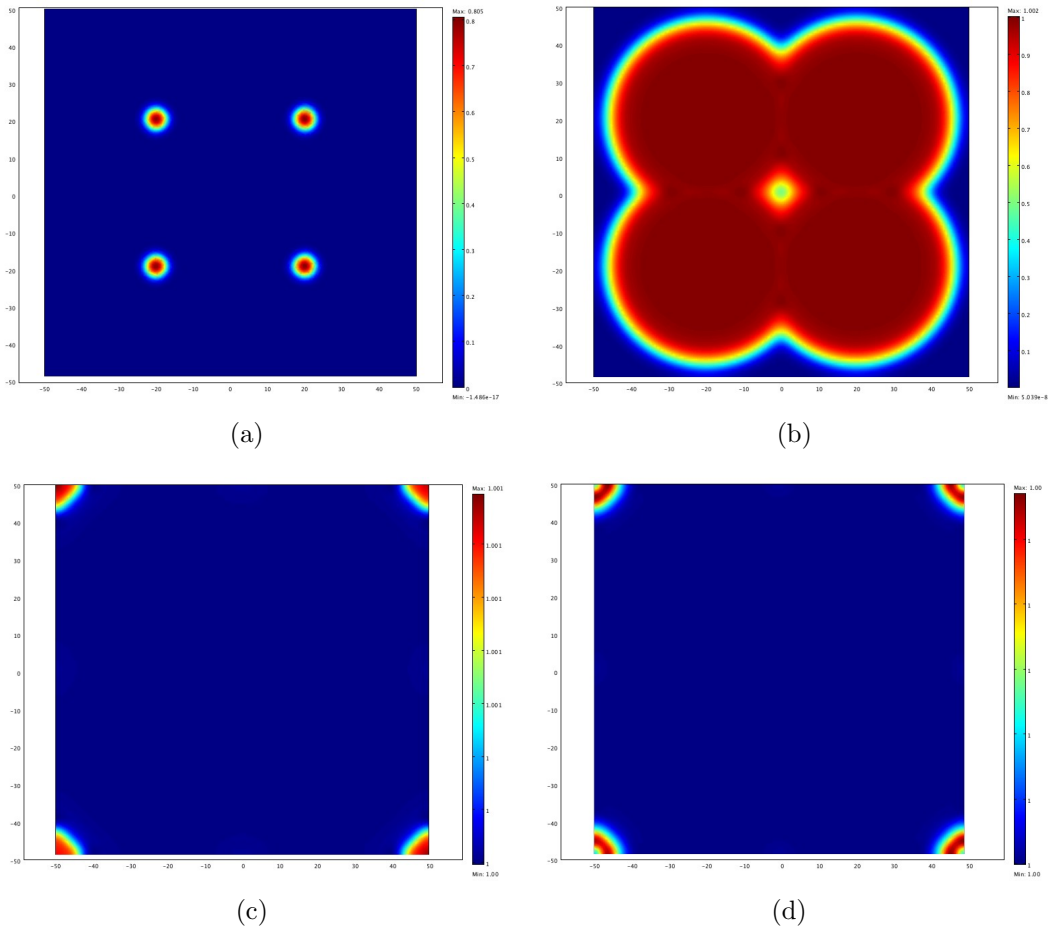

(a) (b)

(c) (d)

Figure 6.17: Two-dimensional solution of system 6.10 "YWD type" when $\sigma = \alpha n(1-n)$. (a) the biomass density, $n(x,t)$ at $t = 1$; (b) the biomass density, $n(x,t)$ at $t = 10$; (c) the biomass density, $n(x,t)$ at $t = 20$; (d) the biomass density, $n(x,t)$ at $t = 30$;. Parameter values are $\alpha = 2$.

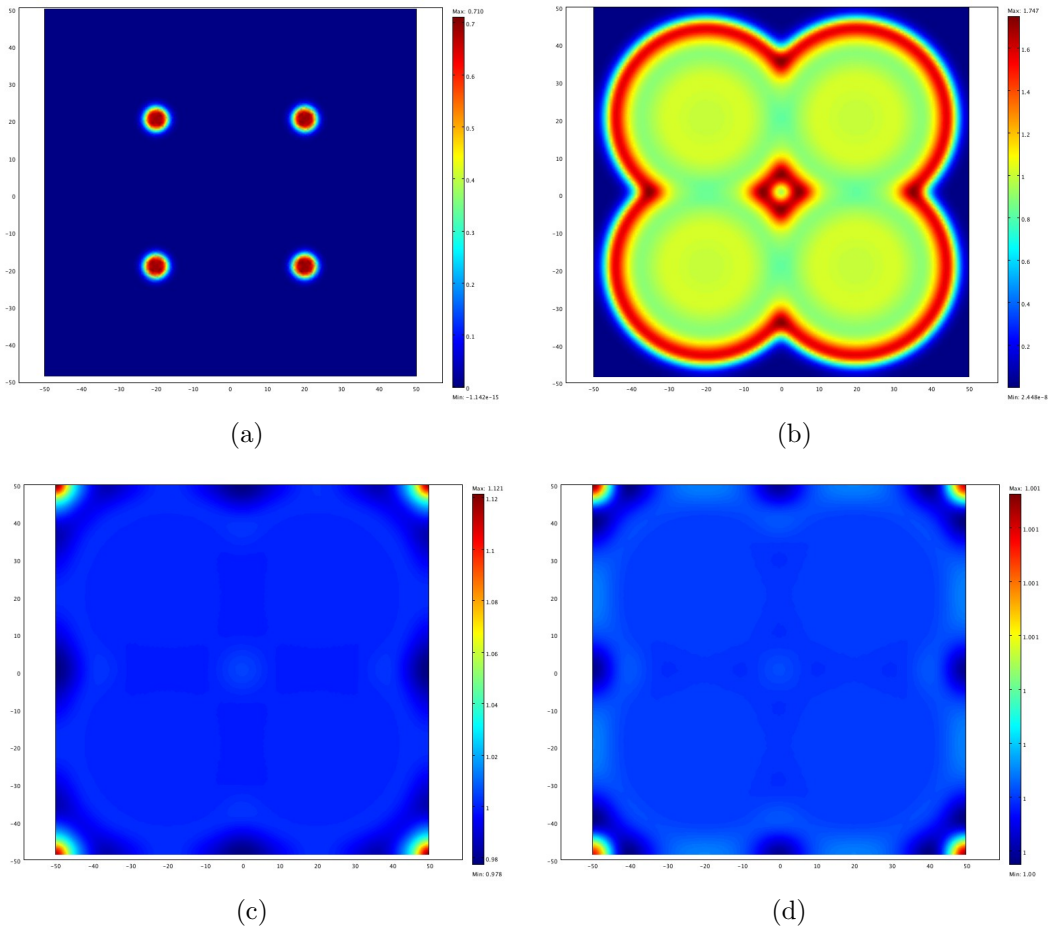

(a) (b)

(c) (d)

Figure 6.18: Two-dimensional solution of system 6.10 "YHD type" when $\sigma = \alpha n(1-\rho)$. (a) the biomass density, $n(x,t)$ at $t = 1$; (b) the biomass density, $n(x,t)$ at $t = 10$; (c) the biomass density, $n(x,t)$ at $t = 20$; (d) the biomass density, $n(x,t)$ at $t = 30$;. Parameter values are $\alpha = 2$.

6.5 2-D Spatially Extended Fungal Growth Model with Substrate

The model system in this case is

$$\begin{aligned} \frac{\partial \rho}{\partial t} &= vns - d(\rho), \\ \frac{\partial n}{\partial t} &= -\frac{\partial (vns)}{\partial x} + \alpha_2 \rho - \beta_2 n\rho, \\ \frac{\partial s}{\partial t} &= -kn, \end{aligned} \tag{6.17}$$

where $\rho(x,t)$, $n(x,t)$, $d(\rho)$, $s(x,t)$, k and $\sigma(\rho,n) = \alpha_2\rho - \beta_2 n\rho$ are defined above. Using COMSOL, we solved FHS: lateral branches tip-hyphae anastomoses with substrate system (6.17) on a square domain $-50 \leq x, y \leq 50$ and used zero flux boundary condition for this simulation. Fig. 6.19 illustrates the substrate density distributions in the all cases. The radial symmetry of three distributions is evident. Notice that the substrate density distributions is start extending see Fig. 6.19(a, b, c), and it is still outward close to the periphery Fig. 6.19,(d), with no change in the centre.

These results are therefore consistent with both the experimental observations described directly above and those of the Chapter 5. Again we see that growth in initially uniform conditions induces radial expansion of substrate accompanied by an expanding annulus of substrate density positioned close to the edge of the substrate distribution. We observed, the speed of substrate starts from 0 to 1 and it is still expanding.

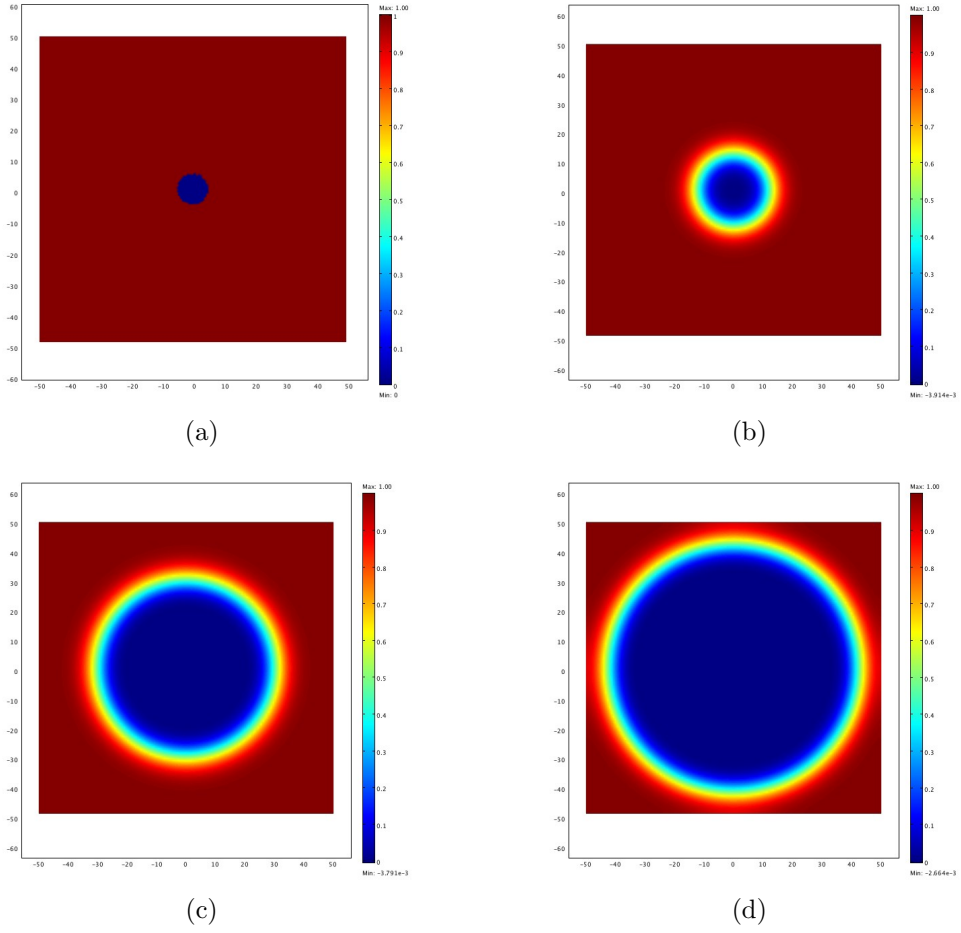

Figure 6.19: Two-dimensional solution of system 6.11: (a) the substrate density, $s(x,t)$ at $t = 1$; (b) the substrate density, $s(x,t)$ at $t = 10$; (c) the substrate density, $s(x,t)$ at $t = 20$; (d) the substrate density, $s(x,t)$ at $t = 30$.

6.5.1 Comparison between FHS type and YWS type

Using the same technique, therefore on a square domain $-50 \leq x, y \leq 50$ and used zero flux boundary condition for this simulation. Fig. 6.20 illustrate the solution of FHS type and YWS type at the same time and the same values of parameters. We note the speed in YWS type is larger than from FHS type for the same values of α, β, k and v. Notice that the substrate density distributions of FWS type is start extending, and it is still outward close to the periphery Fig. 6.20(a), with no change in the centre and the substrate density distributions

of YWS type is start extending, and it is still outward close to the periphery Fig. 6.20(b), with no change in the centre.

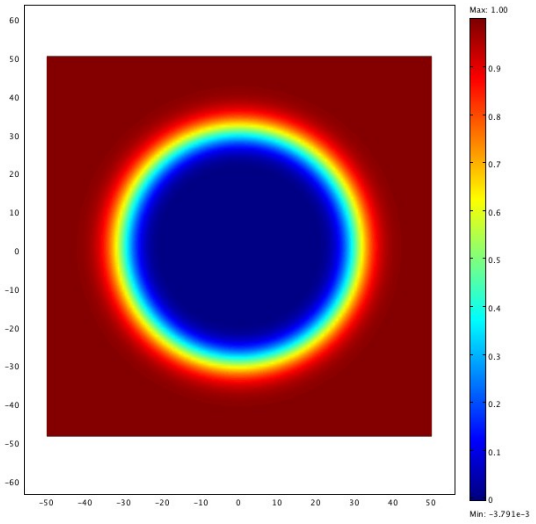

(a)

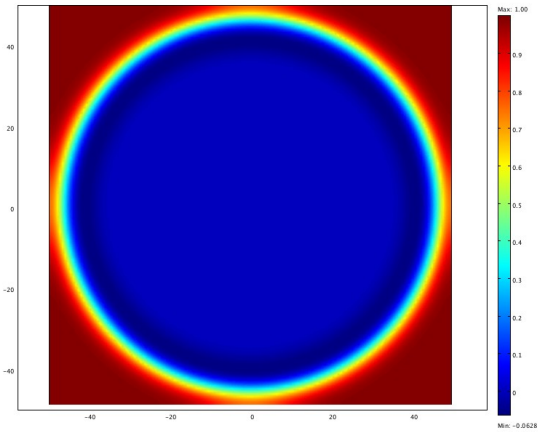

(b)

Figure 6.20: Two-dimensional solution of (a) FHS type, the substrate density, $s(x,t)$ at $t = 20$; (b)YWS type, the substrate density, $s(x,t)$ at $t = 20$. It is clear the waves speed in YWD type are larger than from FHD types for the same values of α.

6.6 Discussion and Conclusion

In this Chapter, we studied 2-D spatially extended fungal growth models. We focused on the system 6.1 for different types of branching. We compared types of branching. The wave speeds in YWD, YHD types are larger than the FHD and FXD types for the same values of α.

We solved FHS: lateral branches tip-hyphal anastomosis with substrate system and we got some results which represented the behaviour of substrate. We compared FHS type and YHS type at the same time and with the same values of parameters. We noted the speed in FHS type larger than the YHS type for the same values of parameters. We noted that the substrate density distributions of FHS type started to extended, outward close to the periphery Fig. 6.20(a), with no change in the centre. Whereas that the substrate density distributions of YHS type started to extended, see Fig. 6.20(b), but a lower centre.

We can of corse study more types of branches using similar techniques but to avoid us repetition.

This Chapter illustrated growth in a two dimensional spatial domain. We confirmed that the form in the radially symmetric case approximates to that in the 1-D travelling wave for large r. Then, we investigated the effects of 2-D on fungal growth equation and fungal growth equation with substrate.

Chapter 7

Conclusions and Future Work

7.1 Conclusions

As already emphasised in the introduction the mathematical models for fungal growth affect the network architecture hyphal tip movement, branching, anastomosis and substrate utilisation.

Much work has already been done on mathematical models of fungi, however as we have found throughout the course of this thesis, many important questions remain unanswered. In this thesis some of these questions have been addressed. It has been shown, both in previous work, and throughout this thesis, that mathematical models of fungi can have rich and more complex solution structures than other mathematical models of fungi (Hardy, 1940; Giovanetti et al., 2011; Edelstein, 1982).

In this thesis we have studied the effects of the hyphal death, diffusion and substrates on growth of network of fungi. Chapter 1 outlines the content and development of the models. In Chapter 2, we presented the background to the

physiology and modelling of fungi. In Chapter 3, we considered the effect of hyphal death or loss on the development of fungal networks.

We studied many cases of branching and we found the solutions by using the mechanism or the methods: non-dimensionalisation; stability of uniform solutions; phase plane; travelling wave solution and numerical solution of the initial value problem. These results are summarised in tables (see table 3.3 and 3.5). We then chose another type for hyphal death $d(\rho)$ which was $d(\rho) = d\rho^k$ and $d(\rho) = \frac{d\rho^k}{\rho_o^k+\rho^k}$, where the parameter d represents the rate of conversion, ρ is the branche concentration, and ρ_o is the Michaelis constant in this context it is the "half maximal death rate". We focused on one type of branching, lateral branching, plus tip - hypha anastomosis (FHD) and we extended to other types of branching using the same techniques (see table 3.6).

The results in Chapter 4, particularly, directed us to understanding the effects of diffusion on the development of fungal networks, and allowed comparison between effects of diffusion and convection separately and together. Again, we summarised the results in the tables (see table 4.1) which illustrate the hyphal (death/ loss) $d(\rho) = 0$ or $d(\rho) \neq 0$. In the previous chapters we focused on two variables ρ, represented the branching and n represented the tips, while in Chapter 5, we added a new variable, s, which explicitly represented a substrate, or energy source.

In the above chapters, we used the methods of non-dimensionalisation, stability of uniform solutions, travelling wave solutions and numerical solution of the initial value problems using MATLAB or MAPLE codes. Using these techniques, we determined a range of important types of fungal network architecture.

In Chapter 6, we studied growth in two dimensional spatial domain. We first confirmed that the form in the radially symmetric case approximates to that in the 1-D travelling wave for large r. Then, we investigated the effects of 2-D on fungal growth equation and fungal growth equation with substrate.

We constructed new models for the development of fungal mycelia. At this scale, partial differential equations representing the interaction of biomass with the underling substrate is the appropriate choice. Models are of a complex mathematical structure, comprising both parabolic and hyperbolic parts. Thus, their analytic and numerical properties are non- trivial. We obtain a understanding of the physiology of growth and function and the varying mathematical techniques used in model construction, we revisit existing models to reinterpret the various model components in a simplified form and we constructed models to compare the growth dynamics of different phenotype. for new species to see if these scale appropriately.

7.2 Future Works

Our suggestion for future work regarding the fungal growth model relates to the fact that the model we developed here is dependent on branches ρ and tips n.

One suggestion would be to investigate " optimal" functions $d(\rho)$ or $\sigma(\rho, n)$ for a given environment to test whether particular network architecture is better suited to a particular simulation.

To add or choose another $\sigma(\rho, n)$ like $\sigma(\rho, n) = (\alpha\rho - \frac{\beta n\rho}{1+\rho^2})$ that results in double travelling wave because in this case will got three steady states.

Our work is dependent on two variables ρ and n where as Edelstein-Kehet and Ermentrout (1989) extended the model and their analysis to higher dimensions where the phenomena are geometrically more complex. A further suggestion would be to add a variable that represents orientation θ (see, for example, (Alt., 1980; Holliday and Ward, 1975) for similar ideas), and to develop this case by studying fungal types:

- Lateral branches with density limitation with hyphal death.
- Dichotomous branches tip-tip anastomoses with hyphal death.
- Dichotomous branches tip-hyphae anastomoses

A further suggestion in 2-D would be to study another type for example (FXS, YWS, YHS) types. We suggestion would be to compare to other investigations for example (Davidson, 1998).

Appendix

Glossary of Biological Terms

Anastomosis The process of a hyphya tip fusing into another hypha tip or into the wall thus creating the mycelial network.

Autocatalysis The process whereby a compound catalyses it is own production.

Autolysis Self-degradation that hyphae undergo after the death of their cells.

Biomass The total quantity of matter in organisms.

Colony A plant community where more or less distinct individuals live and interact in a mutually advantageous way.

Connectivity The degree to which a network is integrated.

Hypha A thread-like filament that is the structural unit in many fungi.

Mycelium A mass of hyphae making up the vegetative stage of many fungi.

Protoplasm Cell contents within and including the plasma membrane.

Septation When a cross-wall develops in a hypha preventing the transport of material.

Translocation The movement of dissolved substances within a fungi.

Bibliography

Alt., W. (1980). Biased random walk models for chemotaxis and related diffusion approximations. *J. Math. Biol.*, **9**:147–177.

Assinder, S. and Rutter, G. (2001). How the mushroom got its spots. *Published jointly by the British Mycological Society and BBSRC.*

Bartton, N. F. (1986). *Reaction - Diffusion Equations and their Applications to Biology.* Academic Press, New York.

Bejan, A. (2004). *Convection Heat Transfer.*

Bird, Stewart, L. (1960). *Transport Phenomena.*

Boswell, G. P. (2008). Modelling mycelial networks in structured environments. *Mycol. Res.*, 112:1015 – 1025.

Boswell, G. P., Jacobs, H., Davidson, F. A., Gadd, G. M., and Ritz, K. (2003a). Growth and function of mycelial fungi in heterogeneous environments. *Bull.Math.Biol.*, 65:447–477.

Boswell, G. P., Jacobs, H., Davidson, F. A., M.Gadd, G., and Ritz, K. (2002). Functional consequences of nutrient translocation in mycelial fungi. *J. Theor. Biol*, 217:459–477.

Boswell, G. P., Jacobs, H., Gadd, G. M., Ritz, K., and Davidson, F. A. (2003b). A mathematical approach to studying fungal mycelia. *Mycologist.*, 17:165–171.

Boswell, G. P., Jacobs, H., Ritz, K., Gadd, G. M., and Davidson, F. A. (2007). The development of fungal networks in complex environments. *Bull. Math. Biol.*, 69:605–634.

Bourret, A., Lincoln, R. G., and Carpenter, B. H. (1969). *Science*, **166**:736.

Bull, A. T. and Trinc, A. P. J. (1977). Adv. *Arch Microbial*, **15**:1.

Caldwell, I. Y. and Trinci, A. P. J. (1973). *Arch Microbial*, **88**:1.

Darrah, P. R., Tlalka, M., Ashford, A., Watkinson, S. G., and Fricker, M. D. (2006). The vacuole system is a significant intracellular pathway for longitudinal solute transport in basidiomycete fungi. *Eukaryot.Cell.*, 5:1111 – 1125.

Davidson, F. A. (1998). Modelling the qualitative response of fungal mycelia to heterogeneous environments. *J. Theor. Biol.*, 195:281 – 291.

Davidson, F. A. (2007a). Mathematical modelling of mycelial : a question of scale. *Fungal Biol. Rev*, **21**:30–41.

Davidson, F. A. (2007b). Mathematical modelling of the form and function of fungal mycelian of scale. *Fungal Biol. Rev*, **21**:30–41.

Davidson, F. A. and Olsson, S. (2000). Translocation induced outgrowth of fungi in nutrient - free environment. *J. theor. Biol.*, **205**:73–84.

Davidson, F. A., Sleeman, B. D., Rayner, A. D., Grawford, J., and Ritz, K. (1996). Contex - dependent macroscopic patterns in growing and interacting mycelial networks. *Proc. R. Soc. Lond*, B **263**:873–880.

Drew, E., Murray, R., Emith, S., and Jakobsen, I. (2003). Beyond the rhizosphere: growth and function of arbuscular mycorrizal external hyphae in sand of varying pore size. *Plant and Soil*, **251**:105–114.

DuChateau, P. and Zachmann, D. (1989). *Applied Partial Differential Equations* . Colorado State University, New York.

Edelstein, L. (1982). The propagation of fungal colonies: A model for tissue growth. *Journal of theoretical Biology.*, **98**:679–710.

Edelstein, L. and Segel, L. A. (1982). Growth and metabolism in mycelial fungi. *Weizmann Institute, Rehovot*, **512**:187.

Edelstein-Kehet, L. (2005). *Mathematical Models in Biology*. Duke University.

Edelstein-Kehet, L. and Ermentrout, B. (1989). Models for branching networks it two dimensions. *Applied Mathematics.*, **49**:1136–1157.

Falconer, R. E., Bown, J. L., White, N. A., and Crawford, J. W. (2007). Biomass recycling: a key to efficient foraging. *Oikos*, 116:1558 – 1568.

Falconer, R. E., Bown, J. L., White, N. A., and Crawford, J. W. (2008). Modelling interactions in fungi. *J. R. Soc. Interface*, 5:603 – 615.

Fife, P. C. (1979). Mathematical aspect of reacting and diffusion system. *In Lect. Notes in Biomathematics*, 28. Springer - Verlag, Berlin-Heidelberg - New York.

Fisher, R. A. (1937). The wave of advance of advantageous genes. *Ann. Eugenics*, 7:353–369.

Giovanetti, M., Fortuna, P., Citernesi, A., and Morini, S. (2011). The occurrence of anastomosis formation and nuclear exchange in intact arbuscular mycorrhizal network. *New Phytol.*, **151**:717–724.

Grindrod, P. (1996). *The Theory and Applications of Reaction - Diffusion Equations - Patterns and Waves.* Oxford University Press, New York.

Gruhn, C. M., Gruhn, A. V., and Miller, O. K. (1992). Boletinellus merulioides alters root morphology of pinus densiflora without mycorrhizal formation. *Mycologia*, **84**:528–533.

Hadley, M. (2002). Fungus fred goes foraying. *British Mycological Society, UK.*

Hardy, G. H. (1940). A mathematician's apology. *Cambridge.*

Hein, M. E. and Neimann, C. J. (1962). *Chem. Soc.*, 84:4487.

Holliday, L. and Ward, I. M. (1975). A general introduction to the structure and properties of oriented polymers (chapter 1), in structure and properties of oriented polymers. *I. M. Ward, ed., John Wiley, New York.*

Humpherson-Jones, F. M. and Cooke, R. C. (1977). *New Phytol*, **78**:181.

Jager, M. J., Lamour, A., Gilligan, G. A., and Otten, W. (2008). A fungal growth model fitted to carbon-limited dynamics of rhizoctonia solani. *New Phytol*, 178:625 – 633.

Jakobsen, I., Abbott, L., and Robson (1992). External hyphae of vesicular-arbuscular mycorriza fungi associated with *Trifolium subterraneum* 1. 1. spread of hyphae and phosphorus inflow into roots. *New Phytol*, **120**:371–380.

Jolicoeur, M., Bouchard-Marchand, E., Becard, G., and Perrier, M. (2003). Regulation of mycorrhizal symbiosis: development of a structured nutritional dual model. *Ecol. Model.*, 163:247–267.

Jones, D. S. and Sleeman, B. D. (1983). *Differential Equatons and Mathematical Biology.* Department of Mathematical Sciences, University of Dundee.

Kolmogroff, A., Petrovsky, I., and Piscounoff, N. (1937). *É*tude de l' *é*quation de la diffusion avec crissance de la quantit*é* de matiére et son application *à* un problème biologique . *Moscow University, Bull Math*, 1:1–25.

Kuto, K. and Yamada, Y. (2004). Multiple coexistence states for a prey-predator system with cross-diffusion. *Journal of Differential Equations*, 197(2):315–348.

Leung, A. W., Hou, X., and Li., Y. (2008). Exclusive traveling waves for competitive reaction-diffusion systems and their stabilities. *Journal of Mathematical Analysis and Applications*, 338:902 – 924.

Luther, R. L. (1906). Rauemliche fortpflanzung chemischer reaktionen. *Z. für Elekronchemie und angew physikalische Chemie*, 12(32):506–600.

Madigan, M. and Martinko, J. (2005). Brock biology of microorganisms. *(11th ed. ed.).Prentice Hall.ISBN).*

Mehrer, H. (2007). Diffusion in solids: Fundamentals, methods, materials, diffusion-controlled processes. *Springer.*

Moore, D. (2001). Slayers, saviors, servants and sex: An expose of kingdom fungi. *Springer-Verlag, New York.*

Murray, J. D. (2002). *Mathematical Biology I.: An Introduction.* New York: Springer.

Odell, G. (1980). *Mathematical Models in Cellular and Molecular and Molecular Biology, pp. 523-67. Edited by L. A. Segel.* Cambridge: Cambridge University press.

Okon, Y., Chet, I., and Henis, Y. (1972). *J. gen. Microbiol*, **71**:465.

Okubo, A. and Levin, S. (2001). Diffusion and ecological problems: Modern perspectives. *New York: Springer-Verlag.*

Persson, C., Olsson, S., and Janssonr, H. B. (2000). Growth of *arthrobotrys superba* from a birch wood food into soil determined by radioactive tracing. *FEMS Microbiol Ecol.*, **31**:47–51.

Probstein, R. (1994). *Physicochemical Hydrodynamics.*

Prosser, J. I. (1995). Mathematical modelling of fungal growth. *In: Gow, N.A.R., Gadd, G.M. (eds), The Growing Fungus. Chapman and Hall, London*, pages 319–335.

Ritz, K. and Crawford, J. W. (1990). Quantification of the fractal nature of colonies of trichoderma viride. *Mycol. Res.*, 94:1138 – 1141.

Ruan, W. H. (1996). Positive steady-state solutions of a competing reaction diffusion system with large cross-diffusion coefficients. *Journal of Mathematical Analysis and Applications*, 197(2):558–578.

Sayer, J. A., Raggett, S. L., and Gadd, G. M. (1995). Solubilization of insoluble metal compounds by soil fungi: development of a screening method for solubilizing ability and metaltolerance. *Mycol. Res.*, 99:987–993.

Schnepf, A. and Roose, T. (2006). Modelling the contribution of arbuscular mycorrhizal fungi to plant nutrient uptake. *New Phytol*, 171:669–682.

Schnepf, A., Roose, T., and Schweiger, P. (2008a). Growth model for arbuscular myorrhizal fungi. *J.R.Soc.Interface.*, 5:773–784.

Schnepf, A., Roose, T., and Schweiger, P. (2008b). Impact of growth and uptake patterns of arbuscular mycorrhizal fungi on plantphosphorus uptake a modelling study. *Plant Soil*, 312:85–99.

Segel, L. A. (1981). *The general balance law and the diffusion equation. In Mathematical Models in Melecular and Cellular Biology, pp. 440-452. Edited by L. A. Segel.* Cambridge: Cambridge University press.

Showalter, K. and Tyson, J. J. (1987). Luther's 1906 discovery and analysis of chemical waves. *J. Chem. Educ.*, 64:742–744.

Swanson, K., Alvord, E., and Murray, J. (2000). A quantitative model for differential motility of gliomas in grey and white matter. *Cell Proliferation.*

Swanson, K. R., Alvord, E. C., and Murray, J. D. (2002a). Quantifying efficacy of chemotherapy of brain tumours with homogeneous and heterogeneous drug delivery. *Acta Biotheoretica*, 50(4):223– 237.

Swanson, K. R., Alvord, E. C., and Murray, J. D. (2002b). Virtual brain tumours (gliomas) enhance the reality of medical imaging and highlight inadequacies of current therapy. *British Journal of Cancer*, 86(1):14–18.

Tlalka, M., Hensman, S., Darrah, P. R., Watkinson, S. G., and Fricker, M. D. (2003). Noncircadian oscillations in amino acid transport have complementary profiles in assimilatory and foraging hyphae of *phanerochaete velutina*. *New-Phytol.*, 158:325 – 335.

van Hees, P. A. W., Rosling, A., Essen, S., Godbold, D. L., Jones, D. L., and Finlay, R. D. (2006). Oxalate and ferricrocin exudation by the extramatrical mycelium of an ectomycorrhizal fungus in symbiosis with pinus sylvestris. *New Phytol.*, 169:367 – 378.

Vetterling, W. T. (1987). Numerical recipes. *University Press, Cambridge, UK.*

Watkinson, A. T. (1975). *J. gen. Microbiol*, **87**:292.

Winfree, A. T. (1980). *The Gemetry of Biological Time*. New York: Springer Veriag.

Yan-ze and Krishnan, E. V. (2006). Exact travelling wave solutions for a class of nonlinear partial differential equtions. *International Journal of pure and Applied Mathematical Sciences*, 3:11–20.